

Rule 110 as it Relates to the Presence of Gliders

Harold V. McIntosh
Departamento de Aplicación de Microcomputadoras,
Instituto de Ciencias, Universidad Autónoma de Puebla,
Apartado postal 461, 72000 Puebla, Puebla, México.

January 29, 1999
revised February 2, 2000
further revised May 14, 2001

Contents

| | | |
|----------|---|-----------|
| 1 | Overview | 11 |
| 1.1 | Introduction | 11 |
| 1.2 | Rule 110 as a consequence of triangular tiles | 13 |
| 1.3 | Some triangle-induced equivalence relations | 17 |
| 1.4 | The simplest mosaics according to Rule 110 | 19 |
| 1.4.1 | T1 mosaic | 20 |
| 1.4.2 | T2 mosaic | 21 |
| 1.4.3 | T3 mosaic | 22 |
| 1.4.4 | ether crystallography | 24 |
| 1.4.5 | T4 mosaic | 26 |
| 1.4.6 | T5 mosaic | 27 |
| 1.4.7 | T6 mosaic | 28 |
| 1.5 | General properties of Rule 110 | 29 |
| 1.5.1 | interpretation of graphs | 29 |
| 1.5.2 | the de Bruijn diagrams | 29 |
| 1.5.3 | cycle, or basin, diagrams | 38 |
| 1.5.4 | ancestors and symbolic de Bruijn matrices | 44 |
| 1.5.5 | subset diagram | 45 |
| 1.5.6 | plaid diagram | 45 |
| 1.5.7 | mean field probability | 46 |
| 1.5.8 | two block probability | 47 |
| 1.6 | Evolutionary generalities | 48 |
| 2 | The Gliders | 51 |
| 2.1 | Gliders not using the ether tile | 51 |
| 2.1.1 | two right in five generations | 51 |
| 2.1.2 | four left in six generations | 55 |
| 2.1.3 | one left in six generations | 57 |
| 2.2 | Cook's A-gliders, with forward velocity $2c/3$ | 60 |
| 2.2.1 | tiling approach | 60 |
| 2.2.2 | de Bruijn approach | 62 |
| 2.2.3 | non-existence of (4,6) A-bar gliders | 63 |
| 2.3 | Cook's B-gliders, with backward velocity $-c/2$ | 64 |
| 2.3.1 | tiling approach to the B gliders at -2 in 4 generations | 64 |
| 2.3.2 | de Bruijn approach to the B gliders | 65 |
| 2.3.3 | tiling by B-bar gliders at -6 in 12 generations | 66 |

| | | |
|----------|---|-----------|
| 2.4 | Cook's C gliders, static with velocity 0 | 67 |
| 2.4.1 | tiling approach | 67 |
| 2.4.2 | de Bruijn approach | 68 |
| 2.5 | Cook's D-gliders, forward velocity $c/5$ | 70 |
| 2.6 | Cook's E-gliders, velocity $-4c/15$ ($\approx -c/4$) | 72 |
| 2.6.1 | tiling approach to $-4/15$ gliders | 72 |
| 2.6.2 | tiling approach to $-8/30$ gliders | 73 |
| 2.7 | Cook's F-glider, backward velocity $-c/9$ | 74 |
| 2.8 | Cook's G-gliders, backward velocity $-c/3$ | 75 |
| 2.9 | Cook's H-glider, velocity $-18c/92$ ($\approx -c/5$) | 77 |
| 2.10 | Cook's glider gun, velocity $-20c/77$ ($\approx -c/4$). | 78 |
| 3 | Glider Collisions | 79 |
| 3.1 | Generalities | 80 |
| 3.1.1 | glider widths and glider parities | 80 |
| 3.1.2 | maps of collision chains | 81 |
| 3.2 | Collisions with A gliders | 82 |
| 3.2.1 | the A - B collision vanishes | 83 |
| 3.2.2 | the three A - C collisions | 84 |
| 3.2.3 | Multiple A - C collisions | 86 |
| 3.2.4 | A - D collisions | 87 |
| 3.2.5 | A - E collisions | 91 |
| 3.2.6 | nA - $E\bar{B}$ collisions | 96 |
| 3.2.7 | nA - F collisions | 98 |
| 3.2.8 | A - G collisions | 102 |
| 3.3 | Collisions with B gliders | 103 |
| 3.3.1 | the three B - C collisions | 103 |
| 3.3.2 | the three BB - C collisions | 104 |
| 3.3.3 | the three BBB - C collisions | 105 |
| 3.3.4 | B - D collisions | 106 |
| 3.3.5 | polyadic B - D collisions | 108 |
| 3.3.6 | B - E collisions | 110 |
| 3.3.7 | B - $E\bar{B}$ collisions | 111 |
| 3.3.8 | B - F collisions | 112 |
| 3.3.9 | B - G collisions | 113 |
| 3.4 | Collisions with $B\bar{B}5$ gliders | 114 |
| 3.4.1 | $B\bar{B}5$ - C collisions | 114 |
| 3.4.2 | $B\bar{B}5$ - E_n collisions | 114 |
| 3.5 | Collisions with $B\bar{B}8$ gliders | 114 |
| 3.6 | Collisions with C gliders | 115 |
| 3.6.1 | C - D collisions | 115 |
| 3.6.2 | C - E collisions | 116 |
| 3.6.3 | C - $E\bar{B}$ collisions | 121 |
| 3.6.4 | C - F collisions | 123 |
| 3.6.5 | C - G collisions | 125 |
| 3.7 | Collisions with D gliders | 127 |
| 3.7.1 | D - E collisions | 127 |
| 3.7.2 | D - $E\bar{B}$ collisions | 127 |

| | | |
|----------|---|------------|
| 3.7.3 | D - F collisions | 127 |
| 3.8 | Collisions with E gliders | 127 |
| 3.8.1 | E - F collisions | 127 |
| 3.9 | Collisions with EBar gliders | 127 |
| 3.10 | Collisions with F gliders | 127 |
| 4 | Running an Obstacle Course | 129 |
| 5 | Conclusions | 135 |
| 5.1 | Acknowledgements and Disclaimer | 137 |

List of Figures

| | | |
|------|--|----|
| 1.1 | A sample of evolution according to Rule 110. | 12 |
| 1.2 | Rules nearby Rule 110 | 14 |
| 1.3 | A (2,2) glider rule | 15 |
| 1.4 | A (4,1/2) glider rule | 16 |
| 1.5 | treeb | 17 |
| 1.6 | treea | 18 |
| 1.7 | Tile format | 19 |
| 1.8 | The plane tiled by T1 triangles. | 20 |
| 1.9 | The plane tiled by T2 triangles | 21 |
| 1.10 | T3 tiling | 22 |
| 1.11 | T3 hexes | 22 |
| 1.12 | squished | 23 |
| 1.13 | Glider map | 24 |
| 1.14 | T4 Tiling | 26 |
| 1.15 | T5 Tiling | 27 |
| 1.16 | allt5 | 27 |
| 1.17 | T6 Tiling | 28 |
| 1.18 | T6 mosaic | 28 |
| 1.19 | Left shifting | 32 |
| 1.20 | Periodic configurations | 33 |
| 1.21 | Right shifting | 34 |
| 1.22 | tolin6 | 40 |
| 1.23 | tolin8 | 41 |
| 1.24 | evolution of T23 | 42 |
| 1.25 | evolution of T26 | 43 |
| 1.26 | Subset diagram | 45 |
| 1.27 | plaid | 45 |
| 1.28 | Mean field curves | 46 |
| 1.29 | Two-block contours | 47 |
| 1.30 | decay1 | 48 |
| 1.31 | t18bdr5 | 49 |
| | | |
| 2.1 | The 2/5 tiles | 51 |
| 2.2 | Some 2/5 gliders | 52 |
| 2.3 | Three alpha species | 53 |
| 2.4 | alfethiface | 54 |
| 2.5 | Two 4/6 tiles | 55 |

| | | |
|------|--|-----|
| 2.6 | First 4/6 species background | 55 |
| 2.7 | Second 4/6 species background | 55 |
| 2.8 | four every six | 56 |
| 2.9 | one every six | 57 |
| 2.10 | left 1/6 second | 57 |
| 2.11 | left 1/6 first | 57 |
| 2.12 | generic 1/6 | 58 |
| 2.13 | T1 based gliders | 60 |
| 2.14 | thin A's | 61 |
| 2.15 | thick A's | 61 |
| 2.16 | De Bruijn diagram for A-gliders | 62 |
| 2.17 | De Bruijn diagram for (4,6)-gliders | 63 |
| 2.18 | T1 based B gliders | 64 |
| 2.19 | De Bruijn diagram for B-gliders | 65 |
| 2.20 | tiling diagram for B-bar-gliders | 66 |
| 2.21 | varied BBars | 66 |
| 2.22 | C gliders | 67 |
| 2.23 | C sequence | 68 |
| 2.24 | De Bruijn diagram for C-gliders | 69 |
| 2.25 | D gliders | 70 |
| 2.26 | Two D variants | 71 |
| 2.27 | E gliders | 72 |
| 2.28 | Ebar glider | 73 |
| 2.29 | F Glider | 74 |
| 2.30 | G gliders | 75 |
| 2.31 | extension of G-gliders | 76 |
| 2.32 | H glider | 77 |
| 2.33 | Glider gun | 78 |
| | | |
| 3.1 | A's and B's colliding with C's | 81 |
| 3.2 | A and B collide, vanish | 83 |
| 3.3 | A and C collide, leave C | 84 |
| 3.4 | A and C collide, leave F | 85 |
| 3.5 | A and D2 collide to make D1 | 87 |
| 3.6 | A and D collide to make C2 | 89 |
| 3.7 | A and E collide | 92 |
| 3.8 | A and E2 collide | 93 |
| 3.9 | A and E3 collide | 94 |
| 3.10 | A and E4 collide | 95 |
| 3.11 | AEBarmeeet | 96 |
| 3.12 | A tetrad and EBar collide producing C2 | 97 |
| 3.13 | AFmeet | 98 |
| 3.14 | A and F collide producing EBar | 99 |
| 3.15 | A tetrad and F collide producing C3 or D | 100 |
| 3.16 | A pentad and F collide producing C3 or D | 101 |
| 3.17 | AGmeet | 102 |
| 3.18 | B and C collide, leave C, D or E | 103 |
| 3.19 | BB and C collide, leave D or E | 104 |

| | | |
|------|--|-----|
| 3.20 | BBB and C collide, leave E's or EBar,A | 105 |
| 3.21 | B and D1 collide, leave E | 106 |
| 3.22 | B and D2 collide, leave EBar and A | 107 |
| 3.23 | AFmeet | 108 |
| 3.24 | nB's and D1 collide | 109 |
| 3.25 | E swatch | 110 |
| 3.26 | B and EBar collide | 111 |
| 3.27 | B and F collisions | 112 |
| 3.28 | B and G collide | 113 |
| 3.29 | Table where C collides with E, EBar, F | 116 |
| 3.30 | C - En collisions | 117 |
| 3.31 | C collides with E23 | 118 |
| 3.32 | C2 collides with E | 119 |
| 3.33 | En eats C3 | 120 |
| 3.34 | EBar can pass C2 | 122 |
| 3.35 | C - F alignment | 123 |
| 3.36 | C1 collides with F | 124 |
| 3.37 | G approaches C | 125 |
| 3.38 | C - G collision tables | 126 |
| 3.39 | EBar collides with F | 128 |
| 4.1 | E's pass C's | 130 |
| 4.2 | chain23 | 131 |
| 4.3 | chain23 | 132 |
| 4.4 | C3eatsE's | 133 |
| 4.5 | ACD | 134 |
| 5.1 | Large triangles are hard to pack | 135 |
| 5.2 | Initial stages of one cell evolution | 136 |

List of Tables

| | | |
|------|---|-----|
| 1.1 | Gliders | 25 |
| 1.2 | nodes and links | 30 |
| 1.3 | Eight generations | 35 |
| 1.4 | Ninth generation left shift | 36 |
| 1.5 | Ninth generation right shift | 37 |
| 1.6 | by cycle and period | 38 |
| 1.7 | Long periods up to cycle length 16. | 38 |
| 1.8 | Evolution to zero | 39 |
| 1.9 | evolution to constant 1 | 39 |
| | | |
| 3.1 | widths | 80 |
| 3.2 | A collisions | 82 |
| 3.3 | B collisions | 82 |
| 3.4 | A polymer collisions | 86 |
| 3.5 | A polyad collisions | 86 |
| 3.6 | A - D collisions | 87 |
| 3.7 | A-En collisions | 91 |
| 3.8 | An-EBar collisions | 96 |
| 3.9 | nA-F collisions | 98 |
| 3.10 | A-G collisions | 102 |
| 3.11 | B - C collisions | 103 |
| 3.12 | B dyad - C collisions | 104 |
| 3.13 | B triad - C collisions | 105 |
| 3.14 | nB - D collisions | 108 |
| 3.15 | BBar5-C collision | 114 |
| 3.16 | BBar5-En collision | 114 |
| 3.17 | BBar8-C collision | 114 |
| 3.18 | C - D collisions | 115 |
| 3.19 | D - E collisions mostly cancel out into A's and B's. a noteworthy exception being the D2E1mid collision which cleanly produces a G glider via a freestanding intermediary T13. In this respect the evolution resembles the commonplace production of an EBar from a single T10. | 127 |
| 3.20 | EBar-F collisions | 127 |

Chapter 1

Overview

Recent correspondence (Fall, 1998) in LifeMail dealt with the possibility of “universal computation” using Wolfram’s (2,1) cellular automaton Rule 110. While awaiting further details participants in the list were referred to an eight page prospectus written by Matthew Cook cataloging the known gliders for the rule. Some of the commentary surrounding his introduction is reproduced and elaborated here, namely the results of the survey of the properties of Rule 110 carried out via the cellular automaton program NXLCAU21. Since then, we have played with glider collisions, and examined Rule 110 from the point of view of tiling the plane with isosceles right triangles.

1.1 Introduction

The one dimensional binary cellular automaton rule numbered 110 in Stephen Wolfram’s system of identification [9] has been an object of especial attention because of glider-like structures which have been observed in samples of evolution from random initial conditions. It has even been suggested that it belongs to that exceptional Class IV of automata whose chaotic aspects are intermingled with regularities of behavior; it is just that the background against which this development occurs is textured rather than quiescent, a tacit assumption in the original classification.

Whatever the merits of the classification, Rule 110 was awarded its own appendix (Table 15) in reference [9], containing specimens of evolution annotated with a list of thirteen gliders compiled by Doug Lind and the conjecture that the rule might be “universal.”

Figure 1.1 contains a similar evolutionary sample, starting out from a sparse collection of ones; the scale of diagrams such as these affects the ease with which gliders are perceived. Complementarity applies; the more visible the glider tracks, the harder to grasp the finer details of their structure.

There does not seem to be much published literature concentrating on Rule 110; the sole exception seems to be some statistical studies [4] done by Wentian Li and Mats Nordahl around 1992. The transitional role of Rule 110, as relates to its Class IV style positioning between Wolfram’s Classes II and III, would seem to be reflected in a slow approach to equilibrium statistics, via a power law rather than exponentially.

As for information available via Internet, Matthew Cook wrote an eight page in-

roduction [1] listing gliders A through H and a glider gun. Cook cites Erik Winfree as having made an exhaustive enumeration of Rule 110 gliders, and cross links to Winfree’s [www page](#), which, however, does not seem to mention this particular feat. Another brief page [10] exists in the Santa Fe Institute ALife archive.

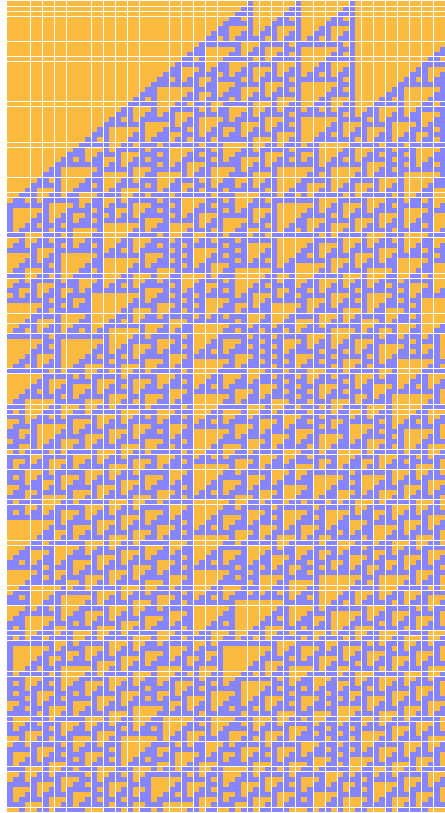


Figure 1.1: A sample of evolution according to Rule 110.

Looking at the rule itself, there seems to be a ubiquitous background texture which Cook calls “ether” although it is but one of many regular lattices stable under the rule’s evolution, and not the one with the smallest unit cell. Calling the artifacts which turn up “gliders” is a way of speaking, no doubt borrowed from experience based on Life. Alternatively, they might be termed “dislocations” and studied as lattice defects.

Taking that approach is suggested by observing that the basic entities in the lattices, the unit cells, are hollow upside down isosceles right triangles of varying sizes. The significance of using Rule 110 could be in guaranteeing recognizably distinct tiles to be assembled, and now that we know that the rule is supposed to be “universal” we might look towards the evolution as a tiling problem, in the sense of Hao Wang. It might even be possible to see fitting elements of one lattice into another as an instance of Post’s correspondence principle, which would establish the computational complexity of the evolution right off.

The choice of words such as “gliders” or “dislocations” is really quite subjective. The name glider originates from John Conway’s Life, to describe small five-cell mobile artifacts relative to the quiescent background of a two-dimensional cellular automaton. It is a mixture of a technical term from crystallography, alluding to a four stage cycle in which mirror images of the phases participate; and a certain whimsy suggesting a gracefulness of motion. It has come to mean anything that moves; moreover in the case of Rule 110, against a background which is no longer quiescent, but textured.

Further complicating the analysis, and suggesting the appropriateness of at least an occasional reference to defects and dislocations, is the fact that two or more distinguishable patterns alternate with one another, or rotate in sequence. When one pattern is highly dominant and the others a rarity, the unusual constituents can be perceived visually as gliders. But roles can be reversed. Even worse, they can occur in approximately equal numbers haphazardly mixed, at which point talking about a disordered, or partially ordered, lattice may be more appropriate than picking out gliders.

In Life, fuses are related to gliders except for extending to infinity. Similar structures abound in Rule 110, where they are readily regarded as the junction of two dissimilar lattices whose interface shifts with time.

1.2 Rule 110 as a consequence of triangular tiles

To the extent that its ability to tile the plane with isosceles right triangles is relevant to the remaining properties of Rule 110, one ought to examine the uniqueness of this characteristic. Consider the eight neighborhoods of a (2, 1) automaton and their relation to tile formation:

| | | |
|-------|---|---|
| 0 0 0 | 0 | quiescent state and interior of the triangle |
| 0 0 1 | 1 | left expansivity, defining hypotenuse |
| 0 1 0 | 1 | permanence of left edge ($x10 \rightarrow 1$) |
| 0 1 1 | a | [square up top left corner] |
| 1 0 0 | 0 | interior, when next to left edge |
| 1 0 1 | b | [close off bottom] |
| 1 1 0 | 1 | permanence of left edge ($x10 \rightarrow 1$) |
| 1 1 1 | 0 | top edge gives way to interior |

Six of the eight transitions are hardly controversial; that the ones marked a and b should evolve to 1, if not evident at first sight, becomes apparent after examining a trial evolution. Leaving the values a and b open for the moment, the Wolfram scheme of rule numbering yields four alternatives,

$$\text{rule} = 70 + 8a + 32b,$$

which are

| | | |
|-----|----|------|
| a/b | 0 | 1 |
| 0 | 70 | 102 |
| 1 | 78 | 110. |

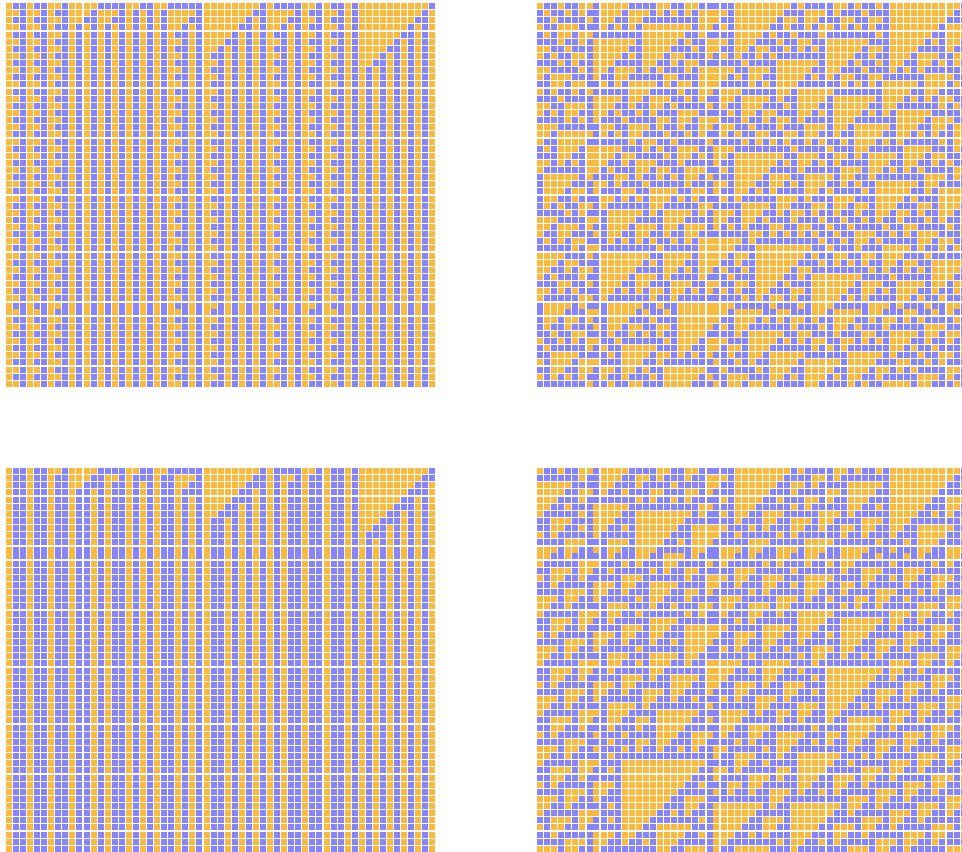


Figure 1.2: Some slight variants on Rule 110, according to the retention of the upper left corner of triangles, and likewise whether the bottom vertex is closed off or not.

In Figure 1.2 we see that Rules 70 and 78 are clearly disappointing, whereas Rule 102 shows some character; nevertheless closing the right-angle vertex leads to lots of diagonal protuberances which do not look very tile-like.

In essence, Rule 110 seems to be uniquely defined for tiling purposes. Of course, we could experiment with triangles with a horizontal hypotenuse, and there may be other interesting figures, even if not available with $(2,1)$ rules. Within the realm of binary, first-neighbor automata, are there other rules for which similar results can be inferred? The Santa Fe AI archive mentions Rule 54 as possibly having computability traits in common with Rule 110.

Generalizing to bigger neighborhoods, $(2,2)$ rules might be a place to start. First choice might be the iterate of Rule 110, which is Rule 729E529E (in hexadecimal). Gliders still exist, although with an altered appearance due to essentially displaying every second generation of Rule 110 and seeing triangles collapse twice as fast because of the new light velocity.

To obtain a rule with the same rate of collapse, a table similar to the one shown above can be constructed. But the results are substantially the same, and there is

much redundancy due to the don't-care conditions on the left to guarantee that the triangle has the desired right-hand structure. In fact, one is practically embedding a (2,1) automaton into a (2,2) automaton by ignoring the outer margin. However the choice of an image for the neighborhood (x x 1 1 0) is less critical, and gives some variation.

In fact, tinkering with any of the rules shouldn't alter their behavior much. Wentian Li and others have studied the amount of tinkering required to drastically change the nature of the rule, and of course found that some rules were more sensitive than others. In general, if any of the diagrams, especially the de Bruijn diagram, have meagre linkages between loops sparsely interconnected, cutting or adding links can have drastic consequences. If the diagrams are more prolifically connected, such changes can go practically unnoticed. There is a perturbation theory of sorts for rules and their graphs.

There are gliders in rules with more than two states, but relating them to a tiling supposes a better idea of what the tiles should look like than has been discussed here. As to why tiling by triangles or other tokens should be different from tiling with individual cells, the answer is that the rule has been subsumed into the shape of the tile, and the requirement is the purely geometric one of filling the plane (perhaps with selected overlap) and the rule need no longer be consulted. Although that just gives bigger tiles, it seems to be useful change of emphasis.

Some (2,2) rules displaying triangles and gliders to some extent or other are: 3CBC3CBC, 3CFC3CBC, 3CBC3CFC, 3CFC3CFC, 7CFCFCBC. The main freedom lies in deciding what to do with short sequences of 1's – start a new triangle, or not.

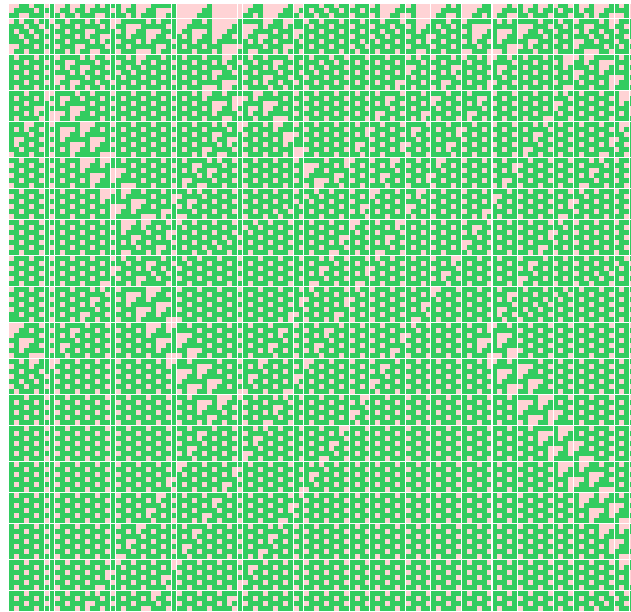


Figure 1.3: A (2,2) rule [3CBC3CFC] with characteristics similar to (2,1) Rule 110.

Figure 1.3 shows a sample of the evolution according to the second neighbor, binary

rule 3CBC3CFC, which resembles Rule 110. Not all triangles are completely rimmed, and the gliders seem to be quite a bit weaker than those in Rule 110. But there are several other nearby rules, all of which show gliders to one degree or another, all waiting to be examined.

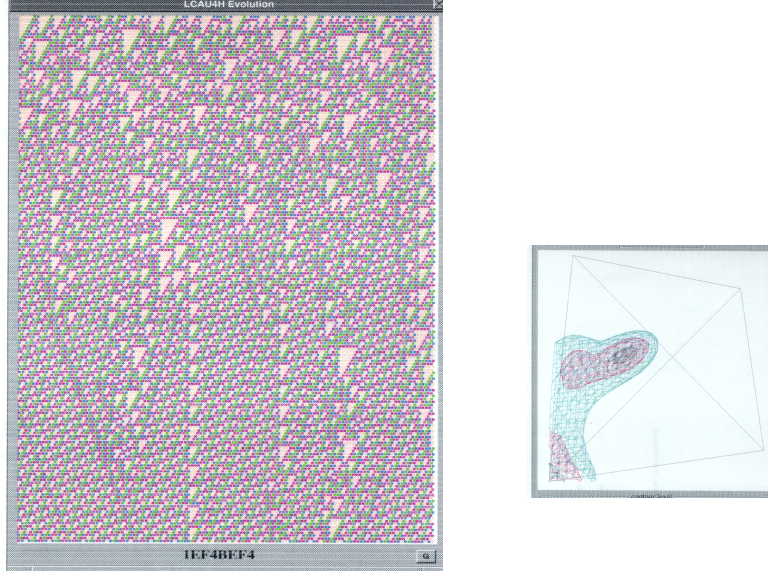


Figure 1.4: A $(4,1/2)$ rule [1EF4BEF4] with characteristics similar to $(2,1)$ Rule 110.

Although it still represents the same rule, there is a blocking technique described by Moore and Drisko [7] which will transform any rule into an equivalent two-neighbor rule. The $(2,1)$ Rule 110 transforms into the $(4,1/2)$ Rule 1EF4BEF4, a sample of whose evolution is shown in Figure 1.4. Gliders and the ether are still recognizable, but the half-integer radius breaks up the planar tiling which is the most evident aspect of Rule 110.

The right side of Figure 1.4 shows some mean field contours for Rule 1EF4BEF4 from which two fixedpoints are evident. one of which reflects the fact that 00 pairs, representing an unused quiescent background, give an unstable fixed point. The other corresponds to a higher density, and presumably relates to the stable background provided by the ether.

1.3 Some triangle-induced equivalence relations

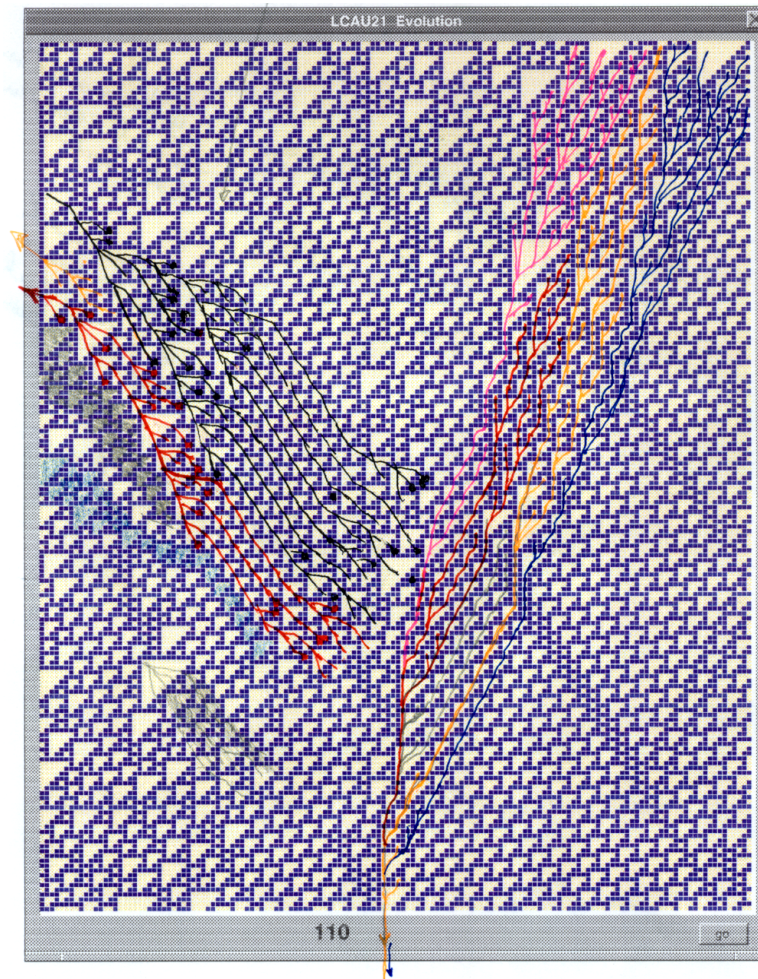


Figure 1.5: Each triangle defines a unique successor in at least four different ways, depending on vertex-contact. Here two tree families are partially sketched for evolution from a random initial configuration.

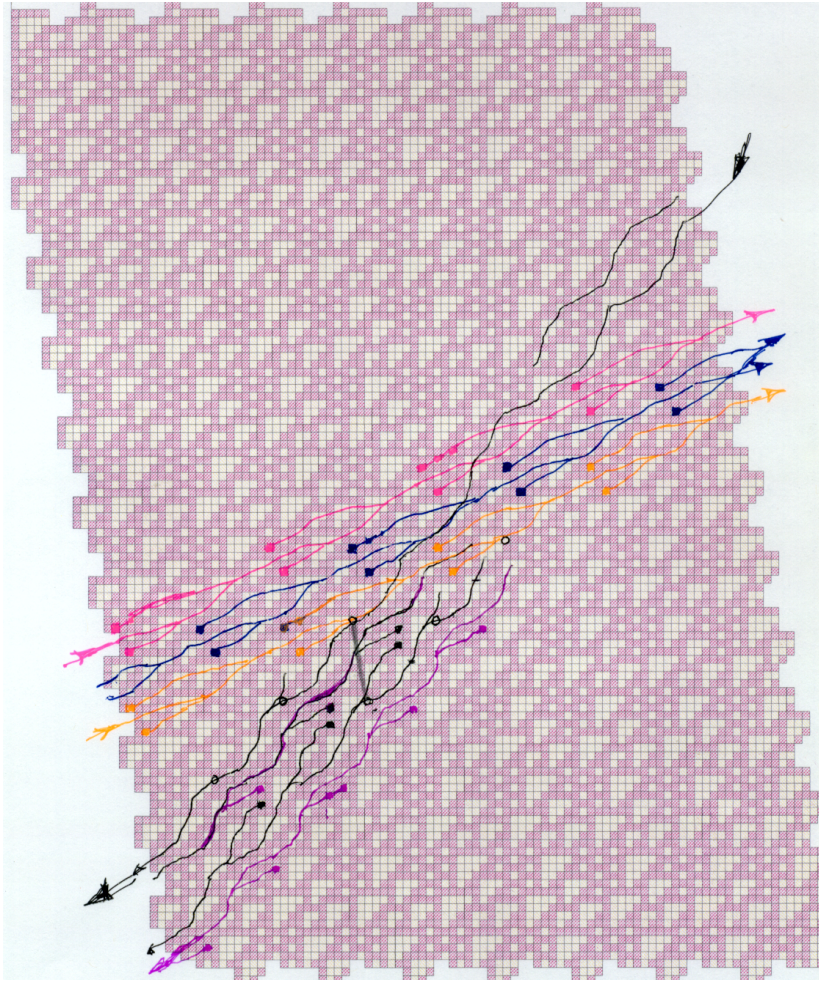


Figure 1.6: Here tree families are sketched for a particular regular lattice.

1.4 The simplest mosaics according to Rule 110

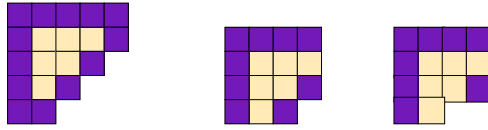


Figure 1.7: Format of the tiles appearing in the evolution of Rule 110, as it affects the appearance of the T3 tile.

Having agreed on the use of triangles as tiles, they can be labelled T_n , where n is the number of zeroes in their top row, and presented as being completely bordered, or semibordered, as in Table 1.7. The semibordered version is easier to work with since the adjacent triangles complete missing border cells, at least along horizontal or vertical edges. Diagonally it is sometimes necessary to overlap a diagonal cell with a top left corner cell. It is never allowed to abut two triangles prolonging a common top edge, which would imply one single large triangle on account of the run; otherwise the tiling is completely geometrical without any reference to the values of the cells they contain.

Superluminal shifts in the LCAU de Bruijn diagrams are a good source of regular lattices in the evolution of any automaton, especially because by taking the form of disjoint loops simple lattices result. However, other shifts and the cycle option can all give lattice examples. For rules such as 110 which have a textured background, which Cook calls the ether, the likely candidates should be found among the lattices of small period or cycle. From the point of view that Rule 110 depends on a triangular tiling of the plane, smaller triangles should be preferred, just on statistical grounds.

1.4.1 T1 mosaic

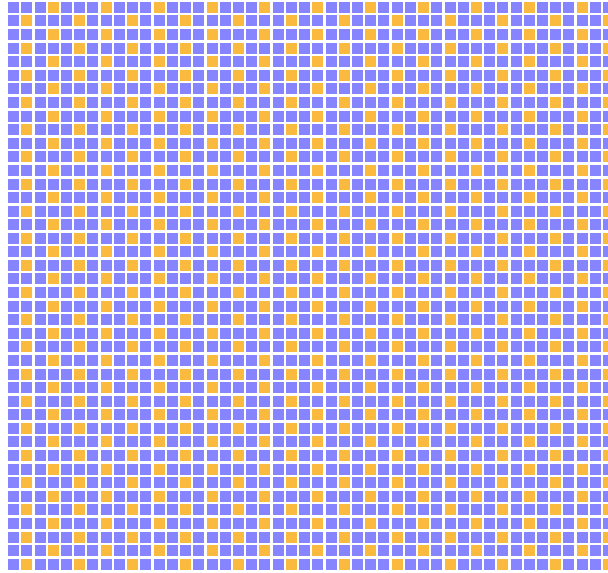


Figure 1.8: The plane tiled by T1 triangles.

Figure 1.8 shows the tiling constructed from the smallest triangles of all, which we have called T1. The triangles stand in columns, alternate columns staggered. The unit cells are square, with three of the four states equal to 1. Therefore the density of this lattice is 75%, which is higher than Langton's ratio [the relative proportion of states in the defining rule], which is $5/8$ or 62.5%, and therefore unlikely as an equilibrium configuration.

1.4.2 T2 mosaic

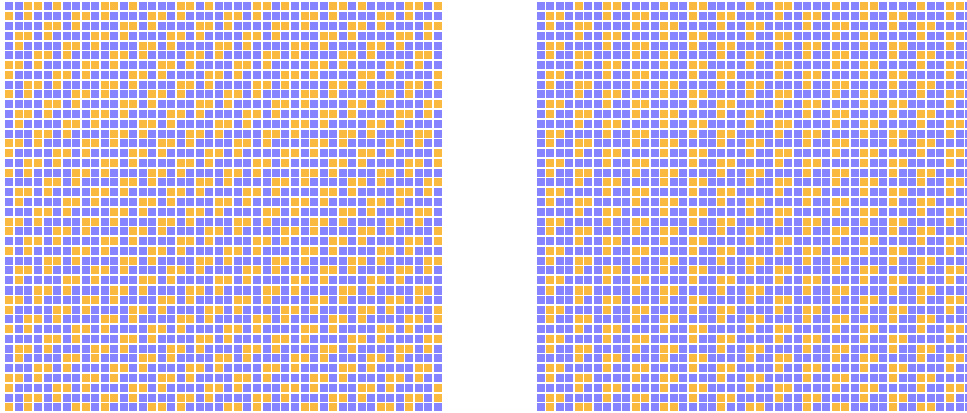


Figure 1.9: The plane tiled by T2 triangles. Left: alpha phase, in which the triangles are stacked diagonally. Right: beta phase, in which they are stacked in columns.

The next larger triangles, T2, can cover the plane in two different ways. One, which could be designated the alpha phase, strings the tiles out along diagonals, as shown in the left mosaic of Figure 1.9. The other, similar to the T1 mosaic, arranges the T2 tiles in columns, for which there is only one way to avoid unwanted sequences of three ones in a row. It constitutes the beta phase, shown in the right mosaic of the same figure.

The density of the alpha phase is $5/8$ or 62.5%, of the beta phase $6/9$ or 67%. In spite of the more favorable densities, neither mosaic is ever a predominant feature of evolutions from random initial configurations.

1.4.3 T3 mosaic

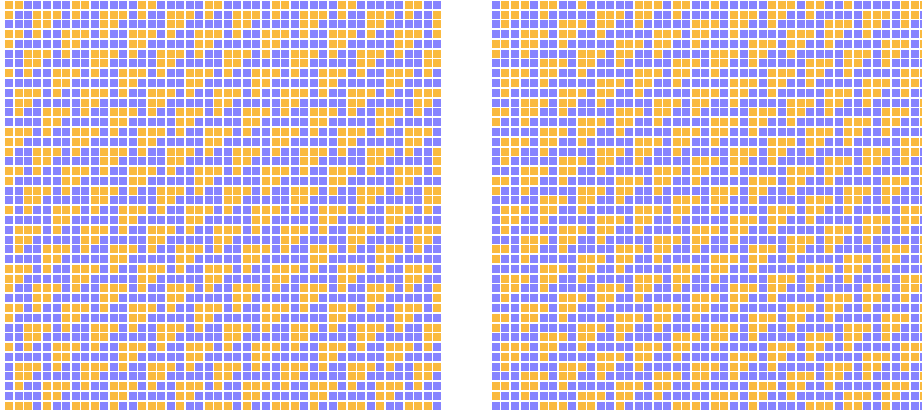


Figure 1.10: The plane tiled by T3 triangles. Left: alpha phase, in which the triangles are stacked diagonally with slope $-1/2$ in periodic rectangular tiles 7×14 . Right: preferred ethereal beta phase, in which they are stacked diagonally with slope -2 in periodic rectangular tiles 14×7 . The beta phase welcomes intercalated T1's, whereas the alpha phase does not,

Continuing, there are two tilings by T3's, likewise designated alpha and beta phases. Both string their tiles along diagonals, as shown in Figure 1.10, The tile to the right sits higher in the alpha phase than in the beta phase, these two diagonal positions being the only ones compatible with Rule 110. Trying to stack T3's in a vertical column would lead to the combination for which Rule 102 was rejected.

Of these two enantiomers (yes, one is a mirror reflection of the other, in the diagonal), the beta form is ubiquitous in evolutions, constituting Cook's ether. It easily combines with other tiles; two mixtures with T1's give the two simplest gliders, designated A and B. By itself it covers the plane with a density of 57%.

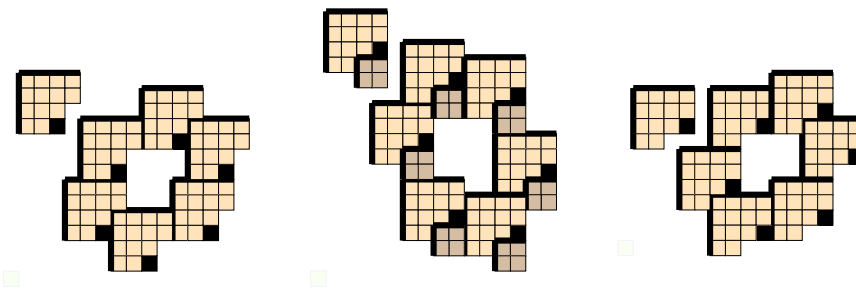


Figure 1.11: Left and Right: the two enantiomers of the T3 tile. Center: The T3 can combine with a T1 to produce a hexagonal lattice with a larger unit cell than T3 alone. Only one of the two enantiomers is shown.

Rule 110 has a predisposition toward the planar hexagonal lattice, on account of the domination of the evolution by upside down isosceles right triangles. On the other hand, the simple mosaics, while clearly displaying the hexagonal format, all differ in the size and orientation of the principal axes since they depend on triangles of different sizes.

The 14×7 unit crystallographic cell for the ether lattice was noted by Lind [9], and evidently has a more convenient periodicity than does the alpha variant. Whatever the reason, the beta version is overwhelmingly preferred as the eventual destination of long term evolution from random initial configurations. One good reason for the asymmetry lies in the packing of T1's with T3's. T1's and T3's have the same symmetry, but the diagonally reflected T1 lattice is incompatible with the rule of evolution; indeed alternate rows belong to the Garden of Eden.

The discrepancy consists in the fact that T1's can, and often are, stacked vertically, but in the mirror reflection they would have to run along horizontally, violating the abutment proscription. Consequently, since columns of T1's often occur in Rule 110 gliders, no enantiomer of a glider with too long a vertical stack would exist.

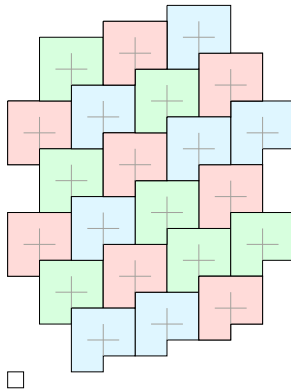


Figure 1.12: The ether lattice is a mosaic of slightly squished hexagons. In common with hexagonal lattices it can be decomposed into three sublattices each of which can be assigned one of three different colors.

1.4.4 ether crystallography

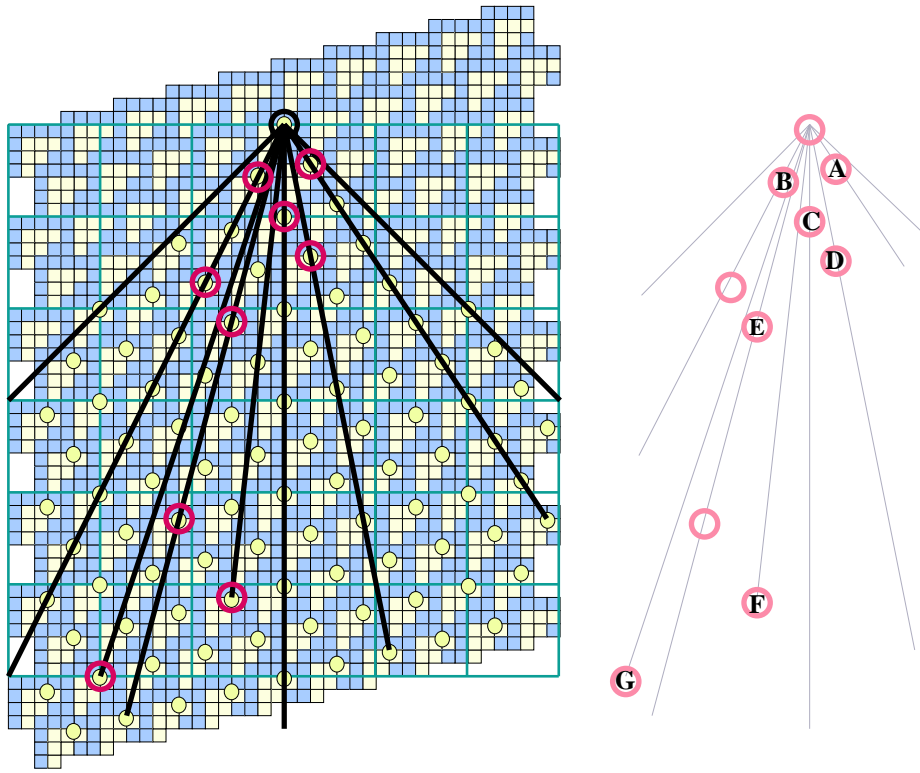


Figure 1.13: The locations of Cook's gliders relative to the ether lattice. The two barred gliders sit lower on the same velocity lines as the unbarred gliders. Small circles on the T3 mosaic show possible positions of compatible gliders, but they could be impossible, duplicates, or so far undiscovered.

By definition, mosaics define crystallographic lattices, relative to which eventual gliders can be seen as dislocations or other defects. Figure 1.13 shows the ether mosaic, together with the position of the light cone and the locations of some of Cook's gliders. The slope of the line connecting any of them to the origin reveals the velocity of the glider. Conversely, these crystallographic faces determine possible velocities whereby it appears that the simpler combinations have already been discovered.

In every generation there are lattice vectors connecting congruent points in the lattice. Those with less than (or exactly) light velocity are listed in Table 1.1, for the first sixteen generations. Note that such combinations as two in three generations and four in six generations refer to the same velocity, but not necessarily the same gliders. Sometimes additional time is required to develop a cycle fully. Of course any gliders obeying m in n will also obey km in kn . Gliders can appear for the first time when $k = 2$ which were absent for $k = 1$; it is more usual that all the old ones remain and either new ones arise, or new interconnections develop between the old ones. And, of course, the value of k can sometimes make no difference, and no gliders may exist at a velocity which otherwise seems reasonable.

| designation | shift | generation | left | generation | right |
|-------------|-------|------------|------|------------|-------|
| A | 2 | 3 | -2 | 3 | 2 |
| B | -2 | 4 | | 4 | |
| B-bar | -6 | 12 | | 6 | 4 |
| C | 0 | 7 | | 7 | 0 |
| D | 2 | 10 | -4 | 8 | |
| E | -4 | 15 | -8 | 9 | 6 |
| E-bar | -8 | 30 | | 10 | 2 |
| F | -4 | 36 | -2 | 11 | |
| G | -14 | 42 | -6 | 12 | 8 |
| H | -18 | 92 | -10 | 13 | 4 |
| glider | . | 77 | | 14 | 0 |
| | | | -4 | 15 | 10 |
| | | | -8 | 16 | 6 |

Table 1.1: Left: Cook's glider list, including Lind's gliders. Right: Some potential glider velocities, arranged by denominator.

1.4.5 T4 mosaic

There is a tiling comprised of pure T4's, in which they lie along diagonals as shown in the left hand mosaic of Figure 1.14. They can share a half-plane with T1's, producing a fuse, or fill the plane by themselves alone. Another combination, shown on the right in Figure 1.14, mixes T1's and T4's, stacking the combination in vertical columns.

There is some delicacy involved in aligning vertical columns of tiles, because three ones in a row evolve to zero. Avoiding the combination while retaining the vertical margin means that an additional one sits either on the left of the spine or the right, but not both. Thus any top margin of a triangle at the right can only attach where there is a zero on the left.

In the case of the T1-T4 combination, there are two umbilical points, leading to the two different alignments which alternate in Figure 1.14. But there is no reason for the full tiling of the plane to be so regular, amounting to an infinitude of phases.

No further mosaics depend on one single T tile, because of the difficulty in evenly filling the lower half of the implicit tile square. Smaller pieces can be incorporated and more elaborate staggering can be arranged, for which there is no lack at all of regular or semiregular tilings for the plane which incorporate at least one of the larger tiles.

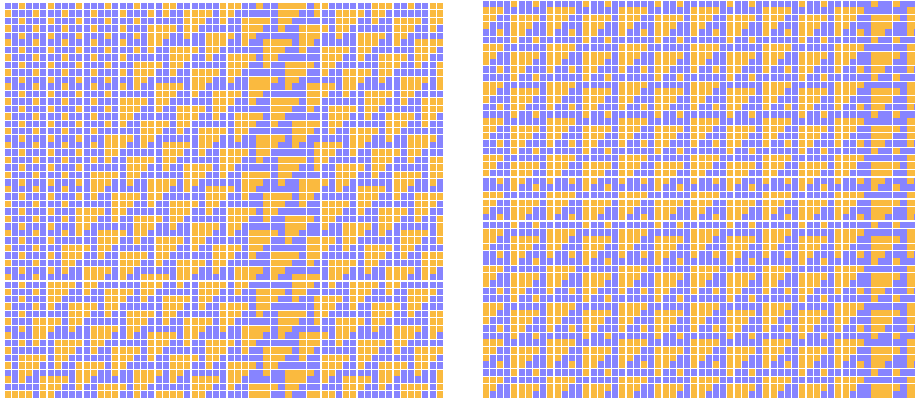


Figure 1.14: To tile the plane, T4 triangles can be stacked diagonally, an arrangement which is compatible with the T1 lattice. Otherwise they have to be paired with some other, smaller, triangle such as a T1 diagonally situated. Once triangles of disparate sizes occupy a unit cell, many combinations still having similar areas are possible.

1.4.6 T5 mosaic

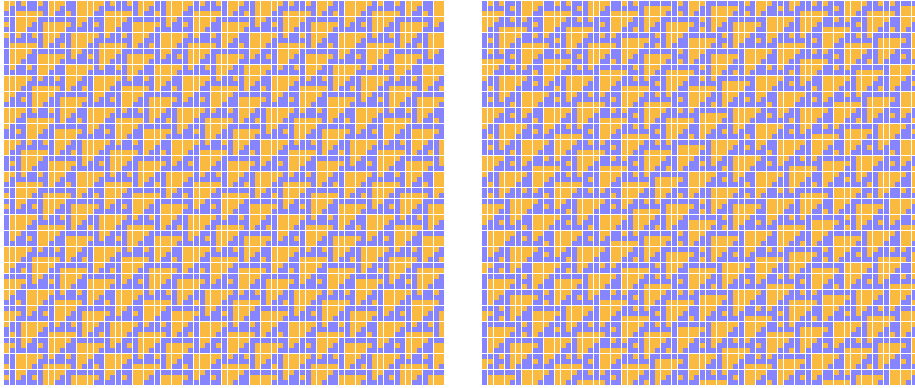


Figure 1.15: To tile the plane, T5 triangles cannot be stacked diagonally, unless they are placed slightly off center, for reasons of parity. There remain interstices which can be filled by one or two T1 tiles, but not by two T1's in a row if Rule 110's evolution is to be respected.

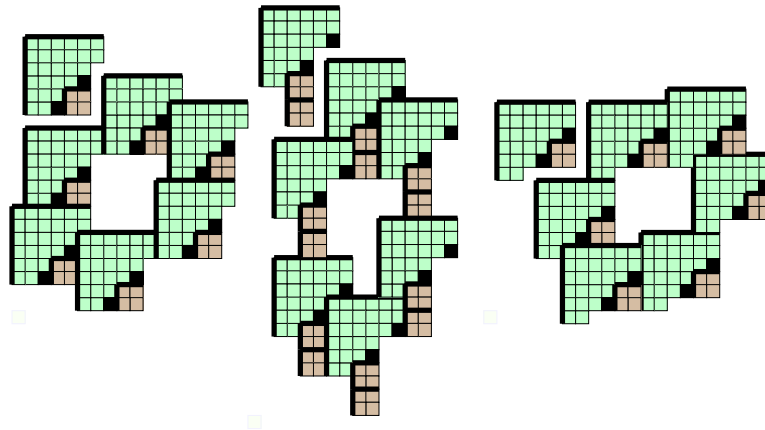


Figure 1.16: Left and Right: the two enantiomers of the T5 tile. Center: The T5 can combine with two T1's to produce a hexagonal lattice with a larger unit cell than T5 and T1 alone. Only one of the two enantiomers of the central figure is shown, since the other would never emerge from a Rule 110 evolution.

1.4.7 T6 mosaic

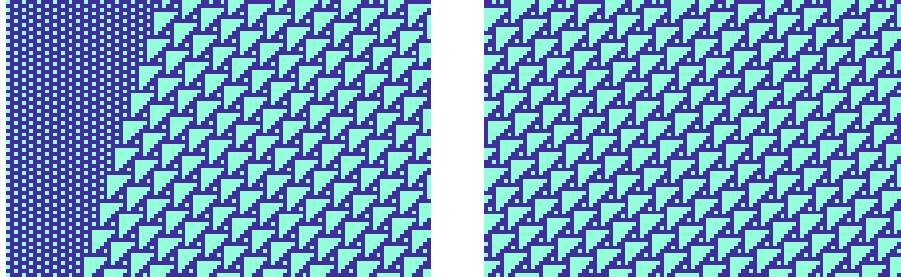


Figure 1.17: Examples of the occurrence of T6 mosaics in the evolution of Rule 110. These designs arise from shift-periodic evolution as detected by the de Bruijn diagram.

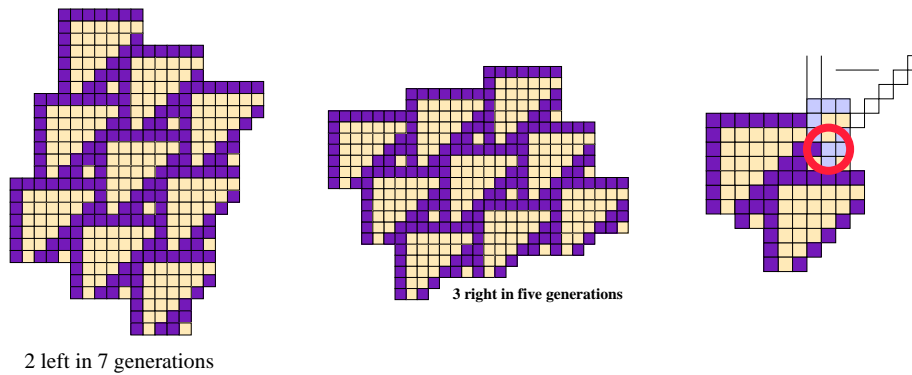


Figure 1.18: The two asymmetric enantiomers of the T6 mosaic. In principle, the T6's could be stacked diagonally, filling the gaps symmetrically with T1's. The T6's group naturally into a hexagonal superlattice. But the layout on the right shows that there is no way to fill the plane without conflicting with Rule 110's requirement that the sequence 111 evolve into 0. Only T1's can nestle against the T6, but whatever is placed above the T1 necessitates a second T1, violating the prohibition against abutting top edges.

1.5 General properties of Rule 110

Running a survey on Rule 110 won't produce much that is really new, but it should fill in some details, and illuminate the results which have already been reported.

1.5.1 interpretation of graphs

The main thing in working with a graph (meaning, digraph, since the distinction is important in this application) is that its loops may be isolated, connected in one direction but not the other, or mutually connected.

With respect to a de Bruijn diagram, the first alternative would mean that there is a simple pattern, persistent or shifting as the case may be, but essentially unique, not admitting any variation. For example, superluminal patterns generally have this form since causality is not operating.

The unilateral connections correspond to fuses, which is an irreversible change of pattern which may be either static or shifting. Many configurations for Rule 110 have this form, including most of the "speed zero" shifts, and in particular the C gliders, which can abut on uniform quiescence, or vacuum. But shift 2 in five generations has a different kind of split field — T1's on the left giving way to a mixture of T3's and T1's on the right, along a right-moving interface. And of course, we have already seen an almost identical combination in Figure 1.14.

Gliders depend on there being a loop generating the "ether" which has another connection to itself constituting the "glider." The ether loop could be an autolink to the quiescent state, but things are different in Rule 110. There might possibly be several handles, signifying distinct forms of gliders or different phases in the evolution of a single glider, all moving at the same velocity.

You can't tell the ether from the glider without a program; this is evident when looking at the A gliders, for example. T1's can intersperse T3's to get the A gliders, but lots of T1's can harbor an occasional T3 for a role reversal. Of course, the T3's figure in lots of other configurations, so it is reasonable to assign them to the ether.

A still more complicated combination has the glider off in a loop of its own, but still having mutual connections to the ether loop. That is the arrangement with respect to the extensible gliders, and can be used to determine admissible spacings, closest approaches, and so on. And it is a property of regular expressions, that if the glider is once extensible, it is multiply extensible.

Once someone is familiar with these ideas, it doesn't really require constructing de Bruijn diagrams to take advantage of the information; however it should make it less surprising when these relationships are observed in practice.

1.5.2 the de Bruijn diagrams

Underlying the existence of the tiling is the fact that Rule 110 has semipermeable membranes. That is just a fancy way of saying that the sequence $x10$ always generates 1 (almost always - the "semi" comes from $111 \rightarrow 0$); more pertinent is that $x10^n$ generates $10^{(n-1)}$ which is another way of characterizing the triangles. Membranes are traceable to configurations in the de Bruijn diagram. It remains to be seen how directly this membrane affects the analysis of Rule 110, even though it is an integral part of the characterization of Rule 110 by tiling.

The reason for mentioning this is that it has been known that some rules have membranes bounding macrocells, within which evolution has to seek a cycle. But not all membranes are permanent, leading to the conjecture that their dissolution might be programmed. This is an idea which has probably never been followed up, but Rule 110 may actually be an instance which fits the pattern, since the evolution depends to a certain extent on the persistence of the left margin of the triangles, and the way in which it eventually breaks up.

In honor of the role of C gliders in Cook's introduction, the dimensions of the arrays in `NXLCAU21` was raised to accommodate seven generations, with the result that they are described in a diagram of 556 nodes and 705 links. It is large for the multiplicity of ways the ether background can join to the T6's which in turn join to ether or vanish. To better manage the diagram, the self-node to the quiescent state can be excised, leaving a diagram of 502 nodes and 632 links; although only a 10% reduction, it takes away lots of stray lines from a map which is still extremely congested.

Table 1.2 summarizes the statistics on all the de Bruijn diagrams up to and including seven generations. The first row of each pair states the number of nodes, the second row, the number of links. When the two numbers coincide the diagram consists exclusively of loops, but not necessarily one single loop. Since zero is a quiescent state, entries of the form (1,1) indicate that it is the only configuration meeting the shifting requirement. In particular, there are no still lifes (except for zero).

The columns follow the degree of shifting, the remainder, pairs of rows, goes by generation.

| | -7 | -6 | -5 | -4 | -3 | -2 | -1 | 0 | 1 | 2 | 3 | 4 | 5 | 6 | 7 |
|--|-----|-----|-----|-----|----|-----|-----|-----|---|-----|----|-----|----|----|-----|
| | 85 | 46 | 26 | 15 | 9 | 5 | 1 | 1 | 1 | 5 | 10 | 19 | 34 | 60 | 106 |
| | 85 | 46 | 26 | 15 | 9 | 5 | 1 | 1 | 1 | 5 | 10 | 19 | 34 | 60 | 106 |
| | 42 | 31 | 22 | 19 | 10 | 1 | 1 | 9 | 1 | 9 | 15 | 5 | 33 | 24 | 90 |
| | 42 | 31 | 22 | 19 | 10 | 1 | 1 | 11 | 1 | 9 | 15 | 5 | 33 | 24 | 90 |
| | 75 | 23 | 38 | 19 | 1 | 5 | 9 | 19 | 1 | 27 | 22 | 37 | 42 | 5 | 134 |
| | 75 | 23 | 38 | 19 | 1 | 5 | 9 | 22 | 1 | 35 | 22 | 37 | 42 | 5 | 134 |
| | 42 | 68 | 26 | 13 | 1 | 41 | 15 | 17 | 1 | 1 | 10 | 13 | 26 | 47 | 109 |
| | 42 | 68 | 26 | 13 | 1 | 49 | 15 | 19 | 1 | 1 | 10 | 13 | 26 | 47 | 109 |
| | 110 | 19 | 1 | 23 | 10 | 58 | 1 | 86 | 9 | 116 | 42 | 38 | 66 | 14 | 161 |
| | 110 | 19 | 1 | 23 | 10 | 63 | 1 | 102 | 9 | 142 | 42 | 38 | 66 | 14 | 161 |
| | 85 | 31 | 94 | 99 | 1 | 27 | 100 | 57 | 1 | 15 | 1 | 126 | 26 | 48 | 85 |
| | 85 | 31 | 100 | 111 | 1 | 27 | 112 | 62 | 1 | 15 | 1 | 164 | 26 | 48 | 85 |
| | 14 | 219 | 9 | 129 | 1 | 266 | 1 | 556 | 1 | 5 | 18 | 1 | 69 | 5 | 169 |
| | 14 | 239 | 9 | 136 | 1 | 287 | 1 | 705 | 1 | 5 | 18 | 1 | 69 | 5 | 169 |

Table 1.2: The number of nodes (upper number) and links (lower number) in the de Bruijn shift diagrams up to and including seven generations.

Points of interest in the table, actually some of Cook's gliders, are the entries at (2,3) [A-gliders], at (-2,4) [B-gliders], and at (0,7) [C-gliders]. [The symbol (x,y) indicates a shift of x, negative to the left, in y generations].

Previously unreported gliders can be found at (2,5), (-1,6), and (-4,6). The (2,5) glider had already been observed in Cook's extensible gliders, but none of the three

connects directly to Cook's ether.

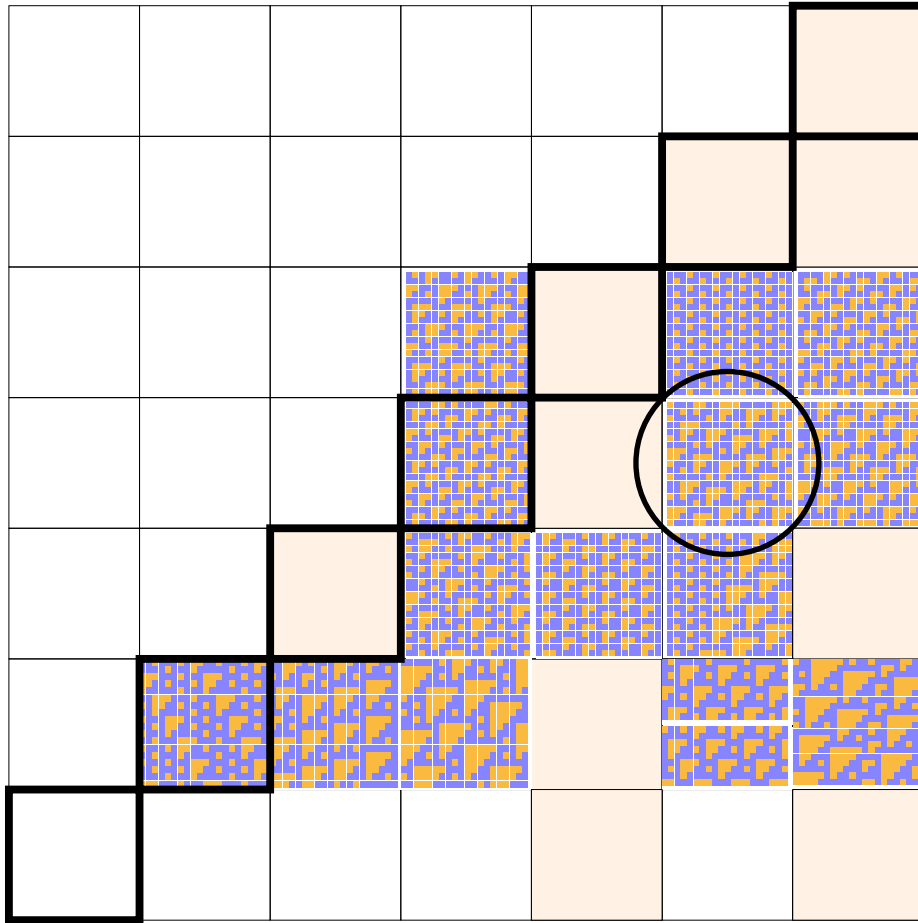


Figure 1.19: Inventory of left shifting configurations. The quiescent configuration is an implicit component of every other shift; sometimes it is the only one. Otherwise it is not shown. When there are still more components, the panel is split into horizontal slices to accommodate them.

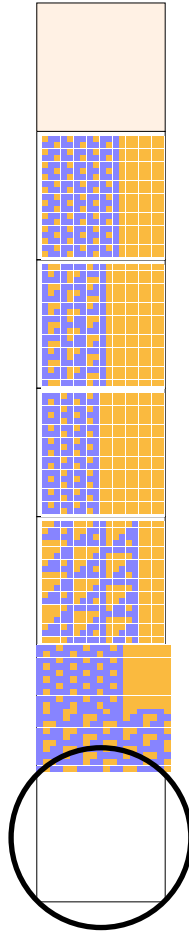


Figure 1.20: Periodic configurations. The quiescent configuration is an implicit component of every other shift; sometimes it is the only one. Otherwise it is not shown. When there are still more components, the panel is split into horizontal slices to accommodate them. That is not the same as a one-sided ideal, in which one single panel divides into two distinctive regions along a vertical fissure.

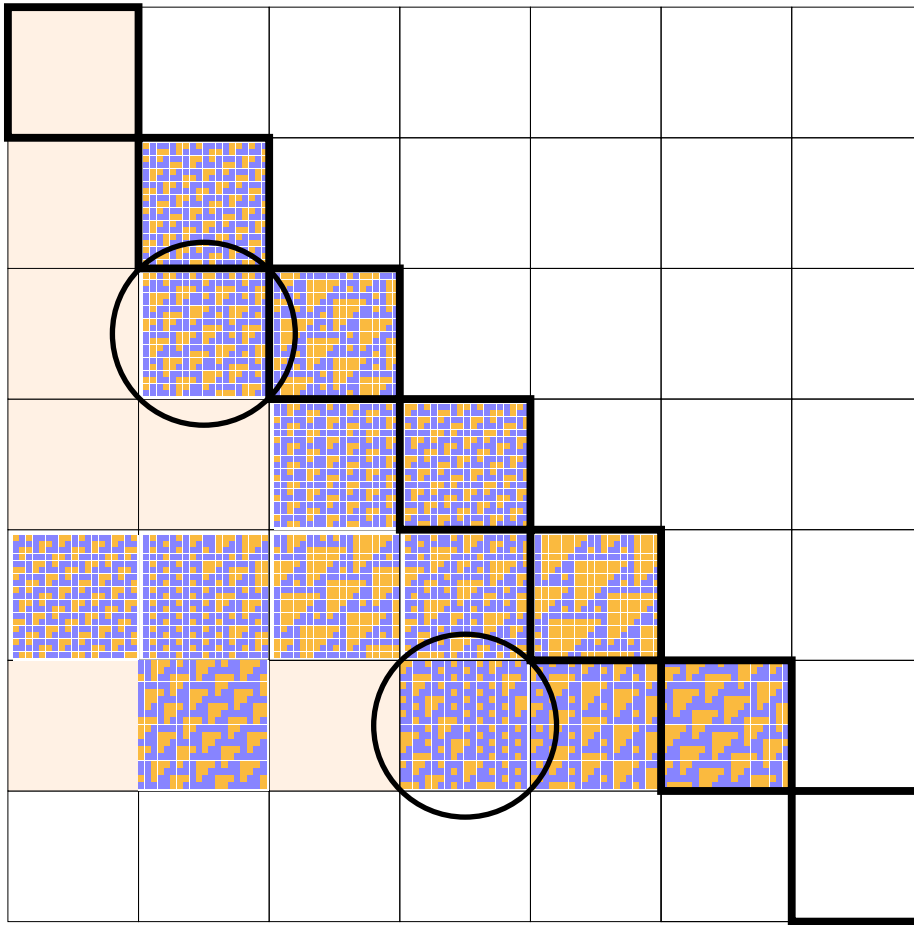


Figure 1.21: Inventory of right shifting configurations. The horizontal coordinate determines the shift, the vertical coordinate the number of generations which have elapsed. The quiescent configuration is an implicit component of every other shift; sometimes it is the only one. Otherwise it is not shown.

| Shift | nodes | links | cycles | comments |
|---------|-------|-------|----------------|--|
| left 8 | 93 | 93 | 1, 4, 8, 90 | |
| left 7 | 56 | 56 | 1, 55 | |
| left 6 | 35 | 35 | 1, 34 | |
| left 5 | 182 | 193 | 2 components | Zero, and two big crosslinked cycles involving T7's. The interlinking makes for two packings, so a glider pairing could be imagined, as in some of the combinations seen previously. |
| left 4 | 381 | 447 | doubled B's | The velocity is the same as for B gliders, with double the time available to complete the shift. The (-2)/4 B configuration must be a subset; it is an absorbing ideal paired with a T5 combination in an emitting ideal. This is a fuse, not gliders, and the figures move parallel to one another. |
| left 3 | 10 | 10 | 1, 9 | |
| left 2 | 37 | 37 | 1, 2x7, 22 | |
| left 1 | 38 | 38 | 1, 37 | |
| static | 41 | 43 | 2 components | T1 emitting ideal connects to zero as an absorbing ideal in a diagram with 33 nodes, 35 links. An independent cycle length 8 contains a T2 mosaic. |
| right 1 | 22 | 22 | 1, 21 | |
| right 2 | 1 | 1 | 1 | |
| right 3 | 1 | 1 | 1 | |
| right 4 | 145 | 153 | 4 components | 1) Quiescent zero configuration 2) T5's over T1's, in 2 phases 3) T1 emitting ideal connects to 4 different absorbing ideals, phases of T3's over T1's, which might be seen as some staggered B gliders. |
| right 5 | 208 | 208 | 1, 2x7, 193 | |
| right 6 | 152 | 152 | various hashes | |
| right 7 | 301 | 301 | several | a variety of cycles, some of them rather pretty. |
| right 8 | 13 | 13 | 1, 4, 8 | |

Table 1.3: The number of nodes and links in the de Bruijn shift diagrams for eight generations.

| Shift | nodes | links | cycles | comments |
|--------|-------|-------|-----------------|---|
| left 9 | 10 | 10 | 1, 9 | Zero, T2's stacked vertically |
| left 8 | 57 | 57 | 1, 4x14 | This combination is important because it is one of the two in the ninth generation in which the crystallography of the ether tiles allows gliders. We see the zero configuration and four of spatial period (cycle) 14, of which one is the ether lattice and the other three phases of a salvo of fat A gliders with seven T1's, even though they conform to a left-moving displacement criterion. Since only the one combination is allowed and there are no alternatives, this mixture might not be a glider even though it has the appearance of one. |
| left 7 | 1 | 1 | 1 | only the quiescent configuration |
| left 6 | 59 | 59 | 1, 3x12, 3x6, 4 | |
| left 5 | 26 | 26 | 1, 25 | |
| left 4 | 216 | 225 | fuse | 4-high A's defer to diagonally stacked T8's. |
| left 3 | 9 | 9 | 1, 8 | |
| left 2 | 370 | 406 | 1, fuse | Zero, and a component in which T1's form the emitting ideal, a combination of T8, T3, and 3 T1's repeat to constitute the absorbing ideal. |
| left 1 | 587 | 666 | 1, mixed | A combination of T8, T3, and two T1's reminiscent of the C glider; they can waver in their vertical alignment in a way which could be construed as forming a glider family. |

Table 1.4: The number of nodes and links in the de Bruijn left shift diagrams for nine generations.

| Shift | nodes | links | cycles | comments |
|---------|-------|-------|--------------|---|
| static | 689 | 771 | big diagram | Includes the T2 emitter, Zero absorber visible in the third generation as one component, There is also a glider bombardment of a T5 wall, and the T5 wall as a source of B glider salvos which annihilate an oncoming A salvo. This is a “black hole” configuration which often forms from two oppositely directed shift configurations. The T5’s form an absorbing ideal which contains <i>one</i> of the two allotropic forms of the gliders previously found in the “four left in six generations” analysis. |
| right 1 | 1 | 1 | 1 | |
| right 2 | 5 | 5 | 1, 4 | |
| right 3 | 1 | 1 | 1 | |
| right 4 | 1 | 1 | 1 | |
| right 5 | 34 | 34 | 1, 8, 25 | |
| right 6 | 604 | 784 | 1, A’s | Zero, all kinds of A’s but nothing evident which was not already visible with the “2 left every 3” row, so there are neither double nor triple A-bar’s. This is the other shift combination for which the ether lattice could have had ninth generation gliders. |
| right 7 | 125 | 125 | 1, 124 | |
| right 8 | 51 | 51 | 1, 50 | |
| right 9 | 94 | 94 | 1, 9, 21, 63 | |

Table 1.5: The number of nodes and links in the de Bruijn static and right shift diagrams for nine generations.

1.5.3 cycle, or basin, diagrams

Continuing the listing of de Bruijn diagrams by looking at cycle diagrams doesn't turn up much beyond what is already in Wuensche and Lesser's Atlas [11]; in fact after increasing the arrays in LCAU they now cover the same range.

| p/c | 1 | 2 | 3 | 4 | 5 | 6 | 7 | 8 | 9 | 10 | 11 | 12 | 13 | 14 | 15 | 16 |
|-----|---|---|---|---|---|---|---|---|---|----|----|----|----|----|----|----|
| 1 | 1 | 1 | 1 | 1 | 1 | 1 | 1 | 1 | 1 | 1 | 1 | 1 | 1 | 1 | 1 | 1 |
| 2 | . | . | . | 2 | . | . | . | 2 | . | . | . | 2 | . | . | . | 2 |
| 3 | x | . | . | . | . | . | . | . | 3 | . | . | . | . | . | . | . |
| 4 | x | . | . | . | . | . | . | . | . | . | . | . | . | . | . | . |
| 5 | x | x | . | . | . | . | . | . | . | 3 | . | . | . | . | . | . |
| 6 | x | x | . | . | . | . | . | . | . | . | . | . | . | . | . | . |
| 7 | x | x | . | . | . | . | . | . | 9 | . | 11 | . | . | . | . | 2 |
| 8 | x | x | . | . | . | . | . | 1 | . | . | . | . | . | . | . | . |
| 9 | x | x | x | . | . | 2 | . | . | . | . | . | 6 | . | . | . | . |
| 10 | x | x | x | . | . | . | . | . | . | . | . | . | . | . | . | . |
| 11 | x | x | x | . | . | . | . | . | . | . | . | . | . | . | . | . |
| 12 | x | x | x | . | . | . | . | . | . | . | . | . | . | 7 | . | . |
| 13 | x | x | x | . | . | . | . | . | . | . | . | . | . | . | . | . |
| 14 | x | x | x | . | . | . | 1 | . | . | . | . | . | . | 1 | . | . |
| 15 | x | x | x | . | . | . | . | . | . | 2 | . | . | . | . | . | . |
| 16 | x | x | x | . | . | . | . | 2 | . | . | . | . | . | . | . | 2 |

Table 1.6: Number of configurations of given cycle and period.

The x's in Table 1.6 mark unavailable periods, but the limit to the lengths of periods increases exponentially leaving little point to trying to incorporate this detail into the table. Equally, there is an exponential limit to the lengths of prime cycles running across columns, to be noted alongside the fact that multiples of periods are periods.

| cycle | period | multiplicity |
|-------|--------|--------------|
| 10 | 25 | 2 |
| 11 | 110 | 1 |
| 12 | 18 | 2 |
| 13 | 351 | 1 |
| 14 | 21 | 2 |
| 14 | 91 | 2 |
| 15 | 295 | 3 |
| 16 | 24 | 6 |
| 16 | 32 | 3 |

Table 1.7: Long periods up to cycle length 16.

Amongst these first sixteen cycle lengths are some which have periods too long for inclusion in Table 1.6; they are listed in Table 1.7.

But in both the de Bruijn diagrams and the basin diagrams there is an interesting item of note, the short height of the basin of attraction for the quiescent state (0, that

is), which doesn't pass 9 and is frequently shorter.

The basin diagram for zeroes is cumulative, since anything which evolves to zero stays zero. But since a line of ones is the only alternative, it is interesting to see what produces ones for each ring circumference. That is where the small height is noticeable.

| cycle | mass | max height |
|-------|------|------------|
| 2 | 4 | 2 |
| 3 | 8 | 3 |
| 4 | 4 | 2 |
| 5 | 32 | 5 |
| 6 | 10 | 3 |
| 7 | 9 | 2 |
| 8 | 20 | 3 |
| 9 | 17 | 3 |
| 10 | 134 | 9 |
| 11 | 35 | 3 |
| 12 | 34 | 3 |
| 13 | 54 | 3 |
| 14 | 67 | 3 |
| 15 | 113 | 5 |

Table 1.8: summary of the structure of the cycle diagrams for evolution to the constant value 0.

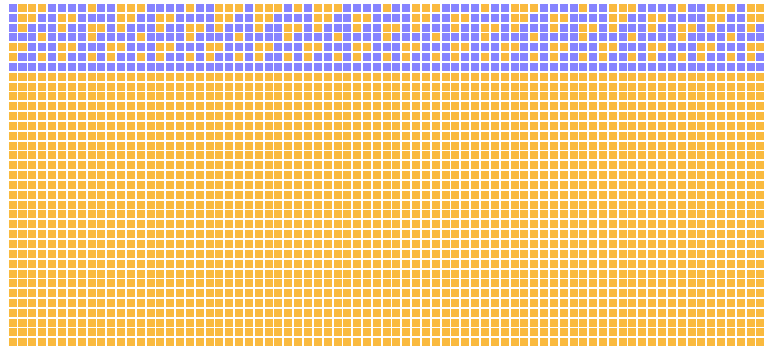
Note that cycles of length 10 seem to be favored. That also shows up in the de Bruijn diagrams for evolution to the constant value 1:

| generation | nodes | links | comment |
|------------|-------|-------|--|
| 2 | 3 | 4 | 2-cycle fused with 3-cycle |
| 3 | 7 | 8 | 3-cycle having common vertex with 5-cycle |
| 4 | 16 | 18 | 2 5-cycles, one way connection in 2 places |
| 5 | 33 | 38 | cycles 5-5-13 all interlinked |
| 6 | 10 | 10 | single cycle length 10 |
| 7 | 32 | 34 | 10-cycle intercommunicates with another |
| 8 | 38 | 40 | 2 10-cycles attached to a 20-cycle |
| 9 | 81 | 90 | several interlinked cycles |
| 10 | 0 | 0 | empty diagram |

Table 1.9: summary of the structure of the de Bruijn diagrams for evolution to the constant value 1.

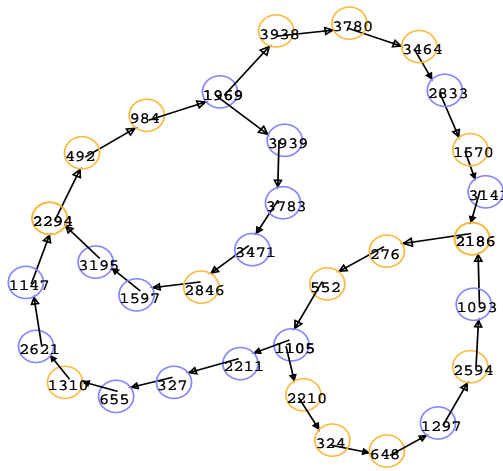
Upon further analysis it appears that the largest triangle which can possibly emerge from the evolutionary process is T42. Of course, larger triangles could be specified as part of an initial configuration, but otherwise they belong to a multiple generation Garden of Eden. Even so, the level ten de Bruijn diagram for evolution to 1 shows that up to ten generations, triangles of any size can be prearranged. The interest in the synthesis of T23 lies in the fact that, as a result of a composite glider collision of a D, a C2, and a packet of four B's, there is no limit to the delay that could be incurred

while waiting for one of them to appear.



evolving to 1 in 6 gen

110



evolving to 1 in 6 generations

Rule 110

December 11, 1998

Figure 1.22: The de Bruijn diagram for evolution to the constant 1 after six generations.

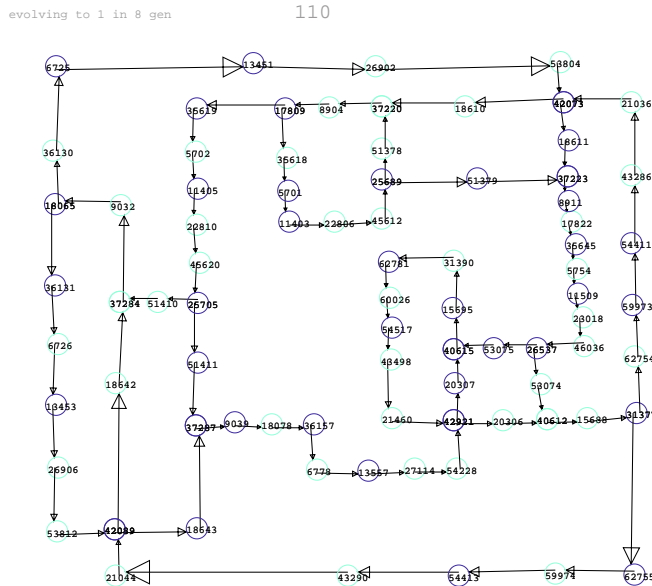


Figure 1.23: The de Bruijn diagram for evolution to the constant 1 after eight generations.

The de Bruijn diagram for evolution to the constant value 1 in nine generations is empty, which simply means that the diagram is acyclic, and its nucleus is empty. The full, unlabelled de Bruijn diagram has a quarter million nodes with half a million links. Approximately half of these evolve to a single 1, of which another half can join with another link to produce a pair of 1's. Actually the percentage remains as high as a half but briefly, drops down to the order of ten percent, and continues to diminish. Altogether, a dozen or two chains remain, overlapping to a degree, with a length of 44 1's.

Since the resultant figure is acyclic, and there are two less 0's in the next generation than there were 1's in the current generation, T42 is the largest emergent tile. Of course, the initial configuration could have arbitrarily long strings of zeroes, whose remnants would still be encountered until the left expansivity of the right margin closed them off.

Except for the fact that the de Bruijn diagram is already quite large, graphs for additional generations could be examined to see whether the necessarily acyclic graphs would have even shorter transients, thereby limiting still further the maximum size of emergent tiles. Working from the opposite direction, finding initial conditions such as the proper positioning of gliders for a future collision, would establish lower limits to the size of emergent tiles.

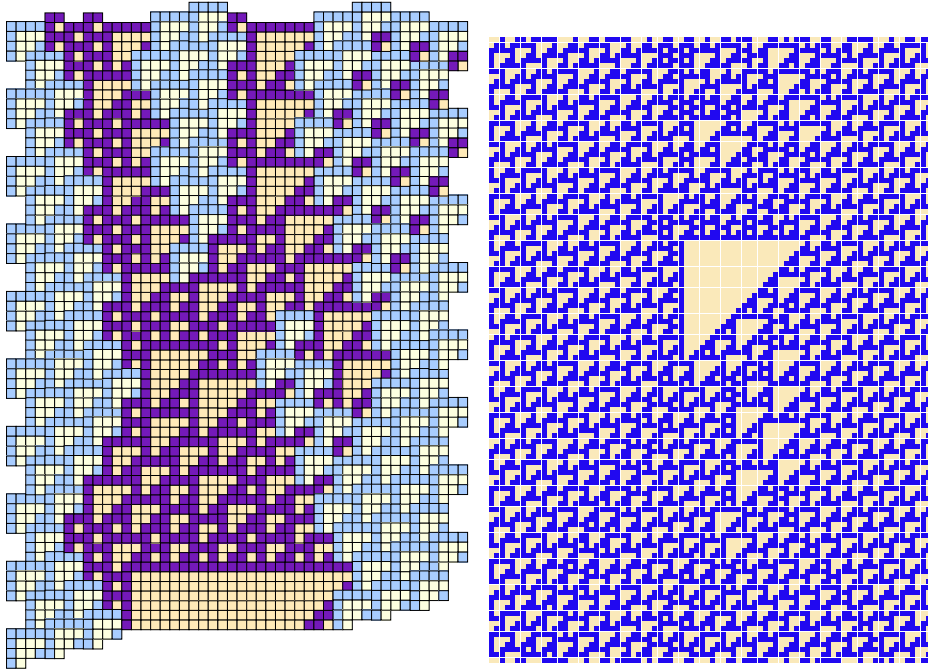
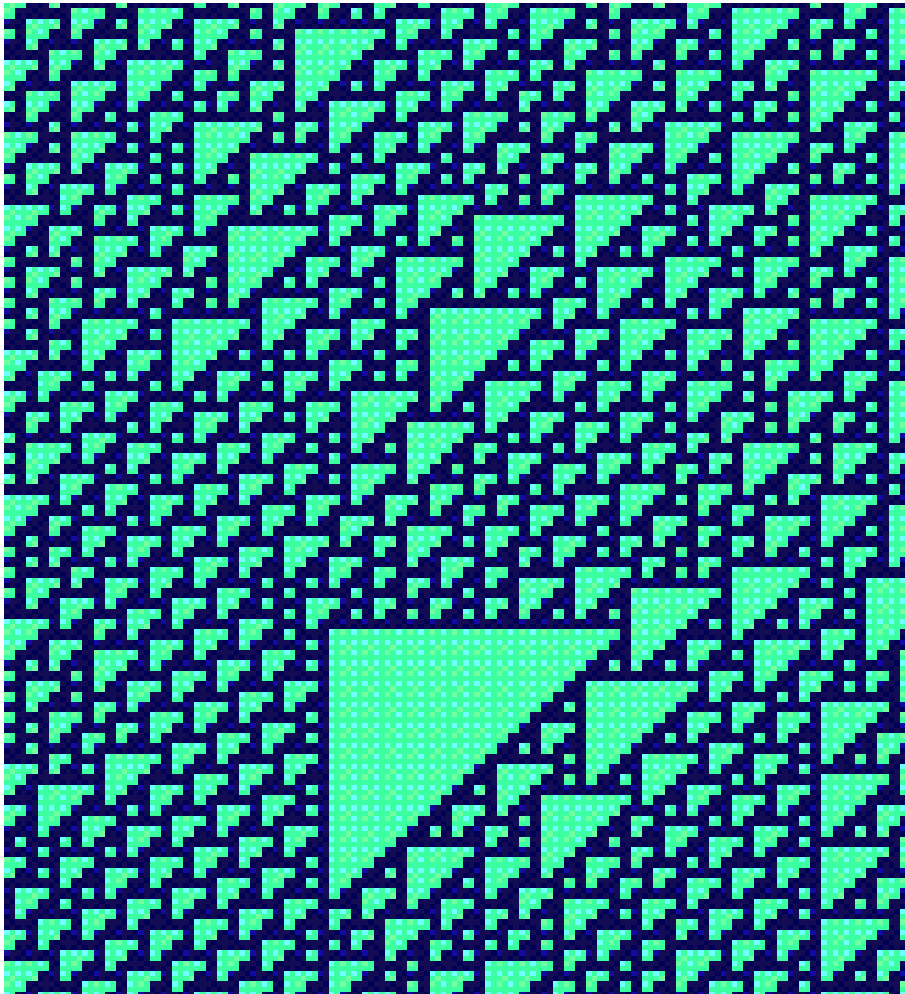


Figure 1.24: One of the largest triangles whose emergence has been observed is the T23. Left: construction by electronic quadrille paper. Right: verification by computer simulation.



decomposition product in a (7 right in 6 generations) lattice

T26

May 30, 2000

Figure 1.25: Large triangles are correspondingly rare, but many of them can be found by systematic search. Some are collision products, which means that they can be formed at arbitrary late times. Others are decomposition products in lattice interfaces, while still others just appear, without having any clear origin.

1.5.4 ancestors and symbolic de Bruijn matrices

By de Bruijn matrix we understand the connectivity matrix of the de Bruijn diagram. Actually there are several de Bruijn matrices according to whether the diagram is labelled or not, and to whether it is taken as a numerical matrix or a symbolic matrix. Accordingly, the A matrix is the part of the de Bruijn matrix labelled according to evolution bearing the label 0, just as the B matrix goes with the label 1. In the case of Rule 110, these matrices are:

$$\begin{array}{c} \text{A matrix} \qquad \qquad \text{B matrix} \\ \hline \begin{bmatrix} 1 & 0 & 0 & 0 \\ 0 & 0 & 0 & 0 \\ 1 & 0 & 0 & 0 \\ 0 & 0 & 0 & 1 \end{bmatrix} \quad \begin{bmatrix} 0 & 1 & 0 & 0 \\ 0 & 0 & 1 & 1 \\ 0 & 1 & 0 & 0 \\ 0 & 0 & 1 & 0 \end{bmatrix} \end{array}.$$

As we see, the A matrix is idempotent, largest eigenvalue 1, and just three nonzero elements, two of which are diagonal ($00 \rightarrow 00$ and $11 \rightarrow 11$) with the other one at $10 \rightarrow 00$ which is only operative in non-cyclic contexts. That means, the only way to get zeroes is to have zeroes, let a solid string of ones evolve into zero, or to have 1 as a left fence without worrying what lies beyond (lots more 1's, for example).

The largest eigenvalue of B is a little larger than 1.32, just less than $\sqrt{2}$, The number of ancestors of a line of ones doubles by adding between 2 and 3 new cells.

The matrices AB and BA are nilpotent, so that there is no point trying to develop long sequences in which 0's and 1's alternate. So much so that 01010 turns out to be the shortest excluded sequence. Following the same route, the regular expression 00^*100^*10 corresponding to a pair of isolated 1's, is also ancestorless, as are numerous other sequences.

With a view toward understanding the occurrence of large triangles, consider powers of the matrix B , which should converge towards the product of its Perron eigenvectors. Its 14^{th} power, as shown in the table below, has the convenient number of 200 ancestors, readily permitting the approximate factorization also shown there.

$$\begin{array}{c} B^{14} \qquad \qquad \text{factored, normalized} \\ \hline \begin{bmatrix} 0 & 16 & 21 & 12 \\ 0 & 21 & 28 & 16 \\ 0 & 16 & 21 & 12 \\ 0 & 12 & 16 & 9 \end{bmatrix} \quad \begin{bmatrix} 0.25 \\ 0.30 \\ 0.25 \\ 0.20 \end{bmatrix} \quad [0.00 \quad 0.30 \quad 0.45 \quad 0.25]. \end{array}$$

The one really clear conclusion is that 00 can never be the trailing edge of an ancestor of a string of 1's. The remaining possibilities are fairly evenly distributed, with a slight preference for beginning 01 and ending 10, and a significantly slimmer chance (1/3 less, roughly) of being surrounded by 11's.

The mixture does not change appreciably between even and odd chains, as would be expected from the uniqueness of the Perron eigenvalue. If the second eigenvalue had been large, an alternation of generations might have been observable in short chains.

1.5.5 subset diagram

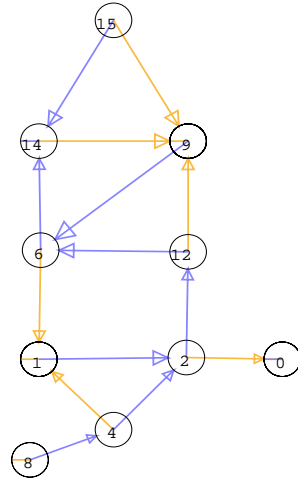
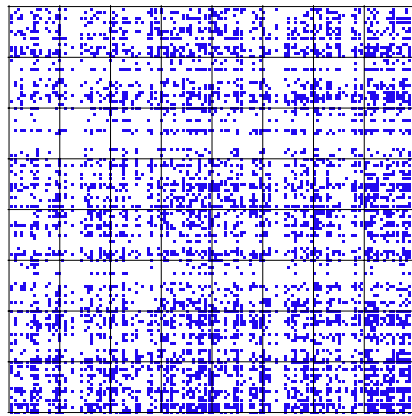


Figure 1.26: Subset diagram for Rule 110. The shortest excluded word is 01010.

There is other information; for example the shortest poison word seems to be 01010, as can be seen by consulting the subset diagram shown in Figure 1.26.

1.5.6 plaid diagram



Rule 110

Figure 1.27: Excluded words are responsible for the plaid diagram's woven texture.

The same information shows up in the plaid diagram. A plaid diagram is obtained by first selecting an origin for a configuration. The sequence of cell states, assuming

they are represented by integers modulo k , the number of states, is then regarded as a k nary number lying in the interval $0 - 1$, which is considered to be the x -coordinate of a point. The same process is applied to the portion of the configuration lying to the left of the origin, except that it is read backwards from the origin, and used as the y -coordinate of a point.

The plaid diagram is made by tracing the trajectories of several initial configurations for a number of generations. Garden of Eden configurations will have a low density because they can only be found at the beginning of a trajectory; their absence will show up as blank strips. Recall that any sequence which begins or ends with an excluded string is also excluded, which gives width to the strips. .

1.5.7 mean field probability

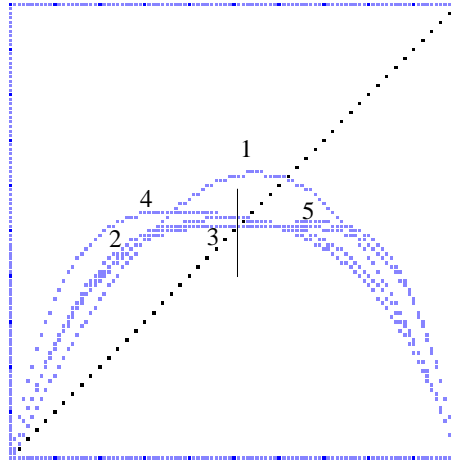


Figure 1.28: Mean field probability distributions for the first five generations of evolution of Rule 110. The uniform 50% distribution tends toward superstability.

As Figure 1.28 shows, the distribution of cell states for Rule 110 tends quickly toward 50%, even though the a priori estimate favors 1's, and any strict alternation of 0's and 1's is ruled out. Note that the curves shown in the diagram are rigorously calculated mean field probabilities for successive composites, or generations of evolution, but that they tend to behave as iterates would.

Although they don't adhere to the first generation fixed point, they tend toward a superstable fixed point at 50%, while the fixed point at zero becomes ever more unstable.

1.5.8 two block probability

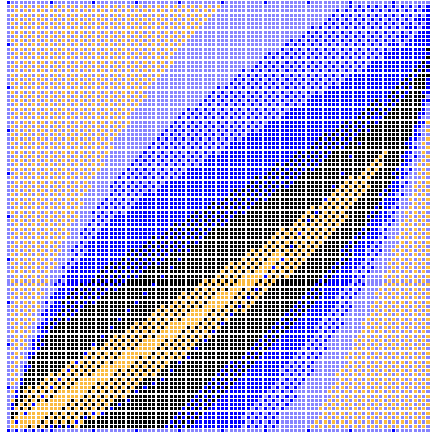


Figure 1.29: Two-block probabilities, showing a linear (rather than quadratic) relation valid at low densities, slope $1/2$, holding over an extensive range.

In the contour map of pair probabilities, shown in Figure 1.29, single 1's, whose frequency forms the horizontal coordinate, tend to occur with double the frequency of pairs of 1's, whose frequency defines the vertical coordinate. That would indicate that the 1's are more likely to form blocks than to be isolated, a predilection compatible with the scarcity of sequences in which 0's and 1's alternate.

1.6 Evolutionary generalities

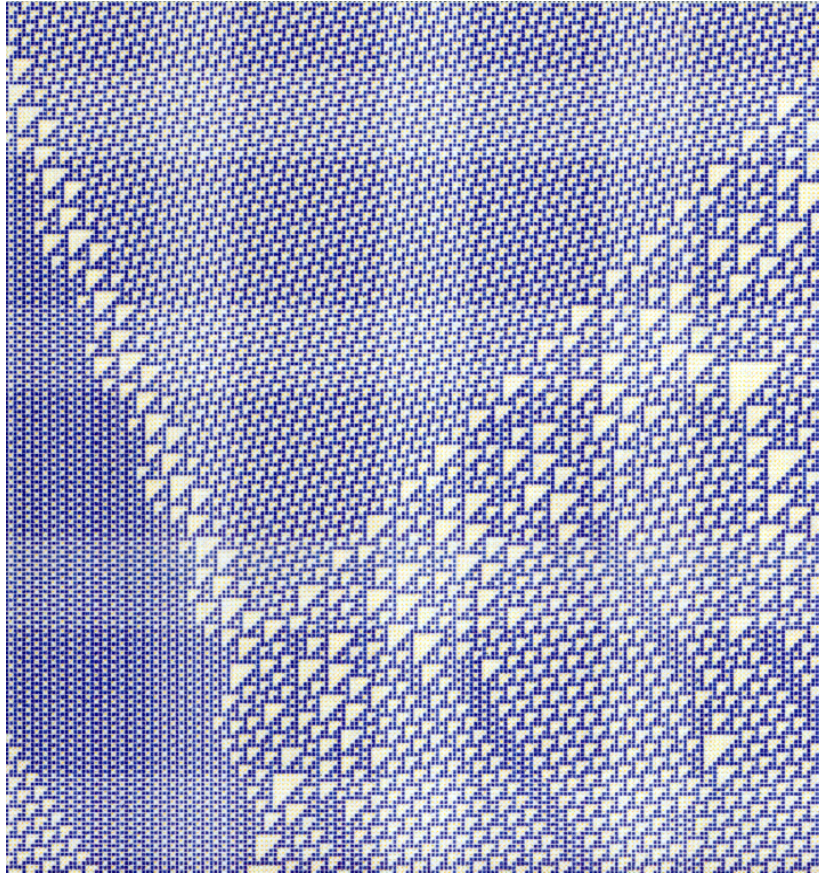
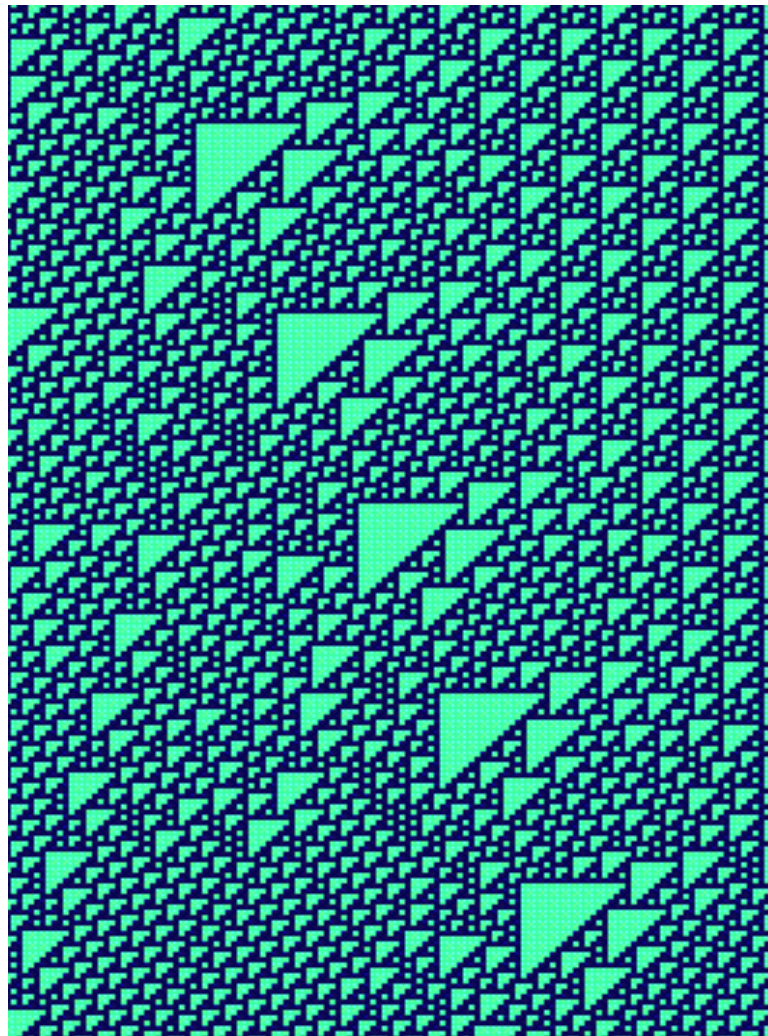


Figure 1.30: A T2 lattice is subject to erosion on both edges. Depending on how the erosion is initiated, and the format of the surrounding environment, periodic interfaces will develop. Here, a T2 lattice decays asymmetrically. To the left, a T1 lattice forms, separated from T2 by a reasonably thin interface; in its turn the T1 merges into the ether. On the right the decay takes longer, is more complicated, and establishes itself after a transient which is still not finished in a hundred generations or two. It remains to be seen whether the D which has formed will be stable under the repeated A salvos, whose existence has stabilized towards the bottom of the figure.



t18 boundary

May 30, 2000

Figure 1.31: A more complicated decay example in which T18's recur periodically in the decay of the left margin of a "shift right seven in six generations" lattice. The T18's themselves shift right fourteen every thirty six generations, which is commensurable with the decaying lattice. They are just barely shadowed by the left spine of the T18 and the T3 (which could be bigger, but can't be smaller, which is all that matters) sitting immediately under it.

Chapter 2

The Gliders

2.1 Gliders not using the ether tile

Since the ether is composed of T3 tiles stacked according to one of the two phases by which they can cover the plane, it might be tempting to call just any T3 an ether tile. To avoid such quibbles, a T3 is an ether tile only if it is part of an assemblage of T3's, especially when providing background.

By this interpretation, T3's may form part of composite tiles, and may have other tiles attached to them, without being ether. On the other hand, many interesting configurations exploit the versatility of considering boundary T3's as sometimes belonging to the ether and sometimes not.

A survey of all the de Bruijn diagrams for shifts through six generations not only revealed three of Cook's gliders, but also three more combinations interpretable as gliders against a background other than the ether. Continuing the survey for additional generations would undoubtedly reveal still more gliders, including the ones which have already been found via search programs.

2.1.1 two right in five generations

Amongst the gliders so far discovered, there seems to be a preference for leftward motion, with only A and D gliders running to the right. However, an additional one, which might be called an alpha glider, was discovered among the de Bruijn diagrams. Once their discovery was made, they were found to be an essential element in the formation of Cook's extensible E and G gliders; others seem to have been aware of their existence, such as their mention by Li and Nordahl [4].

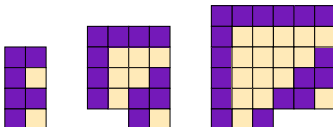


Figure 2.1: There are three species of composite tile from which gliders of velocity $2/5$ c arise.

If the T1's are used, they extend inexorably to the left. On the other hand, the other two can be mixed at will, so that either can be a glider against a background formed by the other. As a philosophical point in glider theory, it should be recognized that a structure is best regarded as a glider when it stands out against a background, thereby supposing a thin glider with fat background.

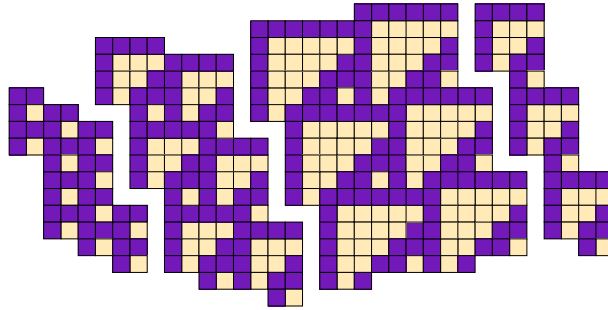


Figure 2.2: Reading left to right, the T1 tiles can be repeated until they meet a T3, following which T3's and T5's may repeat or alternate arbitrarily.

The T3's aren't ether tiles because the T1 is always stuck on to them. But they can readily join up with other T3's, especially in the form of glider collisions. However, the relative positioning of the T1 appendage differs between B gliders and E gliders. In the same spirit, a crosscurrent of B gliders can be seen in a thick layer of the second species, running between source and sink T5's.

Once the de Bruijn diagram for a shift-generation combination is available, the relationships between the different structures visible in the field of evolution is greatly clarified. Of course, it can turn out that the de Bruijn diagram itself defies comprehension, as the number of vertices and links increases with the number of generations.

Figure 2.3 shows the de Bruijn diagram for the α gliders. To begin with, the vertex of ten zeroes is self-linked and isolated from all other vertices. That is the quiescent configuration, which would have any shifting characteristic unimaginable. If it is isolated, then any other pattern must extend to infinity, but if there are interconnections, there may be regions of activity separated by quiescent regions, or there may be quiescent half-spaces. "Islands of chaos in seas of tranquility" was Wolfram's poetic description of Class IV behavior.

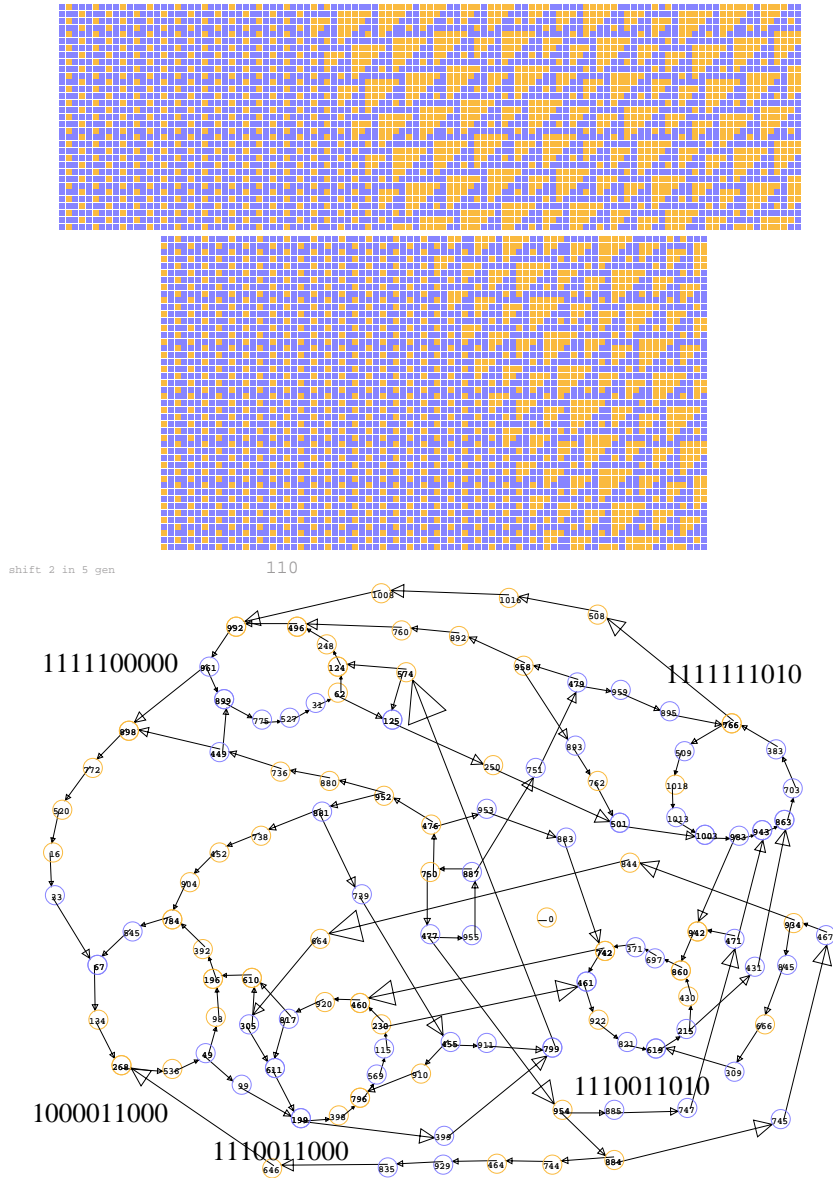


Figure 2.3: The de Bruijn diagram provides the only satisfactory description of the interrelation between the three α species. The cycles of length 10 are the five phases of where T5's and T3's alternate. However there are also domains of pure T1-T5 "squares" and domains of pure B gliders.

Zero need not be the only absorbing component or emitting component, as the loop of length 4 in this diagram shows. As an emitting component, it defines left-hand behavior which, once discontinued, can never resume. The strict loop generates the T1 tiling, the first of the three species of gliders. There are five loops of length ten. If any one of them is followed out, it will be seen to comprise a slice through one T3, one T5, and a T1 nestled between them. It is no one single species, but a mixture having cycle ten and period five; however that turns out to be one of the primitive loops - loops of shortest length in virtue of having no shorter subloop.

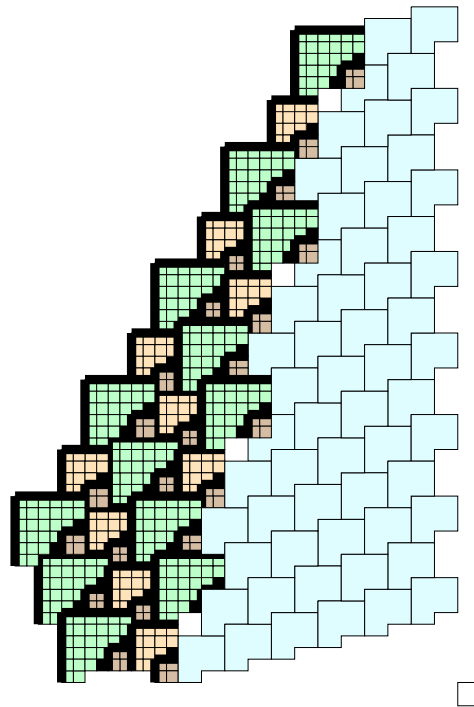


Figure 2.4: Detail of the interface between a sublattice of alpha glider symmetry and the ether lattice. Notice how the location of the marginal T1's should be adjusted to ensure continuity along the interface..

The five loops are not really independent, since they correspond to the five different phases of evolution followed by a cyclic repetition of any one of them. Of course the number of loops could be a divisor of the period of the diagram; but since 5 is prime that could be only 1 or 5, but 1 would mean the strict shift of a sequence unchanging from generation to generation.

One lesson to be learned is that there is not necessarily a strict correspondence between prime loops in the de Bruijn diagram and species of glider.

A detail concerning the alpha lattice which is important for the construction of gliders, but which will not show up until one examined the shift symmetry left four in fifteen generations, is the fact that there are sublattices compatible with the ether lattice.

2.1.2 four left in six generations

There are two more glider situations in the sixth generation. Both are based on the T5 triangle as a base piece, but since its use with the two gliders are diagonal reflections of one another, there probably isn't a clear coexistence situation in which one can overtake the other and produce nice simple collisions. That's something that still has to be tried, however.

In the first combination, there is a shift of four cells after six generations. The two different tiles needed to make up two species are are:

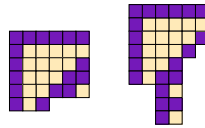


Figure 2.5: One species moves 4 left every six generations against a background generated by the other.

To tile the plane and thus construct an evolution, make diagonals from either tile:

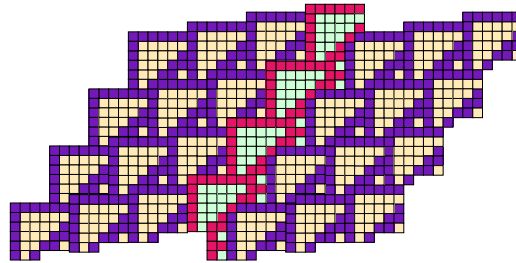


Figure 2.6: The second species is the glider, moving against a background established by the first.

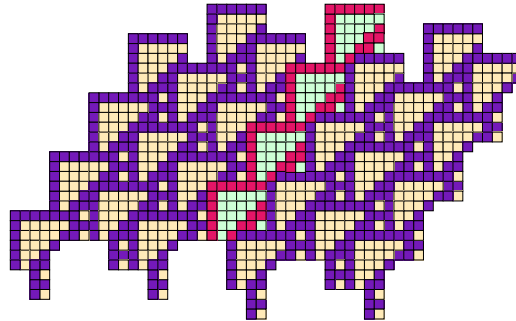


Figure 2.7: The first species is the glider, moving against a background established by the second.

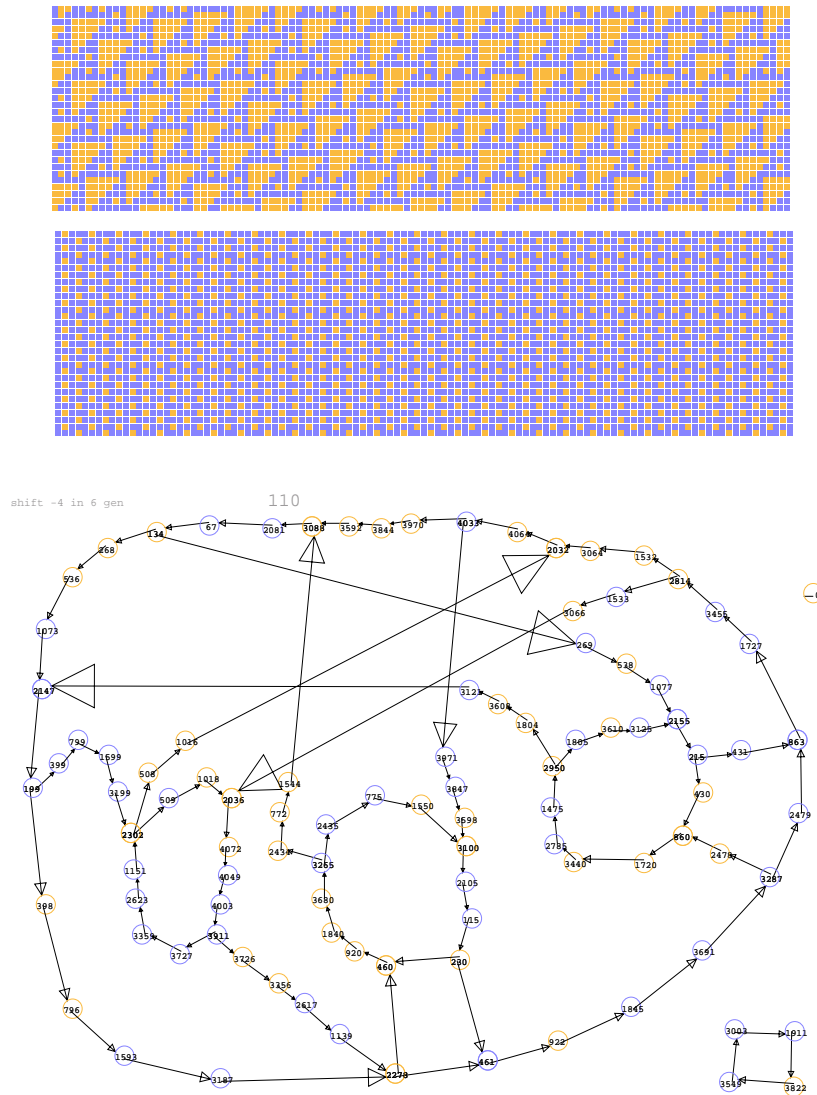


Figure 2.8: The de Bruijn diagram for shifting four cells left in six generations shows the ways in which one of the species can move within a background generated by the other, and all the combinations in between. The diagram has three connected components, one of which is the field of zeroes, meaning that designs belonging to one of them cannot mix with designs belonging to the other. On the other hand, the large component contains several cycles, transitions between which will result in intermingling their patterns.

2.1.3 one left in six generations

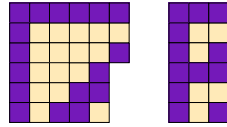


Figure 2.9: One species moves one left every six generations against a background generated by the other. They are based on the same tiles that figure in the α lattice.

To tile the plane and thus construct an evolution, make diagonals from either tile:

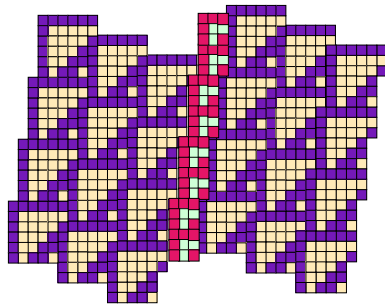


Figure 2.10: The second species is the glider, moving against a background established by the first.

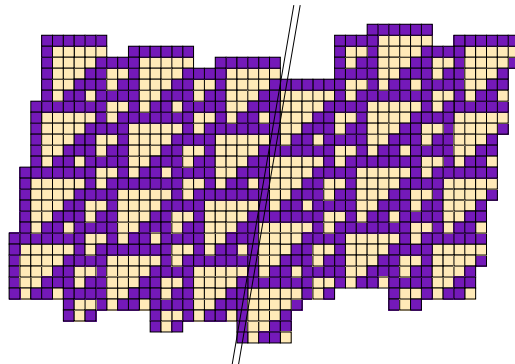


Figure 2.11: The first species is the glider, moving against a background established by the second.

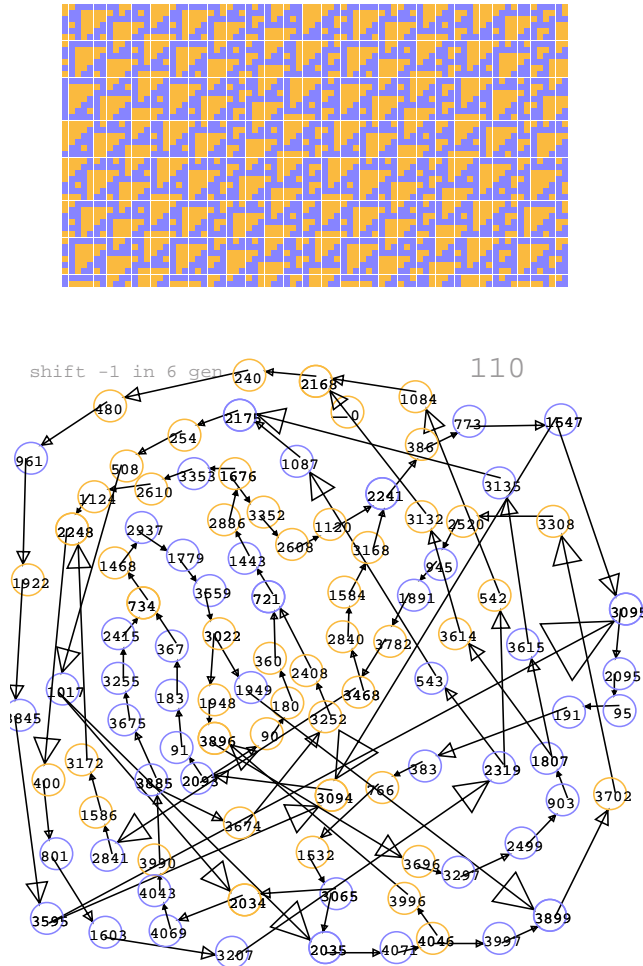


Figure 2.12: Shift periodicity of one left every six generations. Two motifs can be recognized; one moves against a background provided by the other.

Neither this collection nor the one with a shift 2 every five generations is as elegant as the collection which Cook and Lind have shown; nevertheless under some stretch of the imagination or other, these objects do qualify as gliders, giving both new families, and families using different arrangements of tiles than those previously seen.

It is interesting to speculate why the T3 ether fits in with so many other gliders. As we have seen, there are two different T3 packings, one of which lends itself to dislocations (or gliders) and another which does not. Also, if this is going to fit into a Class IV framework, it would be interesting to see how it jibes with mean field theory.

There the criterion was a superstable quiescent state and a superneutral other density. The ether should take the place of the superstable state, which is vaguely accommodated by what appears by such a state at 50% density. It is something to check more closely. Anyway, you do want a tenacious background. As for superneutrality,

that allows a variety of forms to coexist without worrying too much about their exact density.

This is reminiscent of Eigen's Hypercycles, and is probably no more scientific than the reading of tea leaves. As to the question of why other Rules don't show gliders and all, the only readily available comparison is with Rule 22, where they are not in evidence.

This pretty much completes the survey of shifts up through generation 7. There were about as many fuses as gliders, including the property of C gliders that they can just stop at the zero configuration. What might have been expected to be an interesting doubling of the A gliders apparently isn't, although the diagram is much more complicated due to having to describe everything in terms of much longer neighborhoods. Tripling seems to give the B-bar's alongside the B's, although that would need twelve generations - unrealistic - to check and be sure, and the marginally accessible doubling in eight apparently hasn't resulted in anything which has already been observed, dilligent search presumably having been made.

2.2 Cook's A-gliders, with forward velocity $2c/3$

This data is interesting for what it implies about the origins of large triangles, the prime tiles for tiling the plane according to Rule 110. One thing is that when the triangle is big enough, it has a fringe of T1's, T2's and T3's on top. Empirically, large triangles seem to occur - T12's can be seen without trying hard - but the clusters of triangles appearing in the gliders which have been so far reported never seem to be very big.

2.2.1 tiling approach

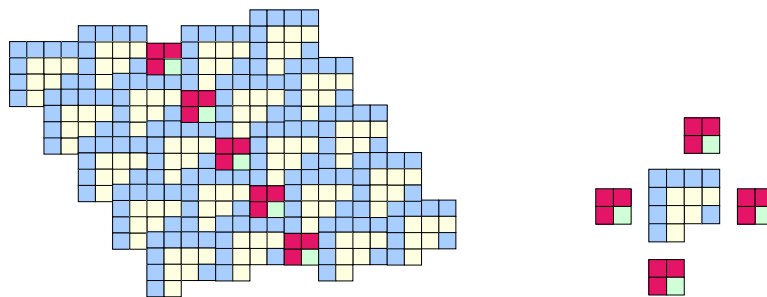


Figure 2.13: T1 based gliders, showing the four ways that they may seem to be attached to the ether tile. Strings of T1's running diagonally downwards are quite conspicuous, and a very common form of glider.

The evolution of random configurations according to Rule 110, especially when viewed under good conditions of scale and coloring, eventually run to a preponderance of the ether tiles, crisscrossed by trajectories which have been called gliders. The smallest, fastest, and most common of these are the A and B gliders, no doubt the reason that they were assigned the first letters of the alphabet. A gliders run right, B gliders run to the left, and both are dislocations in the etheric background caused by T1 tiles.

Speculation as to why the ether is made from T3 tiles and the gliders from T1 should probably start by realizing that the field will not be quiescent because of the left expansivity of the rule. This characteristic keeps zero density of cells in state 1 from being a stable fixed point in the return map of mean field theory; the favored density is somewhat beyond 50%.

Neither is the T1 mosaic favored; its 75% density is larger than the 63% a priori estimate taken from the rule and the mean field fixed point, and in fact higher composites of Rule 110 favor 50% as a superstable fixed point. T3 mosaics come closer to meeting the density requirements, but mesh nicely with T1's to create gliders.

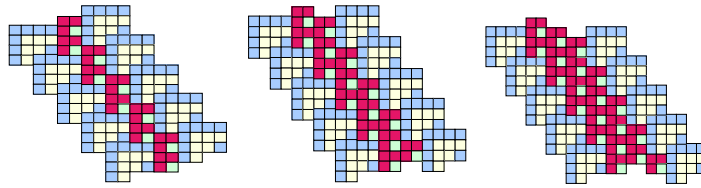


Figure 2.14: Thicker gliders with two, three, and four diagonals of T1's.

thicker A gliders

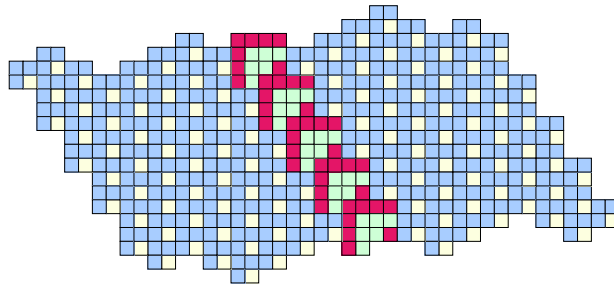


Figure 2.15: Turn about is fair play. T3's can appear to be gliders when displayed against a T1 background.

2.2.2 de Bruijn approach

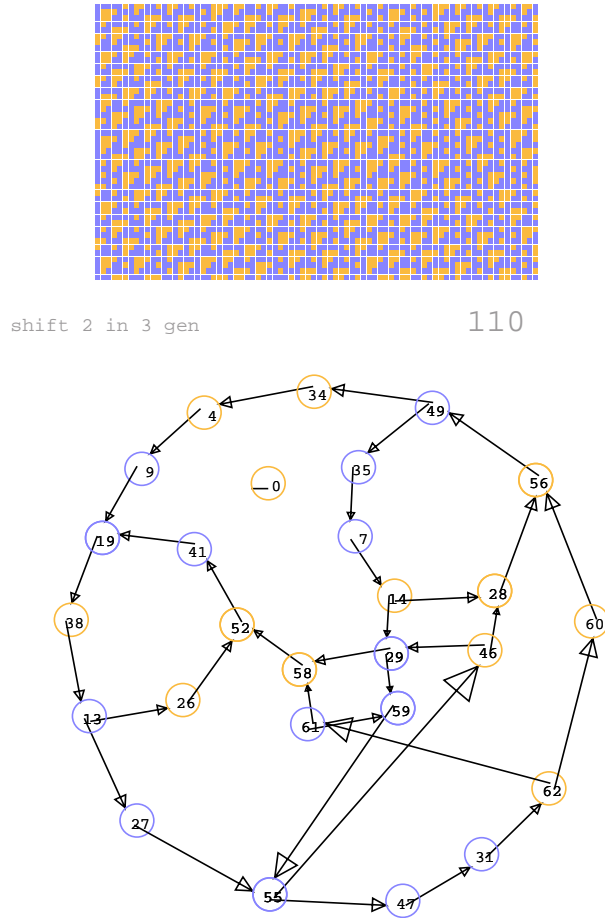


Figure 2.16: Cook's A-gliders and the de Bruijn diagram from which they may be derived. The outer periphery corresponds to the period-7, cycle 14 period rectangle of the ether tiles. If T3's and T1's alternate, there are three phases each of which has a cycle of length of 6. Also, if pure T1's run in succession, there is a loop of length 4 which will generate them. Other mixtures correspond to other paths through the diagram.

2.2.3 non-existence of (4,6) A-bar gliders

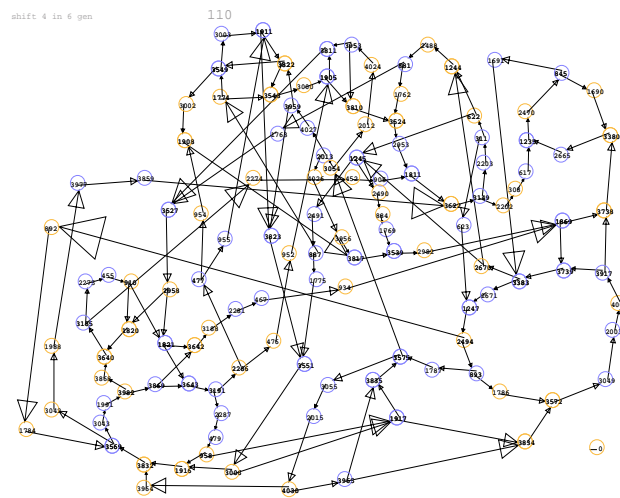
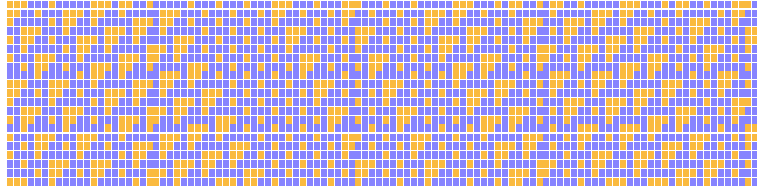


Figure 2.17: The only (4,6) gliders seem to be those already implicit at (2,3): the A-gliders.

2.3 Cook's B-gliders, with backward velocity $-c/2$

Using the second tile gives the illusion of a glider moving against a background generated by the first tile. Using several of the second gives the illusion of a whole fleet of gliders.

Now, the other possibility is where the glider appears to move left just by a single cell every six generations. Once again we need a T5 tile, but with the T1 stuck on a little differently. but the buffer column can be optionally inserted. Again that can be seen as a single glider, but repeating the process produces a fleet.

Their usage is that ether's or B's give way to a left margin, which can be followed by as many interiors as desired, terminated by one of the two right margins, followed once again by ether's or B-bar's.

2.3.1 tiling approach to the B gliders at -2 in 4 generations

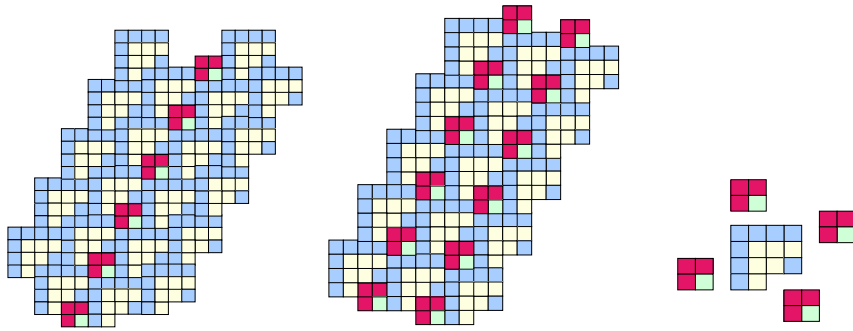


Figure 2.18: T1 based gliders. However, T1 tiles cannot be juxtaposed as they can in the A gliders.

2.3.2 de Bruijn approach to the B gliders

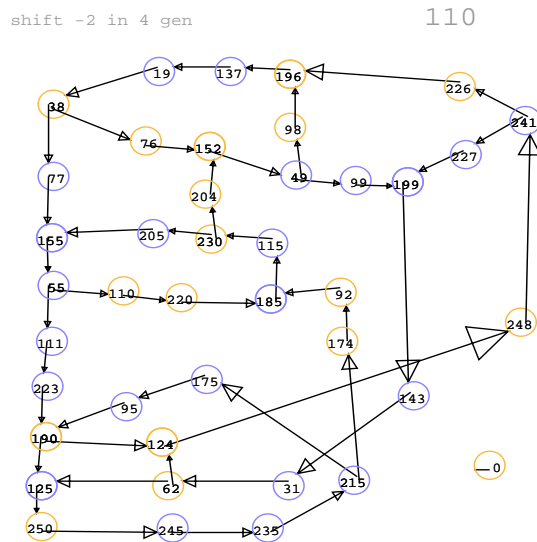
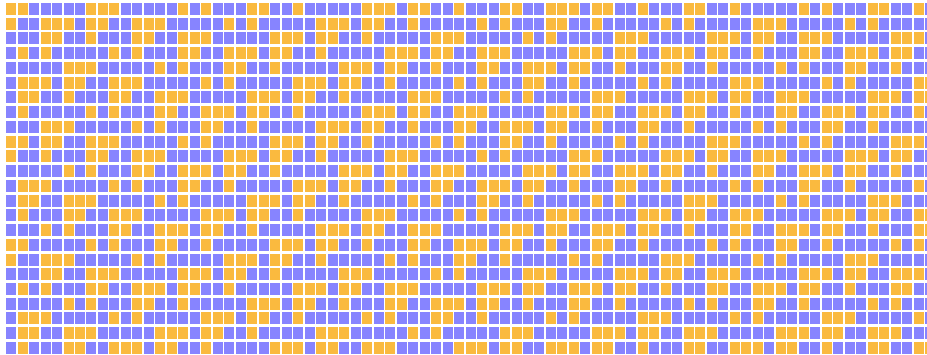


Figure 2.19: Cook's B-gliders and the de Bruijn diagram from which they may be derived. The outer periphery corresponds to the period-7, cycle 14 period rectangle of the ether tiles. If T3's and T1's alternate, there are four phases each of which has a cycle length of 8.

2.3.3 tiling by B-bar gliders at -6 in 12 generations

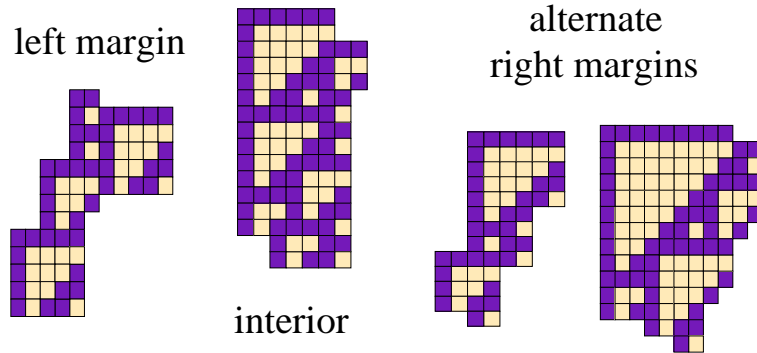


Figure 2.20: B-bar gliders have the same velocity as B gliders, but take three times as long to develop their cycle; however the two types, B and B-bar, may coexist.

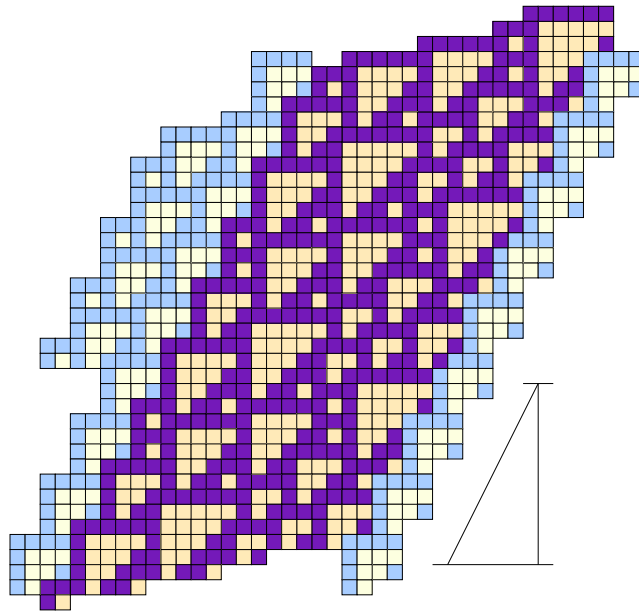


Figure 2.21: B-bar gliders can have varying widths and one or the other of two optional right margins. At least one midsection must be included.

2.4 Cook's C gliders, static with velocity 0

The C gliders don't glide, but that is a technicality; a limiting case.

2.4.1 tiling approach

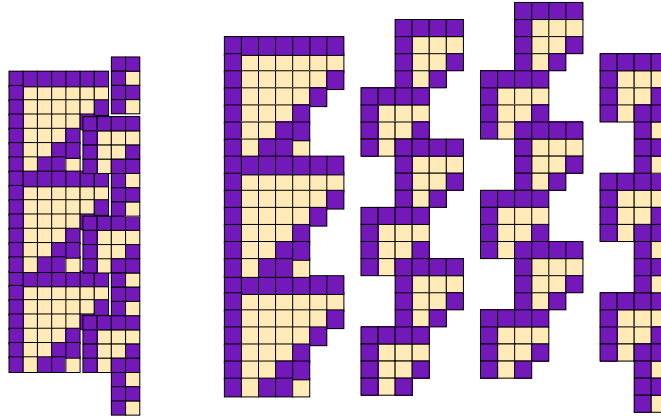


Figure 2.22: T6 based gliders, C in Cook's nomenclature, which actually don't move.

The C gliders are based on T6 tiles, which must be supplemented if they are to fill up the plane. Placing a T1 just under the diagonal at bottom left creates a niche for a T3 just to its right, but which is better kept separate.

Thus the first tile is the combined T1 and T6, which has a height of seven cells. The second tile has two T3's, one above and slightly to the right of the other, for a combined height of eight cells. But this pair can be stacked in a vertical column by aligning the top row of the bottom tile with the bottom row of the lower tile, once again an effective height of seven.

Another combination with a height of seven and stackable in a vertical column compatible with either of the first two tiles, is the third tile shown at the far right in Figure 2.22. It is built from a stack of two T1's nestled under a T3, whose staggered four-three left margin is congruent to the margin in the T3 stack.

The T6ish tiles have a left margin which is a vertical spine – a column of 1's which extends indefinitely, which is just the left margin of a whimsical T_∞ . Meanwhile the third tile, featuring T1's, has a similar right margin. As a result, T6's which have been connected to none or more T3's can reconnect to another T6 to create an environment in which T6's and T3's alternate; or they can connect to a zero half-space, from which there is no return. In other words, a static fuse can exist.

Figure 2.23 summarizes the sequences which can be formed, all of period 7. The columnar form of some of the margins is to be noted; it is related to the ability to interface with a half-space of zeroes, and on a more modest scale, with any large triangle..

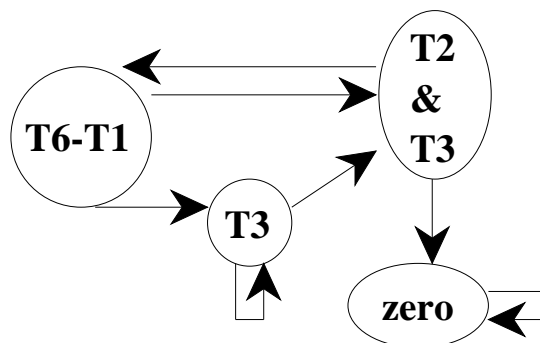


Figure 2.23: Sequence diagram for the tiles in C gliders.

2.4.2 de Bruijn approach

C gliders can occupy a split configuration space, in which the right half is the quiescent zero. That makes the zero vertex an absorbing ideal in the de Bruijn diagram, with its 556 vertices and 705 links. This huge population congests the diagram beyond what will fit nicely on a letter sized page, but removing the zero vertex and all the transients thereby created only reduces the load by about 10%, to 502 nodes and 632 links. No improvement is to be disparaged, however.

The main thing is that the C's pack densely, just like sardines. Basically they are T6's, but a T3 and 3 T1's can be nestled in to get a columnar arrangement of cycle 9. As remarked in Cook's Rule 110 document, there are three different membrane-shift points allowing vertical displacement between successive vertical columns.

As a result the de Bruijn diagram has some cycle-9 loops, although not all of them have been spotted yet. But given that there are seven distinct rows in a C, there ought to be seven of these loops visible in the diagram, the more so because this seems to be the shortest loop present.

There ought to be seven cycle-14 loops as well, containing the unit cells of the pure ether, but they haven't been located, either. On the other hand, since all the nodes have been positioned by hand, it seems certain that the diagram consists of a single component. That does not exclude something communicating just with the zero ideal but not with the nucleus shown in Figure 2.24.

On the other hand, there are readily visible cycles of length 11 sharing part of their arc with cycles of length 20, and there is also a loop of length 17.

What is happening is similar to the layout already apparent for the A and B gliders. Namely, there are some composites which have a shorter cycle length than the full periodicity of the raw ether. The A diagram, for example has a long loop of length 14 which can be taken as the circumference of a big circle, within which there are shorter loops, possibly sharing circumference, which correspond to ether-glider

doublets. There is even a short cycle, sharing circumference with others, generating the T1 lattice of “pure glider.”

In the case of the C's, examination of the cycles shows that they correspond to polymers. This isn't like trees, for which there are polar coordinates and a rather satisfactory diagram can be generated automatically. No doubt, given the interest there is in drawing graphs, there are more suitable programs available, but they haven't been used in this presentation.

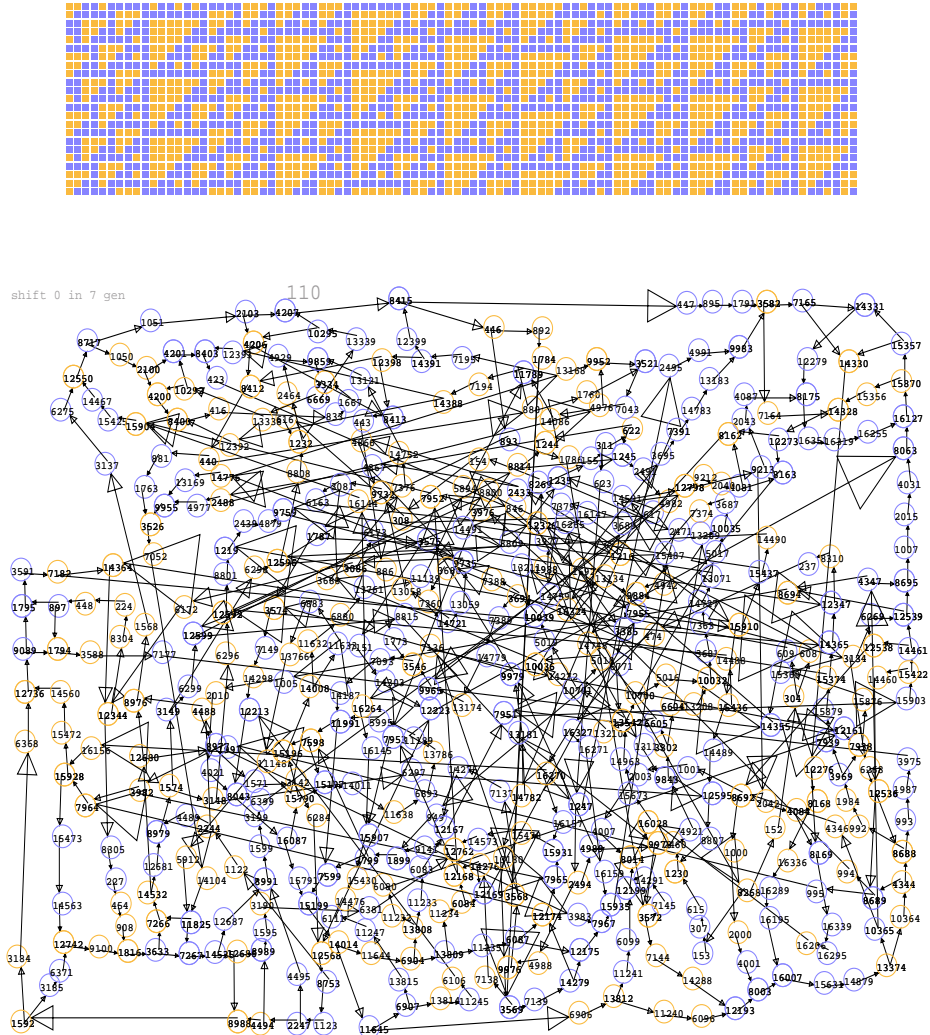


Figure 2.24: Cook's C-gliders and the de Bruijn diagram from which they may be derived. [Zero removed]

2.5 Cook's D-gliders, forward velocity $c/5$

It has been asserted that there are only two D-gliders, running right two every ten generations, and that they are the only right-running gliders besides the family of A's, which run two cells right in three generations, making them about a third as fast as the A's. Note that listing the velocity as $c/5$ is a reduction to lowest terms of the actual relation, which is to advance two cells in ten generations. The only configuration which meets the one-in-five requirement is the alpha phase of the T2's, as seen in Figure 1.9.

Defining the width of a glider has its interesting points. Lind apparently took the cycle-14, period-7 character of the ether for granted, exhibiting an appropriate interlude to define the members of his list. That works well enough except for the E, where 00000 doesn't make a clean insertion. In all the other cases there is varying amounts of slack which often gets taken up by additional ether tiles (taking as ether the 4x4 T3 with a notch cut from the lower right corner). But if you don't do it his way, you can run into phase relationships which have to be explained.

Just gathering up the minimal unit which repeats, supposing that all the ether continuations are implicitly and uniquely defined, The two D-tiles differ quite subtly, the principal difference being where to position the T1 at the upper left of the first tile. As Cook remarks, there is a discrepancy of two or three little dots now and then distinguishing the two gliders.

From diagram experience, these tiles come from loops (several, in fact, if the lines of successive generations are not cyclic permutations of one another) and the ether tile is lurking in there somewhere, either as a loop or in the linkage between the other loops. Well, tile juggling shows that the D1's and D2's can be juxtaposed in any combination at will and separable when desired minimally by an ether strand which can be interpreted as a jittering (D1 to D1) or intermittent (D2 to D2) glider! Or, of course, something even thicker.

Which goes to confirm that the definition of a glider is rather subjective; it depends on which of several tiles is in the minority, generally a strong minority, with respect to the others.

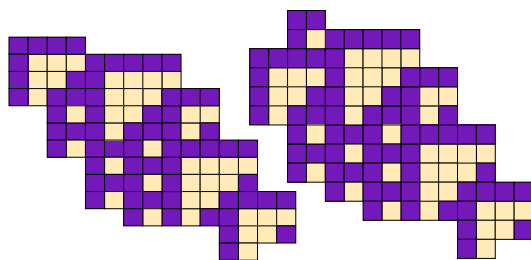


Figure 2.25: T4 based D gliders, which move slowly right. The one on the left is D2, on the right is a D1.

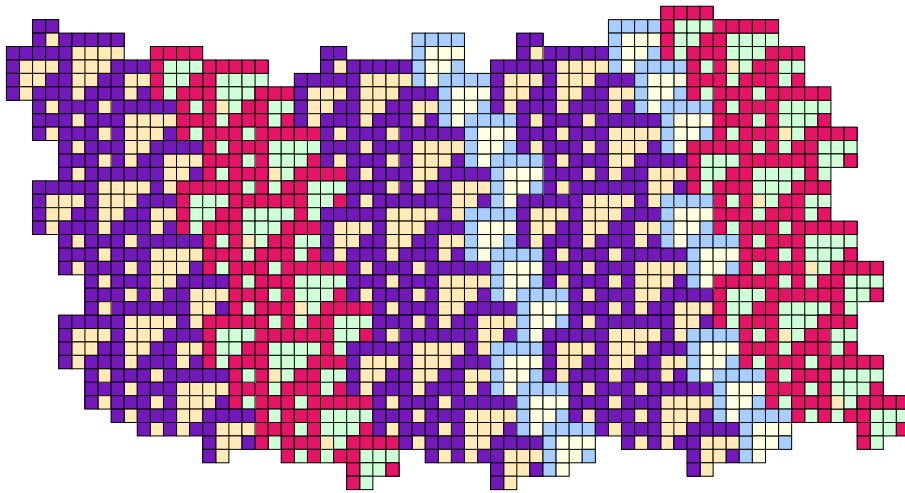


Figure 2.26: There are two kinds of D gliders, each slightly different.

2.6 Cook's E-gliders, velocity $-4c/15$ ($\approx -c/4$)

Going on to the strict E gliders, but still not attempting the E-bar, The E itself is a fairly complex aggregate incorporating a T8, a T5, two T2's, and seven T1's:

2.6.1 tiling approach to $-4/15$ gliders

Although some overlapping of corner pixels is required, the extension can be run out to the right as far as desired. The next course, nestled beneath them, will give the illusion of T5's and T3's gliding off to the right and downwards, at the velocity of two right every five generations. The E's run 4 left every fifteen generations; as Cook remarked, Lind apparently misjudged the velocity of the E2. What is moving at which velocity is something of a subjective judgement; of course the slopes in the evolution diagram are well defined, but the subjectivity lies in whether to call something a glider or not.

The extension tiles can be continued with other tiles of the same velocity. Consistency fixes the lengths of successive rows; all combinations are not possible, and there is apparently no going back to extension tiles without encountering another E base first. So the E is accompanied by a fleet of extensions giving way to the ether again.

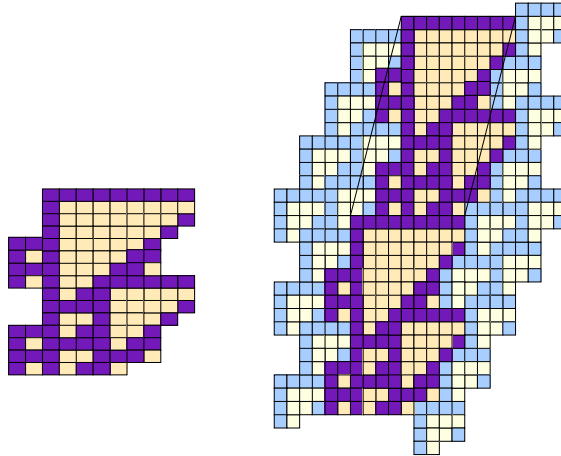


Figure 2.27: T8 based E gliders, which move leisurely leftwards.

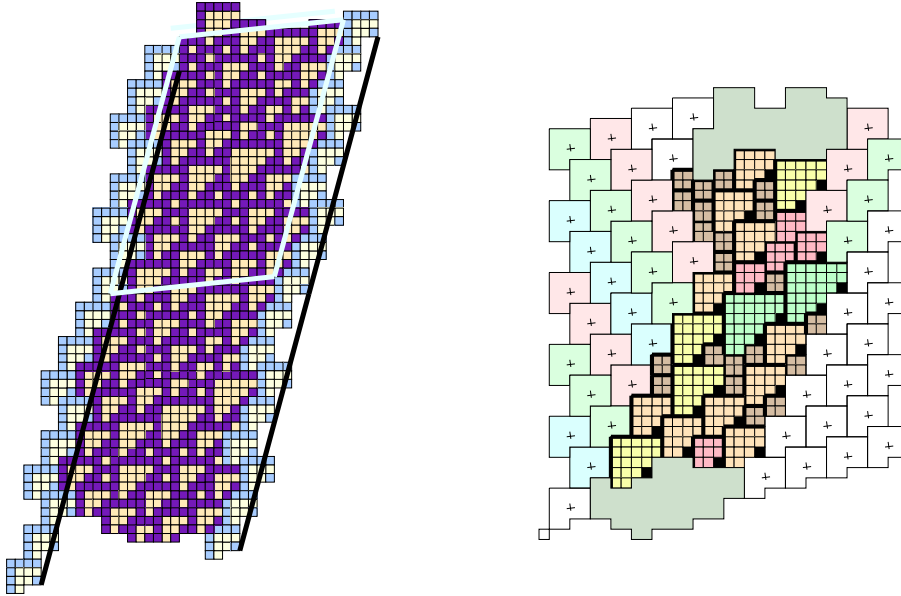
2.6.2 tiling approach to $-8/30$ gliders

Figure 2.28: The E-bar glider has the same velocity as E gliders, but it takes twice as long to go through all its motions. Two periods of the E-bar are shown on the left, to better to see how it fits in with the ether tiles. It is also presented on the right with S tiles, to show the details of its embedment in the ether. Stripped to their barest essentials, two EBars could snuggle quite closely, but that would violate the rule that two top edges cannot abut directly. Some ether tiles must be inserted to avert the problem, following which the gliders can be made to follow each other quite closely.

The EBar glider has coincidentally the same velocity as the E glider (from which it derives its name), but it takes twice as long to complete a period. On the left it spans six ether files, which are the routes along which an A glider would approach. On the right there are only two files, so that it is only necessary to distinguish between low mode and high mode when contemplating collisions with a B glider.

In examining pictures of evolution according to Rule 110, it is fairly noticeable that a single isolated T10 is a precursor to the EBar. Or at least when it interrupts the grain of the ether lattice in one particular fashion (ether one low on the left, one high on the right). A good example is seen in Figure 3.10.

2.7 Cook's F-glider, backward velocity $-c/9$

Cook remarks that the F glider can be triggered from an A-C collision, the details of which are shown in Section 3.2.2.

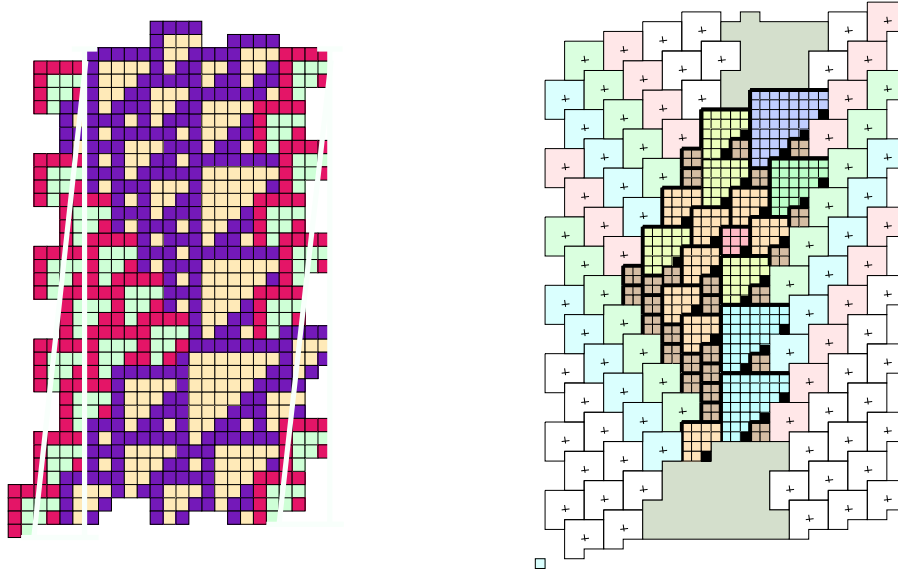


Figure 2.29: The lackadasical F glider, which moves 4 left in 36 generations, for a velocity of $-1/9 c$. Left: the unit cell, expressed with T tiles. Right: presentation with S tiles, showing the different approach aspects. F gliders can be overpacked just as well as EBar gliders, but no such arrangement can arise from natural evolution.

One period of an F glider occupies six ether files on the left, such as would be used in the approach of an A glider. However, it occupies only four files on the right, the path along which a B would approach. The difference is due, of course, to the differences in velocity between A's and B's, given that their orientations relative to the ether are different.

2.8 Cook's G-gliders, backward velocity $-c/3$

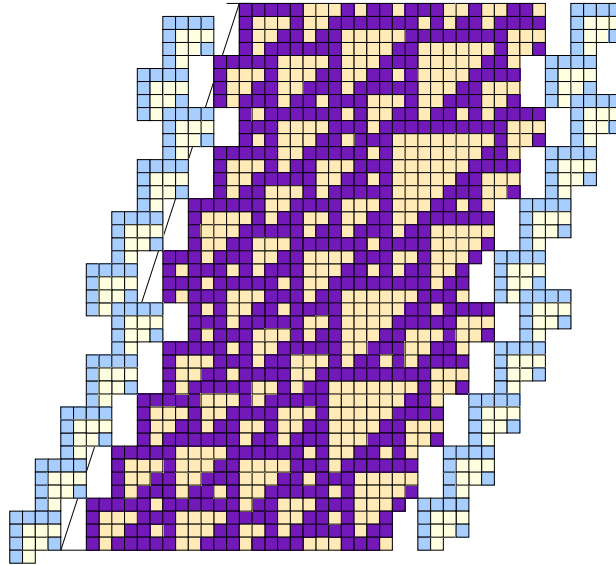


Figure 2.30: G gliders based on a mixture of T5, T6, T7, T8 and smaller ones, which move left at $1/3$ light velocity.

The G family, on the other hand, fulfills its promise of involving the “two right in five” gliders. It differs from the E family in that the two superluminal traces comprising the extension alternate a two-high B strip inside the alpha with a three-high B strip in the same place.

These alphas are not such orphans as seemed at first sight, since they can merge with the ether, fuse style. Moreover, they just plain stop with the left-running slopes appropriate to the E's or B's, which means that their connection to the ether would also show up on the corresponding de Bruijn diagrams.

They also have fuse-like behavior on the left hand, and since the boundary slope is congruent, maybe an effort should be made to embed them totally into the ether. As it is, they need the large triangles in the slim E's or G's to anchor them. But since those large triangles are fairly common, one wonders whether they might extend other gliders. In fact, near the upper right hand corner of Cook's random sample is an episode which fits this description.

Extending the extension occurs when B gliders join up with the latent B's already present, and the process is totally additive, even for two B's right alongside each other. Apparently the effect of A's and B's, as dislocations, is to raise everything vertically by two cells. But that is just the rise needed to put new T5's in the superluminal stream. Since a superluminal stream is a phase effect, it isn't a real glider, and doesn't have to run on and on, as a true glider might.

Since the alphas run out from selected larger triangles, it is also possible to wonder whether there is a family present here, and whether it has any further members?

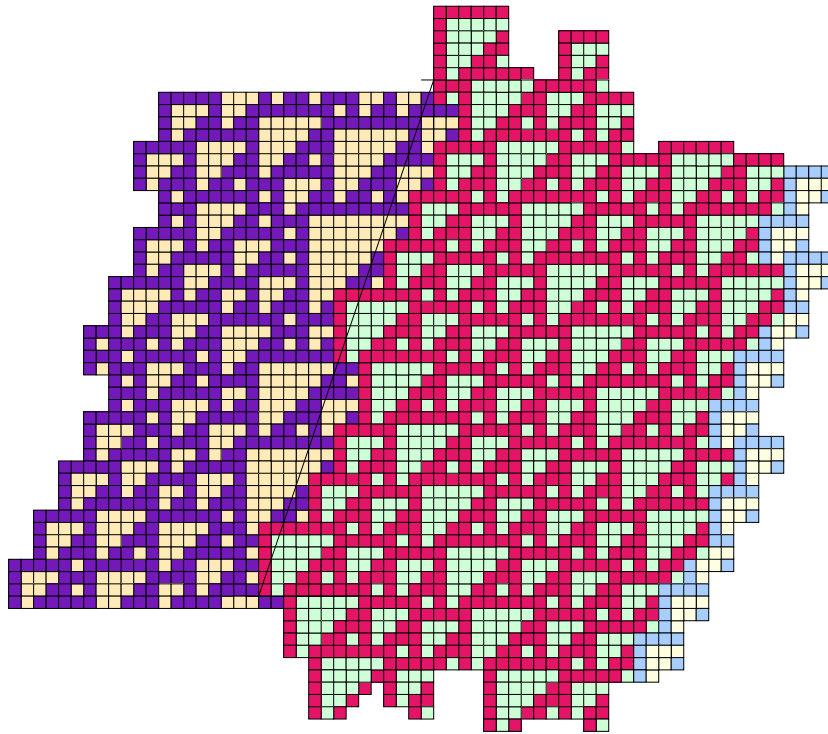


Figure 2.31: The G glider is extensible by the same mechanism which extends E gliders, with the difference that alternative α tiles are used which gives proportional spacing between the T5 chains.

2.9 Cook's H-glider, velocity $-18c/92 (\approx -c/5)$

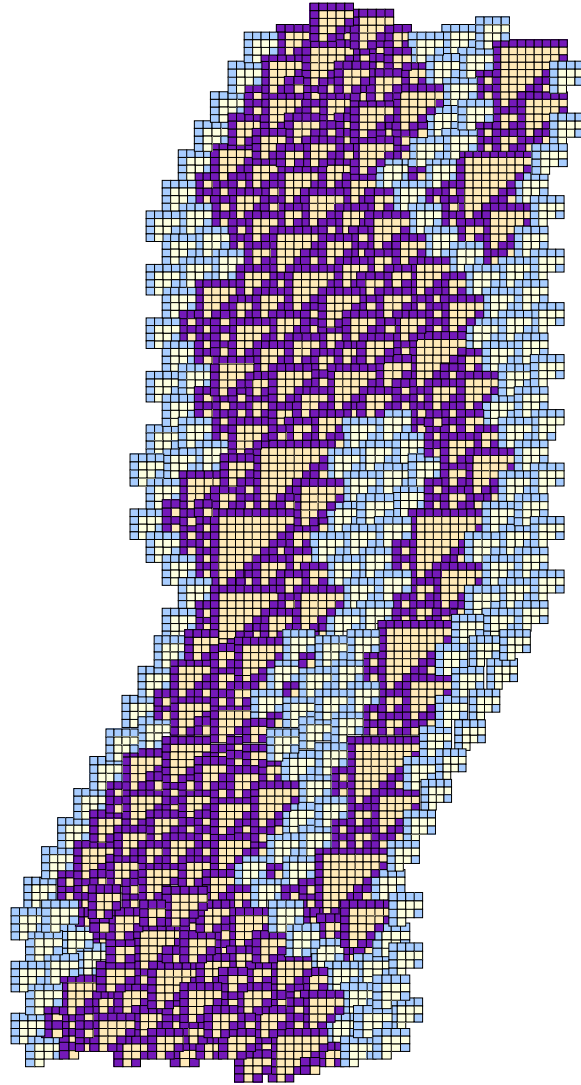


Figure 2.32: The H glider moves left 18 cells in 92 generations, about $-c/5$.

This glider takes so many generations to develop that an analysis by de Bruijn diagram is manifestly beyond reach.

2.10 Cook's glider gun, velocity $-20c/77$ ($\approx -c/4$).

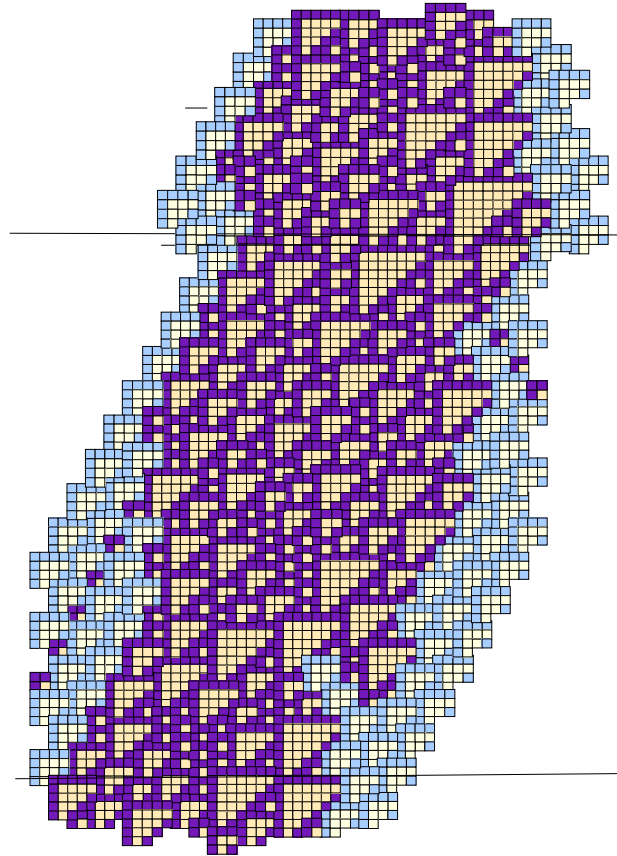


Figure 2.33: The glider gun glides, and having glid, glides on. The horizontal lines delimit one single period.

The glider gun has a velocity intermediate between the velocities of the streams which it launches, giving them ample opportunity to clear the domain of the gun. If A and B gliders annihilate on colliding, there is no obstacle to having a whole phalanx of glider guns, although they won't produce any extra effect on the remainder of the plane (except maybe for spacing) beyond the effect of a single gun.

Chapter 3

Glider Collisions

Most of Rule 110's gliders seem to have been known at the time of Wolfram's World Scientific book [9], although Cook seems to be justifiably proud of discovering the "useless" glider gun and the highly convoluted H-glider, which he reveals to be the product of a three-glider collision. When his results were announced to Life-Mail, search programs were reported to have discovered his list of gliders and none others. Whether there are others is still a moot question; statistical considerations favor their existence (even after discounting complicated extensions of the known families), although it is evident that those which do will have to have longer periods and more complicated cycles than those now available.

Just having gliders doesn't do much for reaching the higher levels of understanding the behavior of a cellular automaton; the evident place to start the analysis is to study the glider collisions. Cook mentions such studies, but his report [1] did not include any of them,

Given a half dozen or more gliders, most of them with extensive variant families, the study of even the binary collisions is going to be long and laborious, although it does reveal some interesting patterns and regularities. These include the systematics of glider extension and reduction, and also some solitons.

3.1 Generalities

3.1.1 glider widths and glider parities

| glider | width | width mod 14 | parity |
|--------|-------|---------------|--------|
| nA | $6n$ | $6n \bmod 14$ | even |
| nB | $8n$ | $8n \bmod 15$ | even |
| BBar5 | 22 | 8 | even |
| BBar8 | 39 | 11 | odd |
| C1 | 23 | 9 | odd |
| C2 | 17 | 3 | odd |
| C3 | 25 | 11 | odd |
| D1 | 25 | 11 | odd |
| D2 | 19 | 5 | odd |
| E1 | 19 | 5 | odd |
| E2 | 27 | 13 | odd |
| E3 | 21 | 7 | odd |
| En | +10 | every $n + 3$ | odd |
| EBar | 21 | 7 | odd |
| F | 29 | 1 | odd |
| G | 38 | 10 | even |
| H | 59 | 3 | odd |

Table 3.1: The widths of Cook's gliders.

3.1.2 maps of collision chains

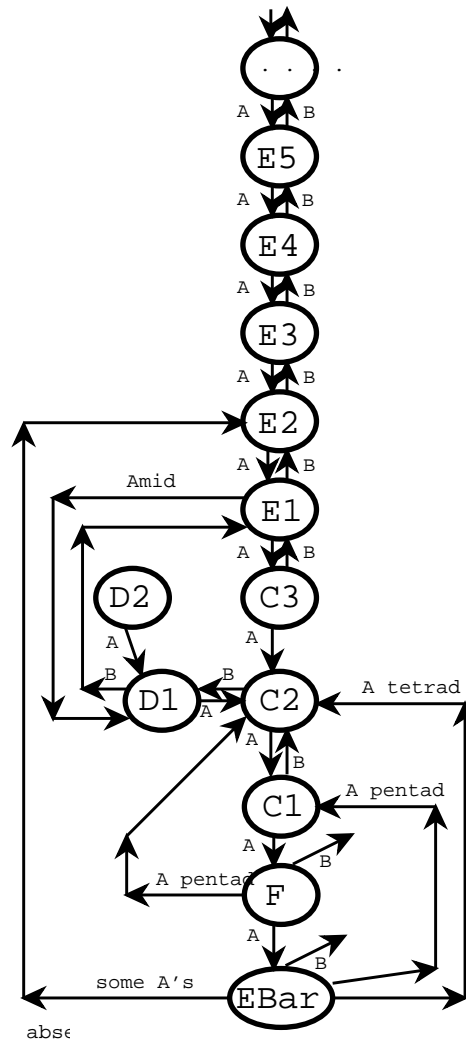


Figure 3.1: A's and B's meeting E's, C's, and some others. All A labels have the A either in the high or the low position. Exceptions are one link marked "A mid," and the tetrad, pentad links, whose collisions stop BBar and F solitons of all aspects.

3.2 Collisions with A gliders

Although glider collisions and puffer trains are not the real province of de Bruijn diagrams, some information can occasionally be gleaned from the diagrams. For instance “black hole” configurations are often interpretable as collisions. Just manually adjusting the coexistence of A and B gliders, it looks like they should begin to collide in the generation-9 de Bruijn diagrams. These are still within computational limits, being 16 times as big as the generation-7 diagrams, but will involve millions of nodes.

However, two kinds of collision are easily described, and are discussed below. Besides the A - B collisions and the A - C collision converting into an F, there is the whole class of collisions by which B gliders extend the E or G gliders, but which has already been incorporated in the foregoing analysis. For A collisions, we can make the following table:

| target | residue |
|--------|---------|
| B | null |
| C1 | F |
| C2 | C1 |
| C3 | C2 |
| D1 | C2 |
| D2 | D1 |
| E1 | D1 |
| E2 | E1 |
| E3 | C2 |
| F | EBar |

Table 3.2: Collisions between right moving A’s and others.

Similarly, a table can be constructed for B collisions:

| target | residue |
|--------|----------|
| A | null |
| C1 | C2 |
| C2 | D1 |
| C3 | E1 |
| D1 | E1 |
| D2 | EBar + A |
| E(n) | E(n+1) |
| F | varied |

Table 3.3: Collisions between left moving B gliders and others.

Besides simple encounters, there is a multitude of collisions between glider polymers, and still more between closely spaced groups of polymers.

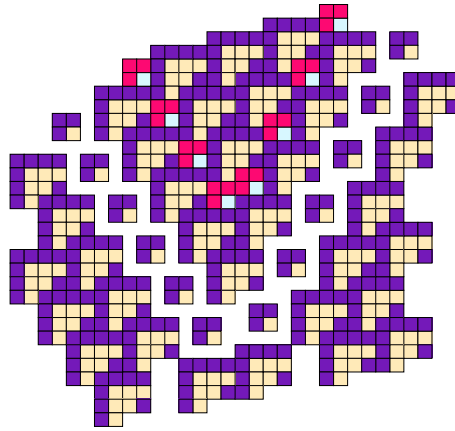
3.2.1 the A - B collision vanishes

Figure 3.2: A and B gliders, travelling in opposite directions, can collide. They leave no trace of their former existence.

A and B gliders, along with their polymers, induce simple fault lines in the ether lattice along which the ether is displaced vertically by two cells but with relative offsets which run in opposite directions. So collisions just balance the offsets, leaving the difference as the overall result. An A polymer colliding with a B polymer of equal weight leaves no trace; otherwise the higher polymer continues its course, appropriately diminished.

3.2.2 the three A - C collisions

The simplest, and presumably amongst the commonest, gliders are the A's, B's, and C's. Because of their simplicity, it is relatively easy to catalogue the multitude of collisions which results from different alignments and relative phases of the oncoming gliders. The A's move right, C's are static and B's move left, leaving A - B - C as the only ordering which needs detailed examination.

The C's embed into the ether according to three possible alignments of the vertical spine formed by the left edges of the column of T6's with T3's on the left. Since A gliders are formed by inserting some number of T1's just below each T3 in a slanting file of slope $-2/3$, the net effect of an A glider or a barrage of n A's is to move everything a distance $2n$ downwards along a fault line.

However, the T6's have period 7 in contrast to the even displacement occasioned by the T1's of the A's, which means that A's arriving in the wrong phase, or in sufficient numbers, can disrupt the alignment, which otherwise just shifts in accomodation.

On the right, there is less freedom, because there is but one alignment of ether T3's with respect to the T6's of a C. As a result there will always be a rearrangement, seen at first from the position of the C as an exchange of the points at which a T1 and a T3 tile connect to the hypotenuse of the T6. But of course that provokes greater change as the generations go on.

There are nine possibilities for the simplest collisions, according to the realignment required to match up the A's followed by the reaction to that alignment in the aftermath of an oncoming B. By separating the A's from the B's only six cases need to be considered unless the A's and B's arrive simultaneously or nearly simultaneously.

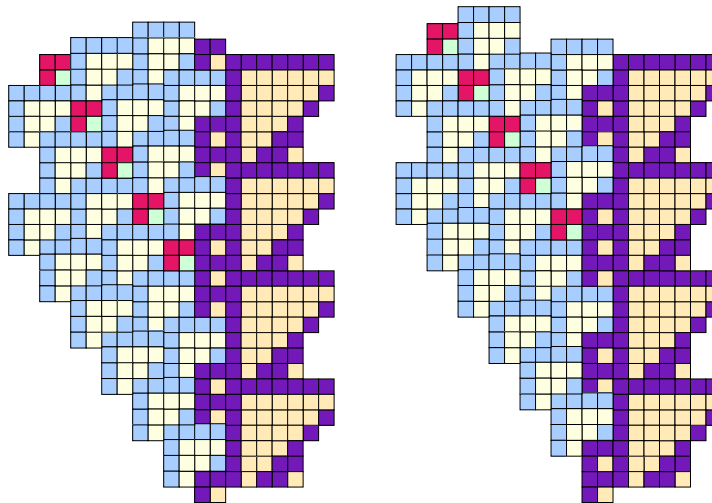


Figure 3.3: Two of the three phases of an A - C collision rotate the phase of the C tiles relative to the lefthand ether.

In Figure 3.3 the collisions are shown for the alignments “lower T1” [C2] which converts into “upper T1,” [C1] on the left, and “T3” [C3] which converts into “lower T1,” [C2] on the right.

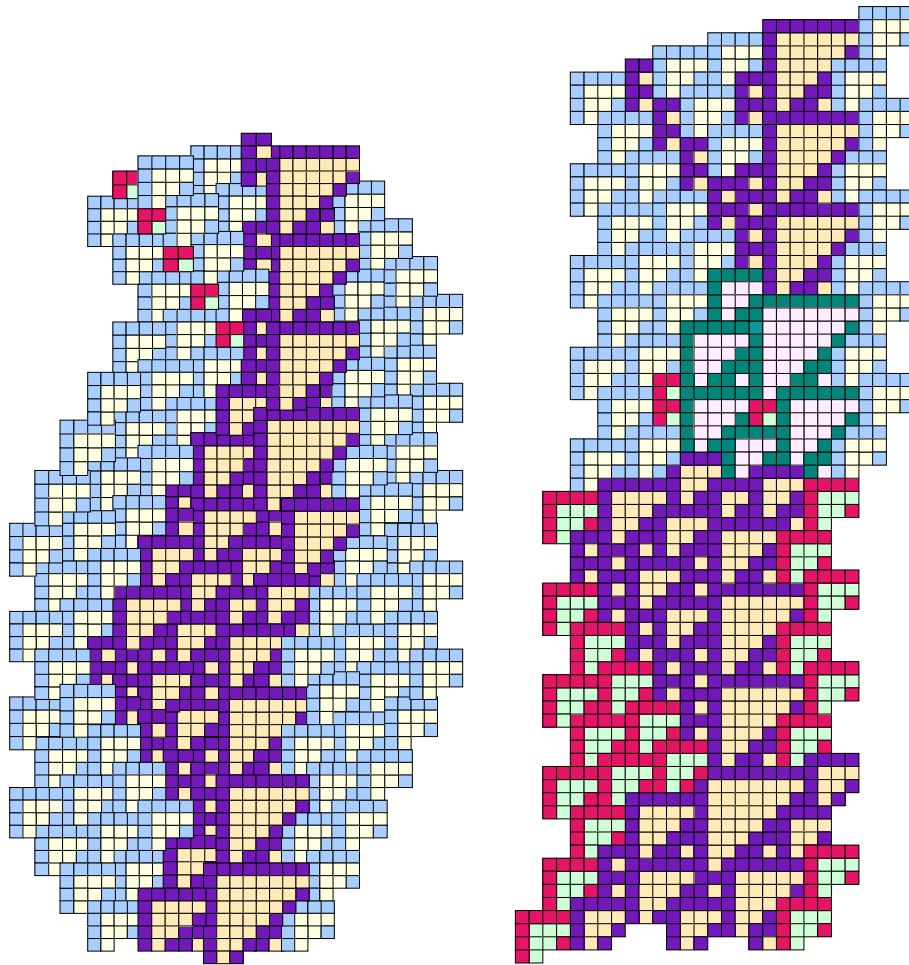


Figure 3.4: A and C gliders, colliding just right, coalesce into an F. Left: ordinary A glider collides. Right: Instead, an A dimer participates in the collision.

In Figure 3.4, the remaining collision does not rotate “upper T1” [C1] into “T3” [C3] but rather converts the collision mass into an F glider after a slight delay. An F glider moves leftward at one ninth the velocity of light. Actually Figure 3.4 also includes a similar reaction based on an incoming doubled A glider to produce the same final result.

3.2.3 Multiple A - C collisions

When the T1 which constitutes an A glider finally makes contact with a C glider, it adds its height, which is 2, to the T1's in the C margin. The result is a shift in the indices of the C, decrementing them except at the discontinuity at C1, which enlarges the C1's T6 to a T7, which transforms the C1 into an F. As long as the effect is shifting, there is no restriction on the spacing between successive A's. From then on, the spacing matters, due to the internal structure of the F or any subsequent intermediaries.

Any spacing at all is possible between A's, from zero onwards, leading to innumerable sequences of A gliders. Two arrangements occur often enough to examine them separately and give them names. The term *polymer*, or more specifically monomer, dimer, trimer, ... refers to a cluster of T1's without any spacing at all. On the other hand, *polyad*, as in monad, dyad, triad, ... contemplates streams of T1's separated by one single ether tile.

| polymer | C1 | C2 | C3 |
|-----------|----------|----------|----------|
| monomer | F | C1 | C2 |
| dimer | EBar | F | C1 |
| trimer | EBar + A | EBar | F |
| quadrimer | E1 | EBar + A | EBar |
| pentamer | D1 | E1 | EBar + A |
| ... | | | |

Table 3.4: Collisions of A polymers with the three C gliders.

| polyad | C1 | C2 | C3 |
|--------|------|------|------|
| monad | F | C1 | C2 |
| dyad | EBar | F | C1 |
| triad | E2 | EBar | F |
| tetrad | E1 | E2 | EBar |
| pentad | D1 | E1 | E2 |
| ... | | | |

Table 3.5: Collisions of A polyads with the three C gliders.

3.2.4 A - D collisions

| target | residue |
|--------|---------|
| D1 | C2 |
| D2 | D1 |

Table 3.6: A - D collisions

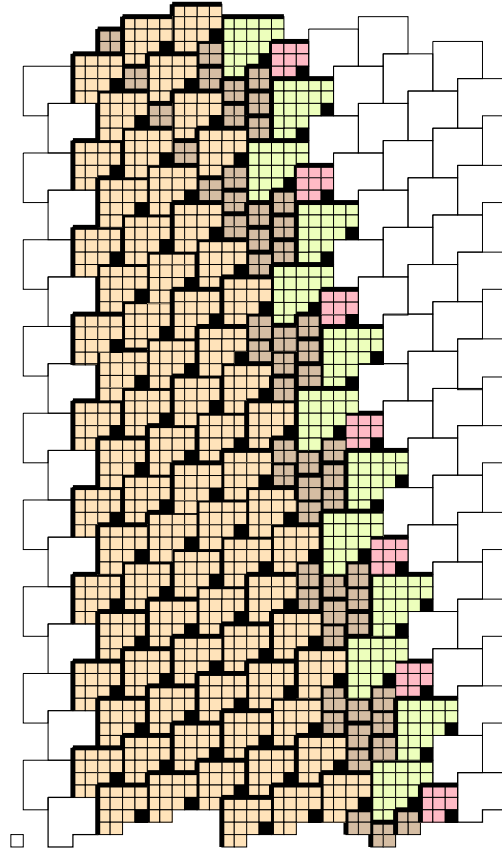


Figure 3.5: An A glider transforms D2 into D1 after a short while.

There is only one way that an A glider can approach a D glider, but there are two species of D glider, according to the way its left margin matches the ether. The two results are very different, because the collision rapidly promotes a D2 to a D1, but the conversion of a D1 into a C2 takes about twice as long. In Figure 3.6 the process is drawn using electronic quadrille paper.

The drawing on the left contains an error, but the drawing has been reproduced because it is a common error with instructive consequences. The main problem is that the first representation of the Rule 110 triangles which was used includes the hypotenuse as part of the tile. However, the upper left vertex of a tile contacting

the hypotenuse must overlap the hypotenuse. The reason is that otherwise three ones in sequence would evolve into a zero, and not the one which forms the left edge of the triangle. It is extremely easy to overlook this requirement, especially if a small triangle like a T2 is being brought in.

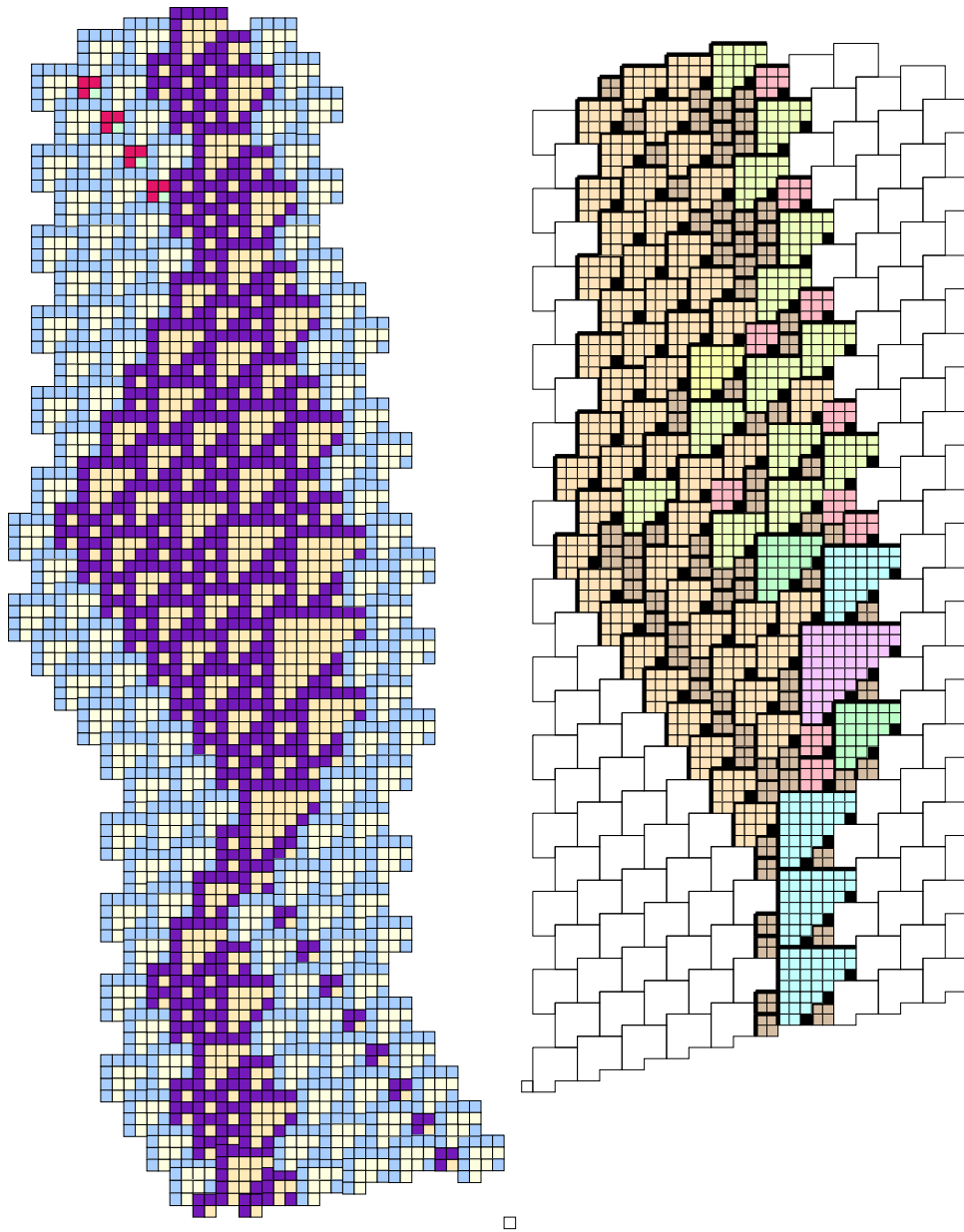


Figure 3.6: An A glider transforms D1 to a C2 after many generations, which is shown in the right diagram; but the drawing on the left contains a common error towards the very end giving, of course, a wrong result.

It is safer to leave the hypotenuse off the tiles, and to invent a T0 – just a single live cell – to fill in the parts of the diagonal which remain unused. In fact any T0's necessarily occupy alternate positions along the diagonal, and that is the only place where they are to be used. Which means that there are two parities for every tile, as can be seen upon close inspection of actual evolutions.

If it were simply a matter of an annoying error, the matter could be forgotten, or at least saved and brought out as a warning for anyone drawing an evolution by hand. But the results are often extremely interesting, even if they aren't part of a legitimate sequence of events. For example, Figure 3.6 was originally seen as providing a unit delay, which could have been useful in a circuit-theory approach to realizing a computation with glider collisions. As frequently happens, the errors are often more artistic and more interesting than true results.

An interesting way to exploit this blunder would be to work with a probabilistic cellular automaton, in which Rule 110 would be modified to the extent that the evolution of the neighborhood 111 to 0 could be reduced slightly by assigning it a probability of 97% or some similar figure, maybe even negligibly but still reliably less than 100%.

3.2.5 A - E collisions

There are three relative alignments at which A and E gliders may meet, which could be called high, medium, and low. Besides that, since the E glider is extensible, there is a whole infinity of E thicknesses, which are actually paddings with α gliders. Therefore, the discussion of A-E collisions turns into a survey of α demolitions.

| n | main | extra | n | main | extra |
|----|----------|-------|----|----------|--------|
| 1 | D1 | . | 17 | D1 | 2B |
| 2 | E1 | . | 18 | E | 2B |
| 3 | EBar | A | 19 | EBar | A, 2B |
| 4 | EBar | . | 20 | EBar | B |
| 5 | EBar | B | 21 | EBar | 2B |
| 6 | F | B | 22 | F | 2B |
| 7 | C1 | B | 23 | C1 | 2B |
| 8 | C2 | B | 24 | C2 | 2B |
| 9 | D1 | B | 25 | D1 | 2B |
| 10 | EBar | 2A, B | 26 | EBar | 2A, 3B |
| 11 | E2 | B | 27 | E2 | 3B |
| 12 | EBar | B | 28 | EBar | 3B |
| 13 | EBar | 2B | 29 | EBar | 4B |
| 14 | BBar + F | B | 30 | BBar + F | 3B |
| 15 | BBar + F | 2B | 31 | BBar + F | 4B |
| 16 | C2 | 2B | 32 | C2 | 4B |

Table 3.7: A mid-collisions with E_n are periodic, repeating every time n increases by 16, with the proviso that an additional B glider is always produced every time n increases by 8.

When the A glider meets the E_n glider in the low position, the reaction is very clean, always resulting in E_{n-1} except that the nonexistent E_0 is a C3. Even so, the indexing is consistent because A collisions with C's lower their indices, C1 turning finally into an F.

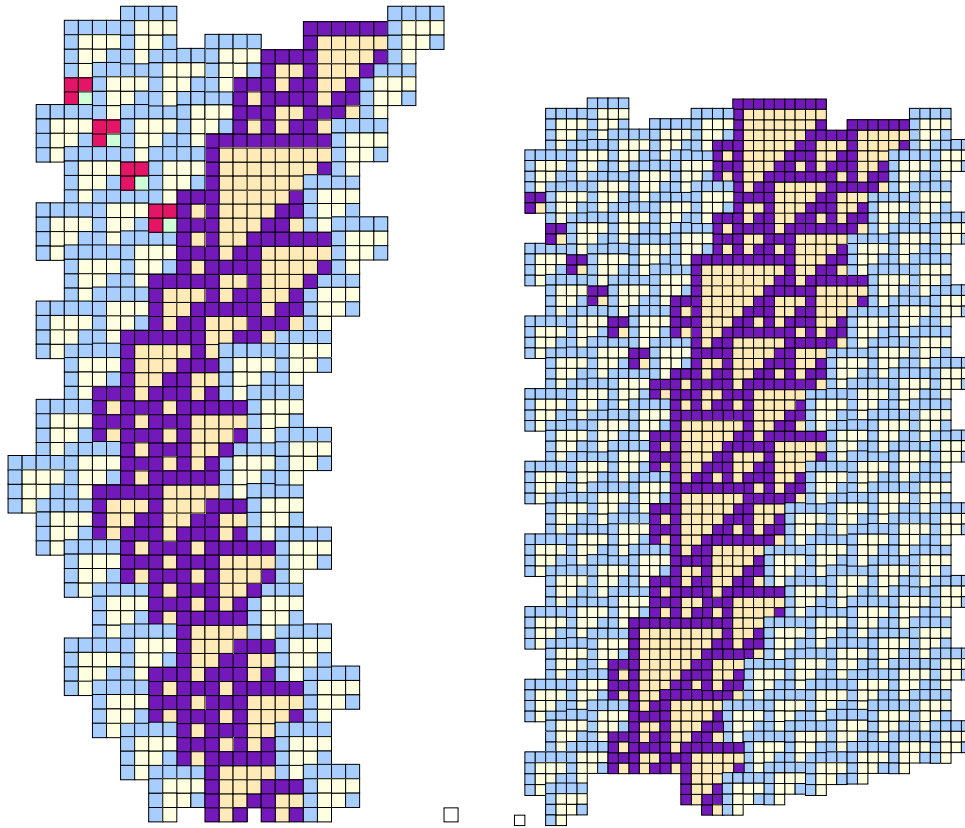


Figure 3.7: Left: An A glider in a “mid” collision can be absorbed by an E glider which promptly transmutes into a D. Right: But in a different alignment, whatever E retracts, which makes a nice counterpart to the extension occasioned by B-E collisions.

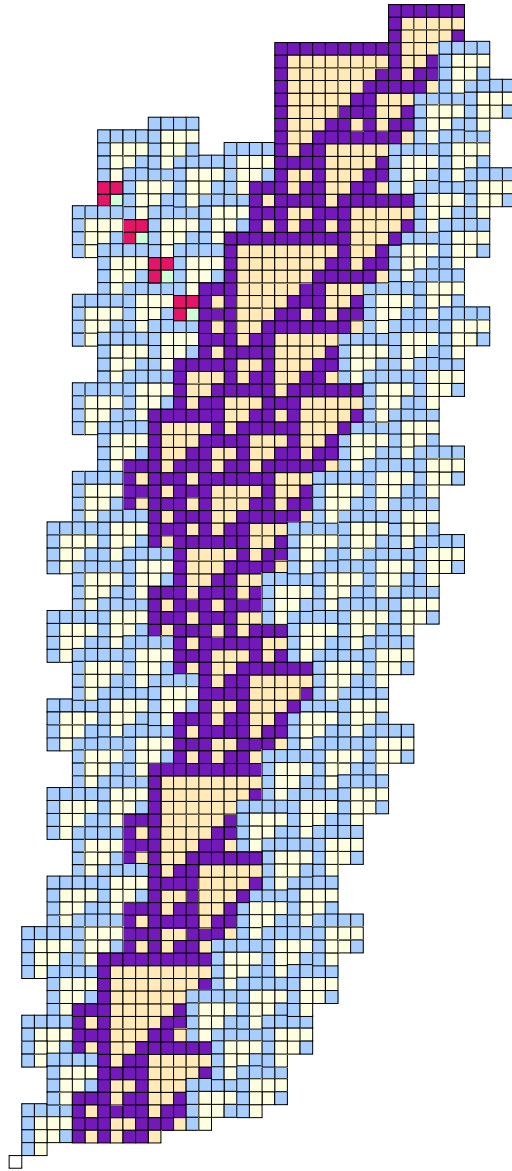


Figure 3.8: An A glider can be absorbed by an E2 which then reverts to an E1.

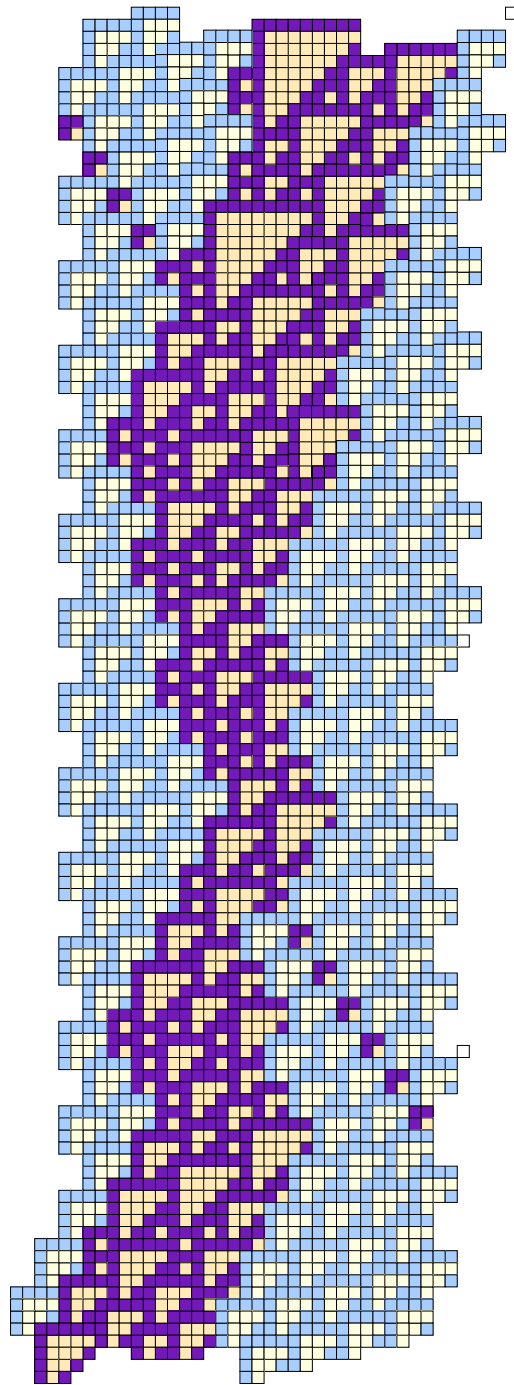


Figure 3.9: An A glider can be absorbed by an E3 which thereupon reverts to an EBar rather than to an E2, emitting a rightrunning A in the process. The alternative result is due to the different relative alignment of the oncoming A.

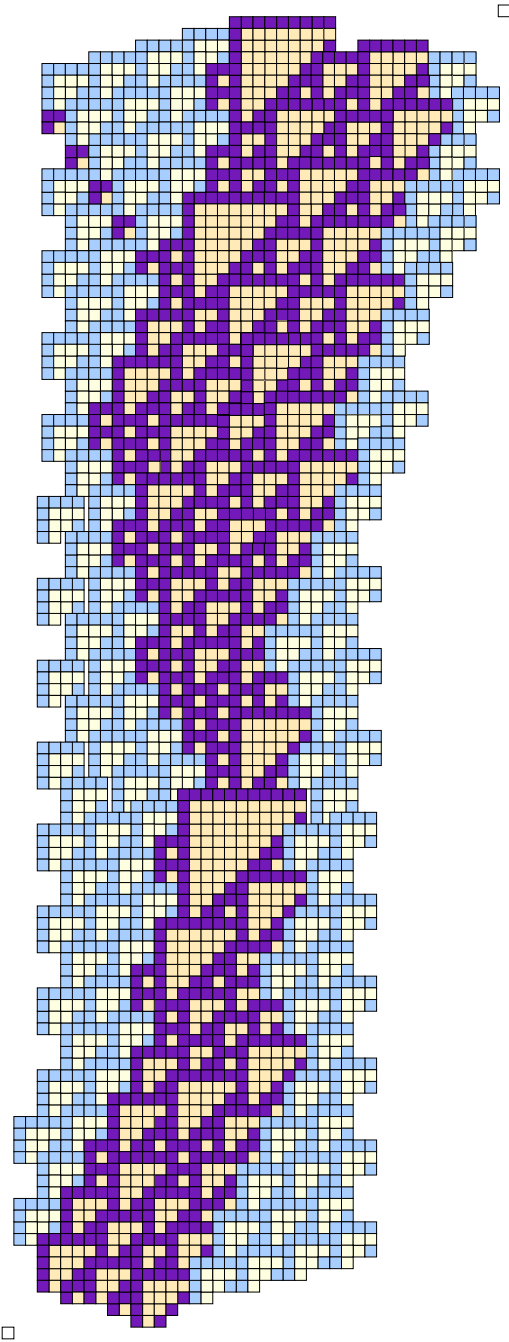


Figure 3.10: An A glider can be absorbed by an E4 which reverts to a BBar rather than to an extended E. Note the isolated T10, which is a sure precursor of the EBar.

3.2.6 nA - EBar collisions

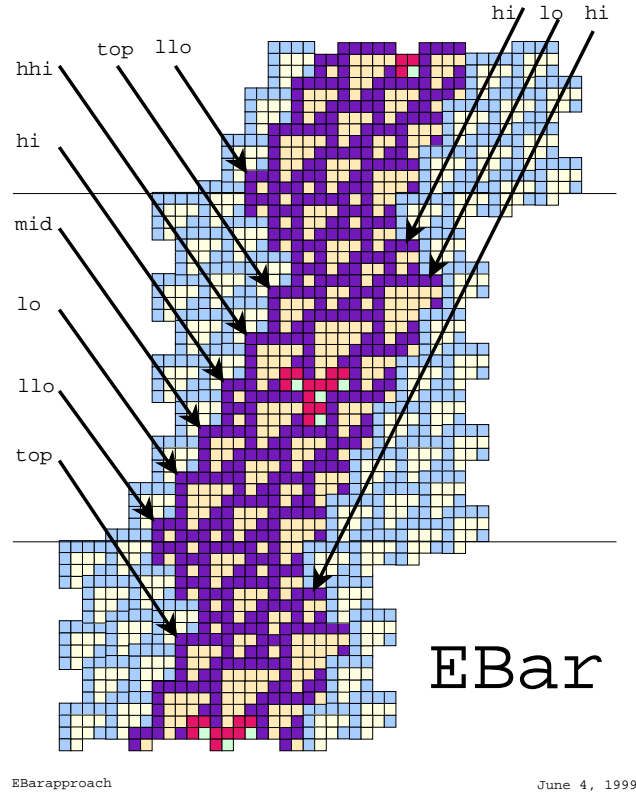


Figure 3.11: There are six different alignments for an A glider approaching an EBar; they also serve as points of reference for A complexes and D's.

| align | monomer | dimer | trimer | tetramer | tetrad | pentad |
|-------|---------|-----------------|--------------|------------|--------|--------|
| top | E2 | E1 | D1 | C2 | C2 | C1 |
| hhi | E2 | EBar, 2 B, Atet | D1 | EBar, Atet | C2 | C1 |
| hi | EBar, A | EBar, 2 A | C3 | C2 | C2 | C1 |
| mid | EBar, A | D2 | D1 | C2 | C2 | C1 |
| lo | EBar, A | E1 | F, BBar, 2 B | F, BBar, B | C2 | C1 |
| llo | EBar, A | E1 | D1 | EBar, Atet | C2 | C1 . |

Table 3.8: A's can almost pass EBar's, except that in the two highest alignments they turn them into E2's and stop. An A tetrad (four equally spaced vs tetramer [block of four]) uniformly yields C2's.

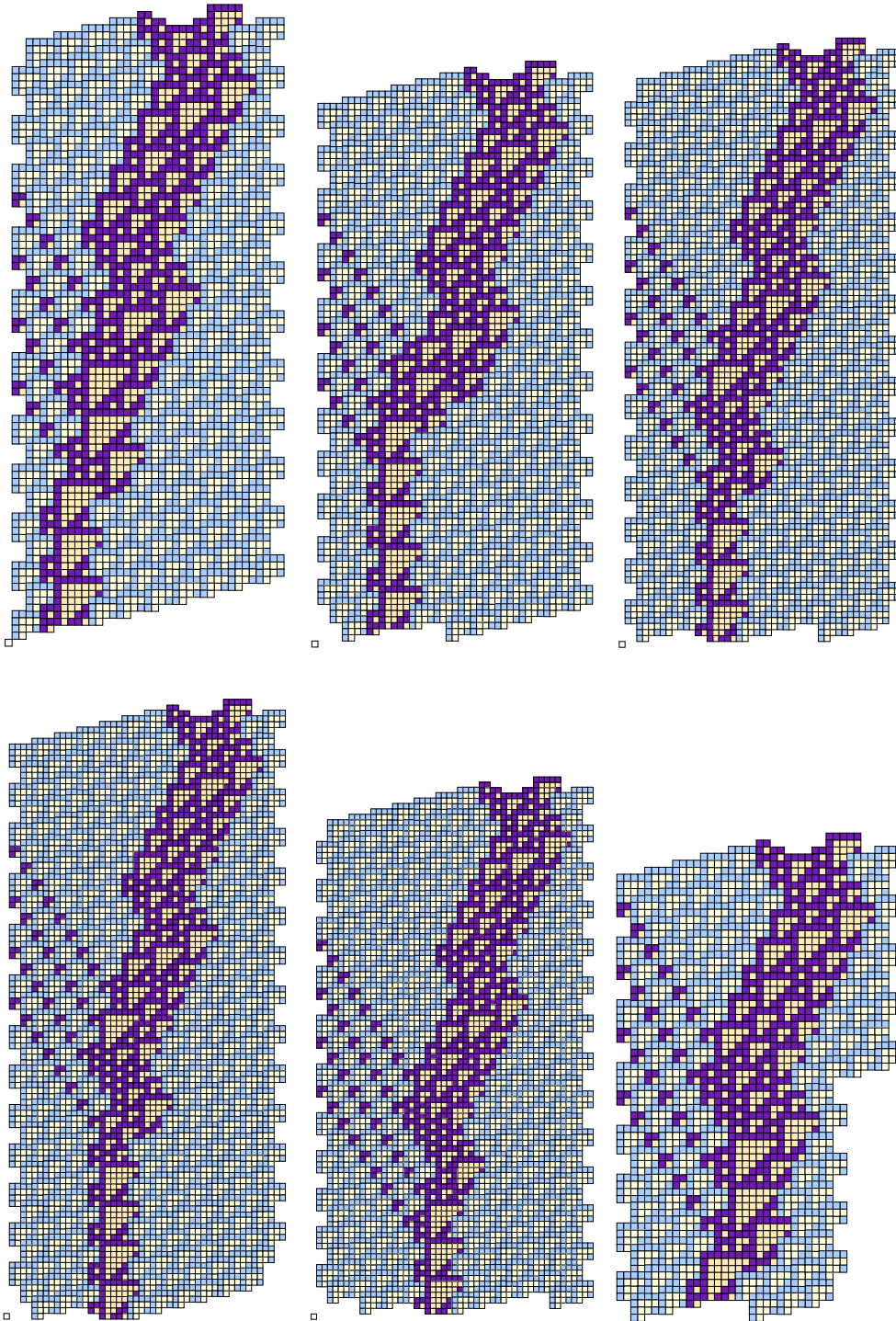


Figure 3.12: A tetrad of A gliders striking an EBar produces C2's from whatever aspect. Since the spine of the column of C2's is already formed, the subsequent arrival of another A, say as a member of a pentad, will simply promote the C2 to a C1.

3.2.7 nA - F collisions

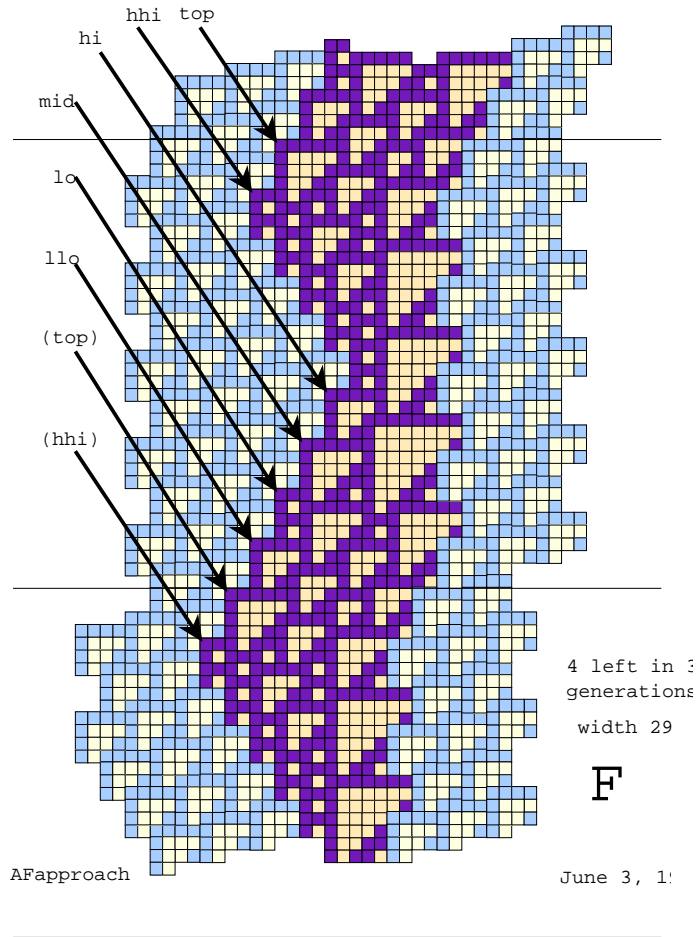


Figure 3.13: There are six different alignments for an A glider approaching an F; they also serve as points of reference for A complexes and D's.

| align | monomer | dimer | trimer | tetramer | tetrad | pentad |
|-------|---------|----------|---------|---------------|--------|--------|
| top | EBar | C1 + 3 B | C1 + 2B | C1 + B | C3 | C2 |
| hhi | EBar | EBar + A | E1 | D1 | D1 | C2 |
| hi | EBar | EBar + A | E1 | E1 + A | D1 | C2 |
| mid | EBar | E2 | E1 | D1 | D1 | C2 |
| lo | EBar | EBar + A | E1 | BBar + F + 2B | D1 | C2 |
| llo | EBar | EBar + A | C1 + 2B | C1+ B | C3 | C2 |

Table 3.9: A single isolated A will transmute an F into an EBar. However, if a second A arrives before the reaction is complete, the results could be quite different. In any event, once the F has changed, any subsequent collider would have to deal with the EBar.

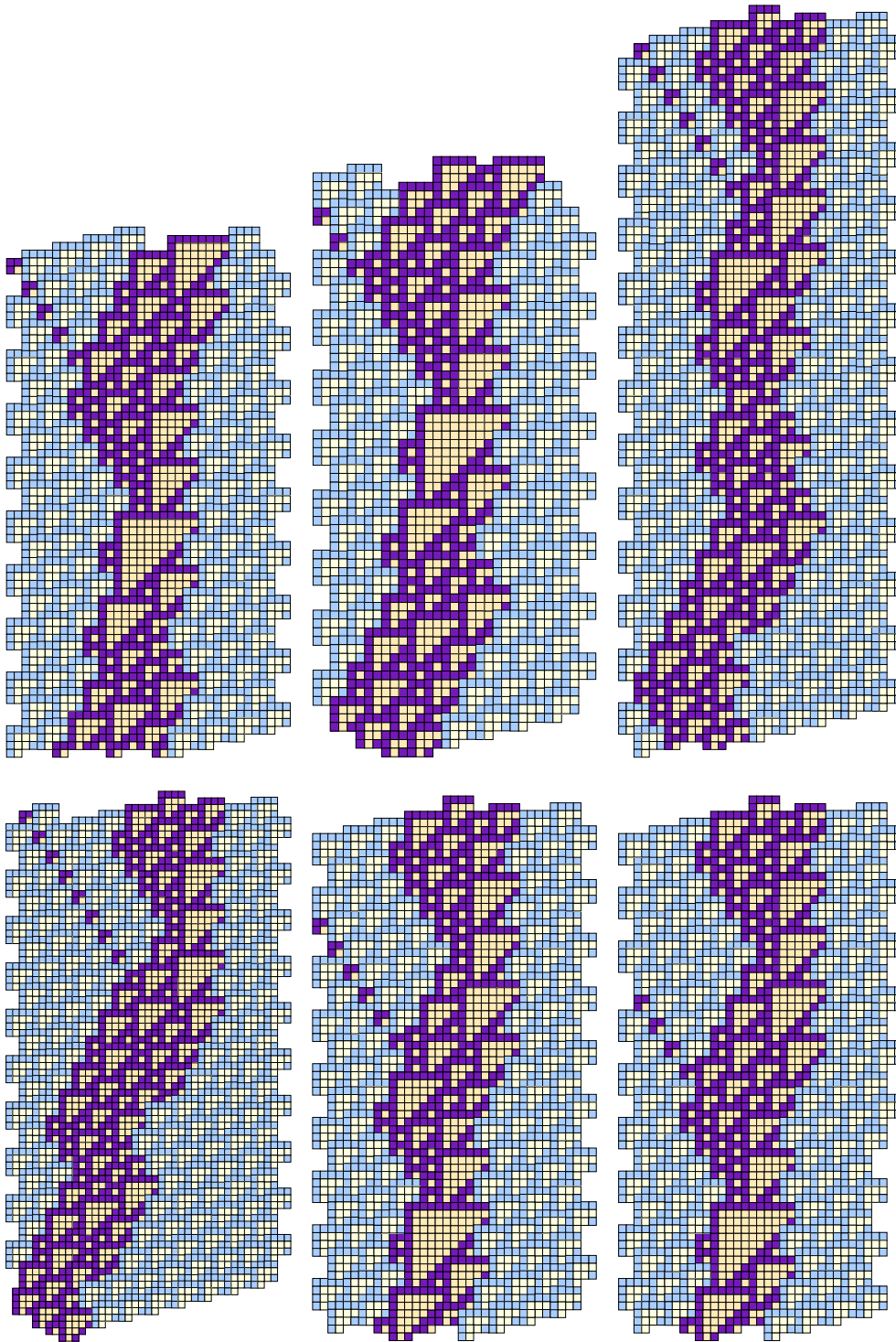


Figure 3.14: A single A glider can strike an F with any alignment to create an EBar glider, which is faster. Note that in many cases an isolated T10 presages the EBar's emergence some twenty generations later on, starting out by producing a T5 - T6 pair.

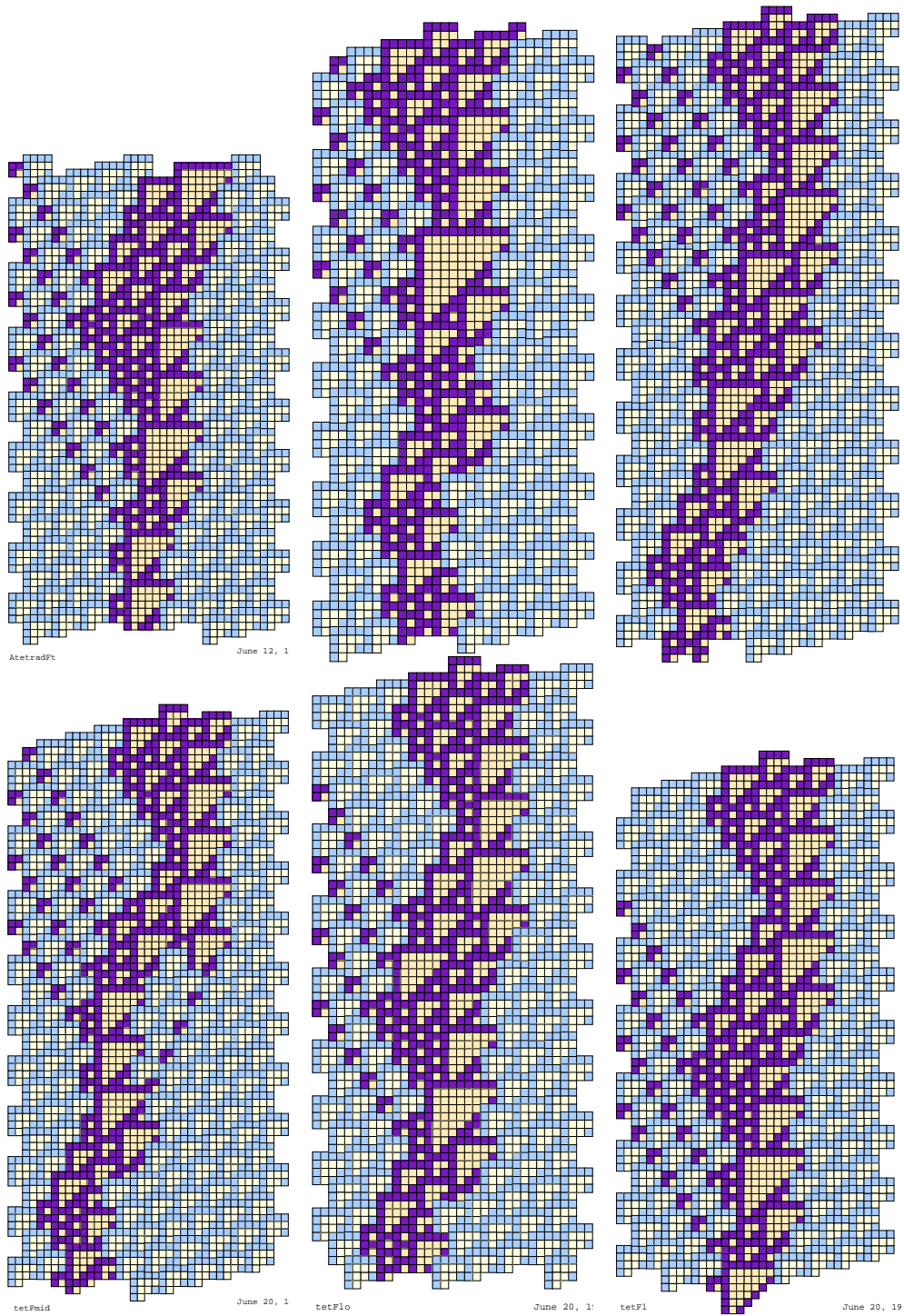


Figure 3.15: A tetrad of A gliders can strike an F to produce either C3's or D1's.

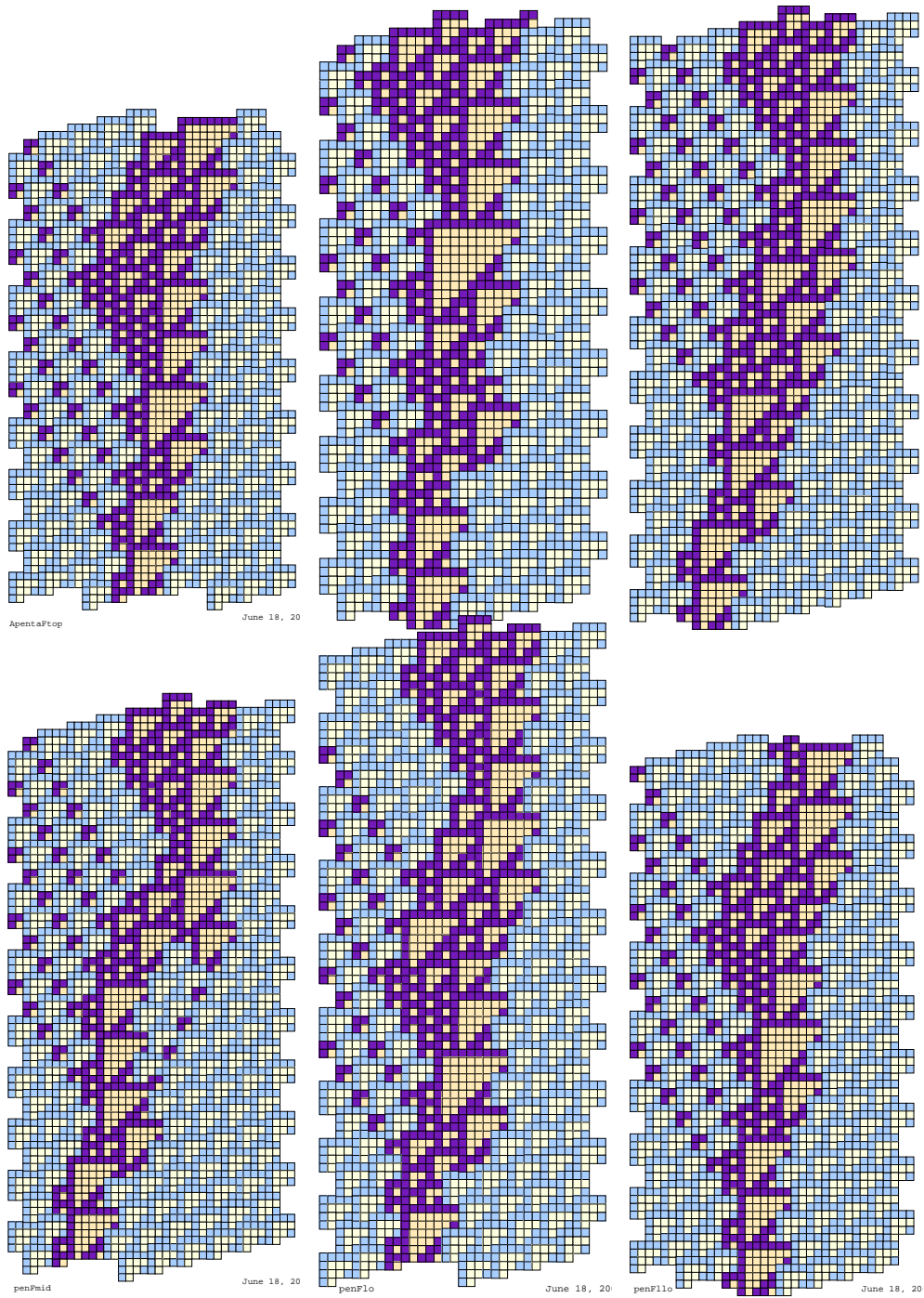
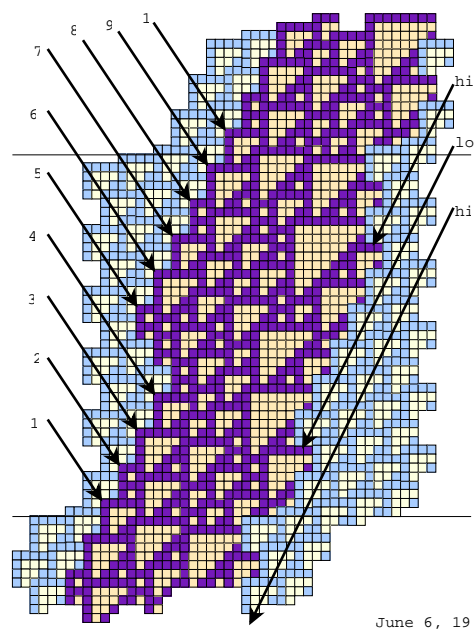


Figure 3.16: A pentad of A gliders can strike an F to produce C2's no matter what.

3.2.8 A - G collisions



A - G collis:

| aspect | monome |
|--------|-----------|
| 1 | C3 + D2 |
| 2 | A + G |
| 3 | C1 + EBar |
| 4 | C1 + F |
| 5 | 2B |
| 6 | 2F |
| 7 | 2B |
| 8 | 2B |
| 9 | C1 + EBar |

AGtabl

May 21, 20

Figure 3.17: There are nine different alignments for an A glider approaching a G; they also serve as points of reference for A complexes and D's.

| align | monomer | dimer | dyad | triad |
|-------|-----------|---------|---------------------|--------------|
| 1 | C3 + D2 | BBar5 | A + 2B | null |
| 2 | A + G | A + 2B | C1 + EBar | A + C2 + D1 |
| 3 | C1 + EBar | 2C3 | C2 + E1 | C2 + C3 |
| 4 | C1 + F | B | A + 2B | null |
| 5 | 2 B | B | B | null |
| 6 | C3 + D2 | A, 2B | A + A dimer + B + G | A dimer + 2B |
| 7 | 2 B | 2B | B | null |
| 8 | 2 B | B | B | null |
| 9 | C1 + EBar | C2 + E1 | C2 + E1 | C2, C3 |

Table 3.10: The collisions between A gliders and a G glider are quite varied. Note that the break in the G margin comes at aspect 5.

3.3 Collisions with B gliders

3.3.1 the three B - C collisions

| target | residue |
|--------|---------|
| C1 | C2 |
| C2 | D1 |
| C3 | E1 |

Table 3.11: B - C collisions

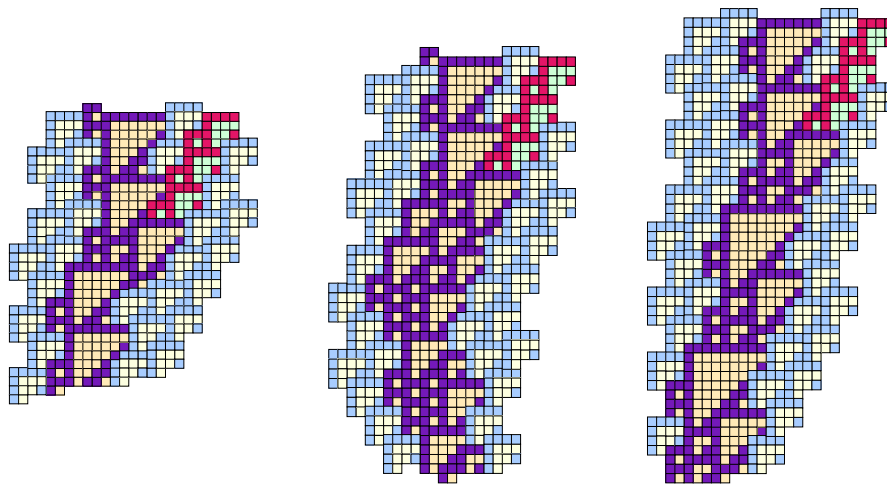


Figure 3.18: B and C gliders, when the C tile is in the “upper T1” [C1] alignment, displace the C stack leftwards by four cells and turns it into a “T2” [C2].

3.3.2 the three BB - C collisions

| target | residue |
|--------|---------|
| C1 | D1 |
| C2 | E1 |
| C3 | E2 |

Table 3.12: B dyad - C collisions

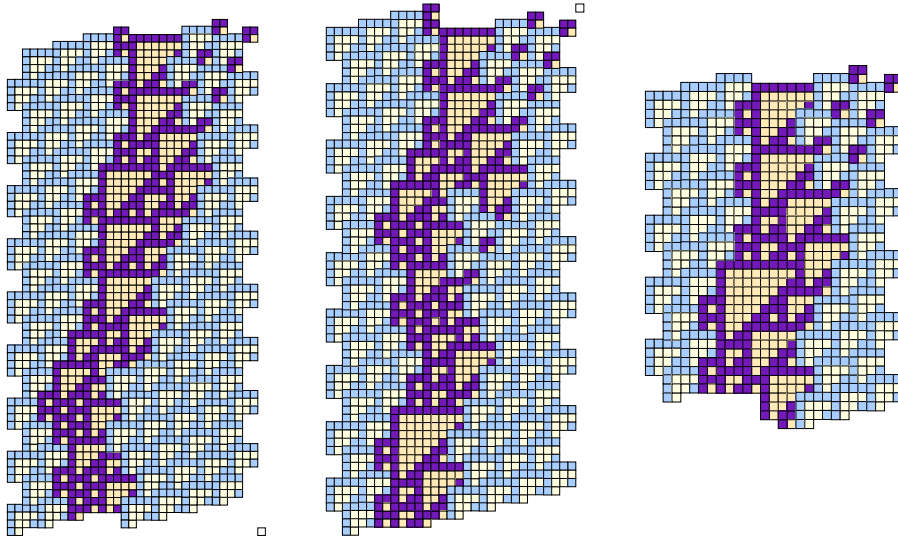


Figure 3.19: The collision of a B dyad with each of the C gliders follows the same sequence as the collision with a single B, except that the result is advanced one step in the general B-C collision chain. In other words, there is no penalty for the second B having followed in close succession to the first.

3.3.3 the three BBB - C collisions

| target | residue |
|--------|---------|
| C1 | E1 |
| C2 | EBar, A |
| C3 | E3 |

Table 3.13: B triad - C collisions

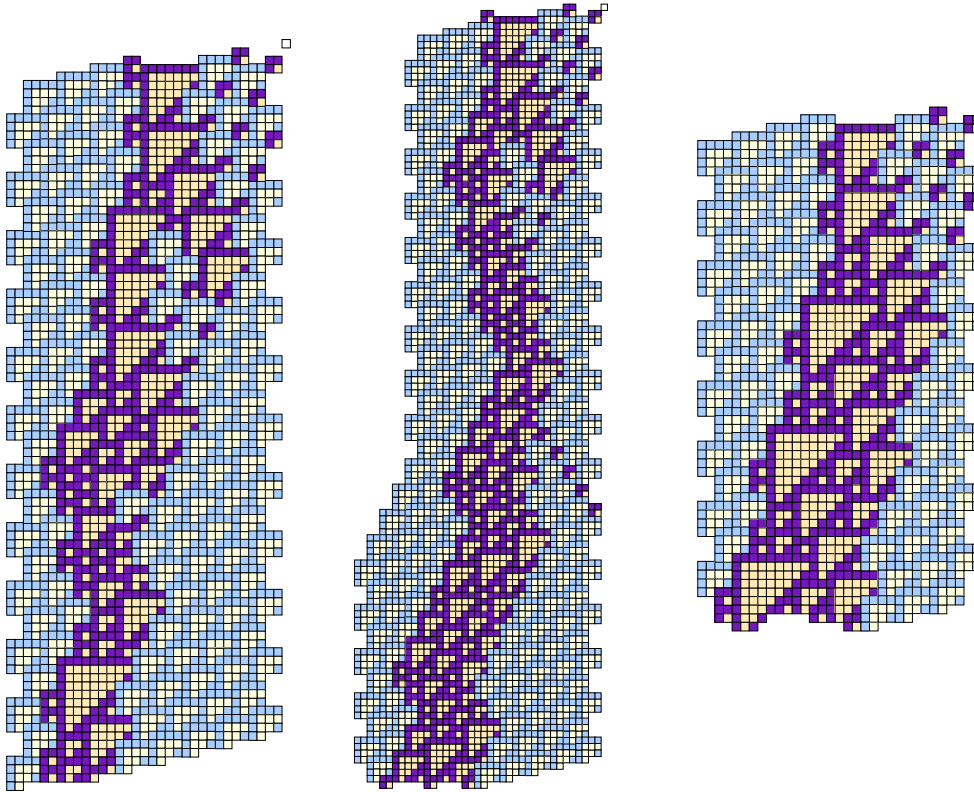


Figure 3.20: The collision of a B triad with each of the C gliders almost follows the same sequence as the collision with a single or double B. However, in the C2 collision, the secondary salvo of B's meets the developing D prematurely, placing a T3 instead of a T5 at a critical point, culminating in the release of an A and the formation of an EBar after a longer delay than was experienced in the other two collisions. In the C3 collision, the secondary B salvo is hidden in the α fragment which forms part of the evolution.

3.3.4 B - D collisions

B gliders can approach a D glider from two offsets.

| | low | high |
|----|----------|----------|
| D1 | E1 | E1 |
| D2 | EBar + A | EBar + A |

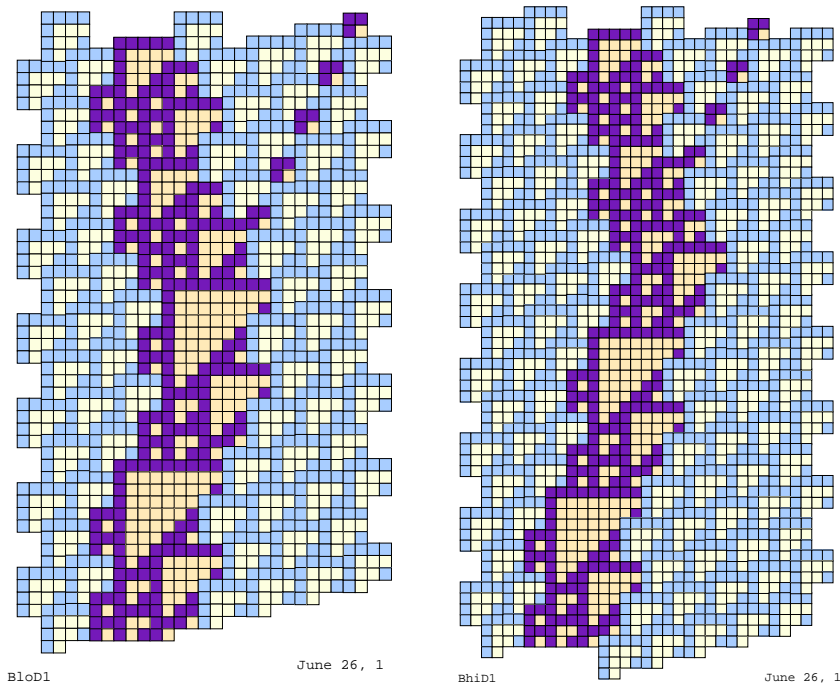


Figure 3.21: B and D1 collide, leave E. Although the same glider results from either collision, the intermediates differ slightly, as do the final positions of the resultants and the delay in their formation. The low collision on the left gives an instant result, whereas the high collision on the right *almost* creates an E, which only comes forth in full bloom thanks to the fact that its essential ingredients were already there.

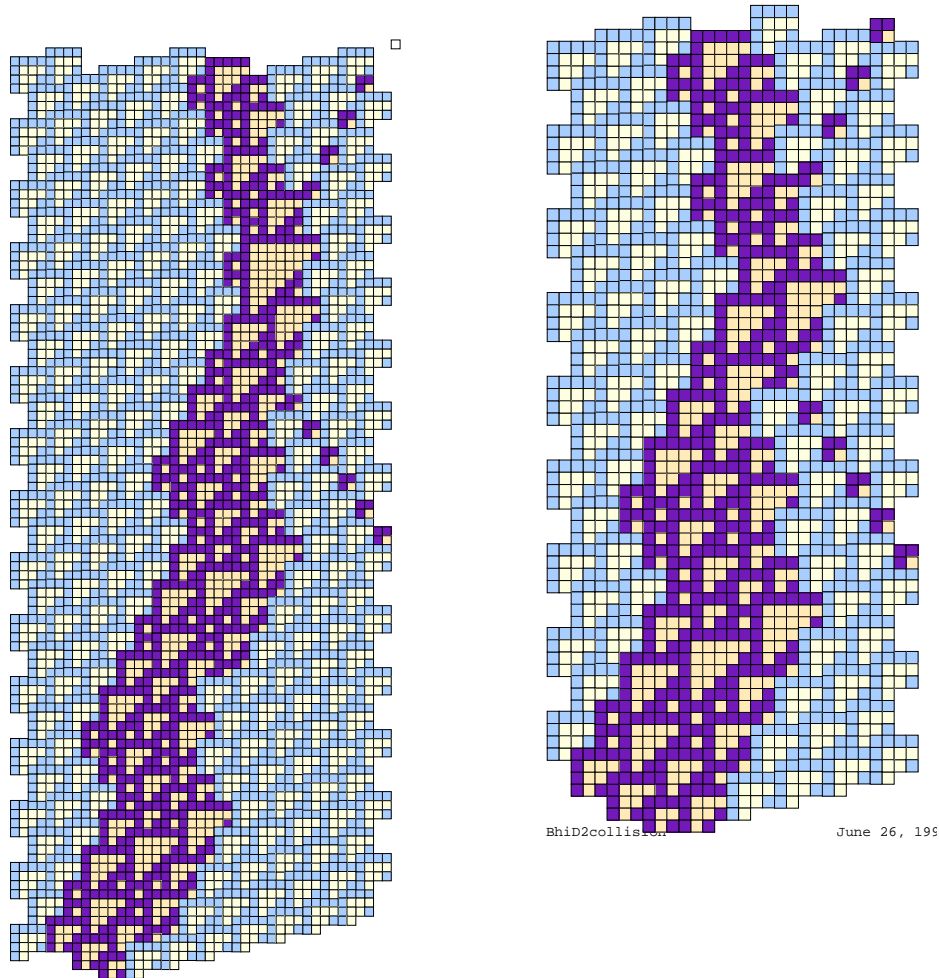


Figure 3.22: B and D2 collide, leave EBar and A, respectively, but following different routes. In the hi collision (right), the incoming T1 meets the D's T2 allowing the formation of a T5 two other heights later, which in turn becomes an EBar glider after the emission of an A. In the lo collision (left), the incident T1 meets a T4, immediately generating a T8 which promptly falls into the hi sequence. Except for the discrepant intermediates and their corresponding delays, both B - D collisions produce the same eventual results. Still, they will respond differently to multiple B collisions.

3.3.5 polyadic B - D collisions

| n | main | extra |
|---|------|-------|
| 1 | E | . |
| 2 | EBar | A |
| 3 | EBar | . |
| 4 | EBar | B |
| 5 | F | B |
| 6 | C1 | B |
| 7 | C2 | B |
| 8 | D1 | B |

Table 3.14: 8.

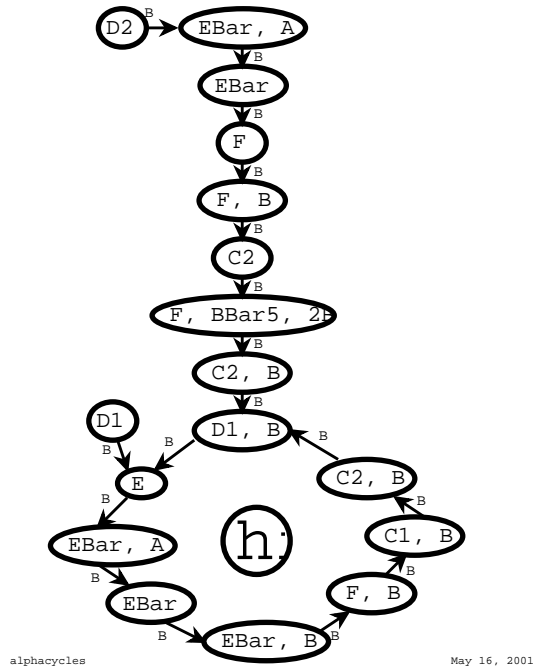


Figure 3.23: Bombardment of any structure by a salvo of B gliders takes on the character of an erosion of the alpha lattice. Therefore it can be expected that it will eventually become periodic. Here the target can be D1 hi, which itself belongs to a cycle of eight, or D2 hi, which evolves into the D1 hi cycle after a transient, also of length eight.

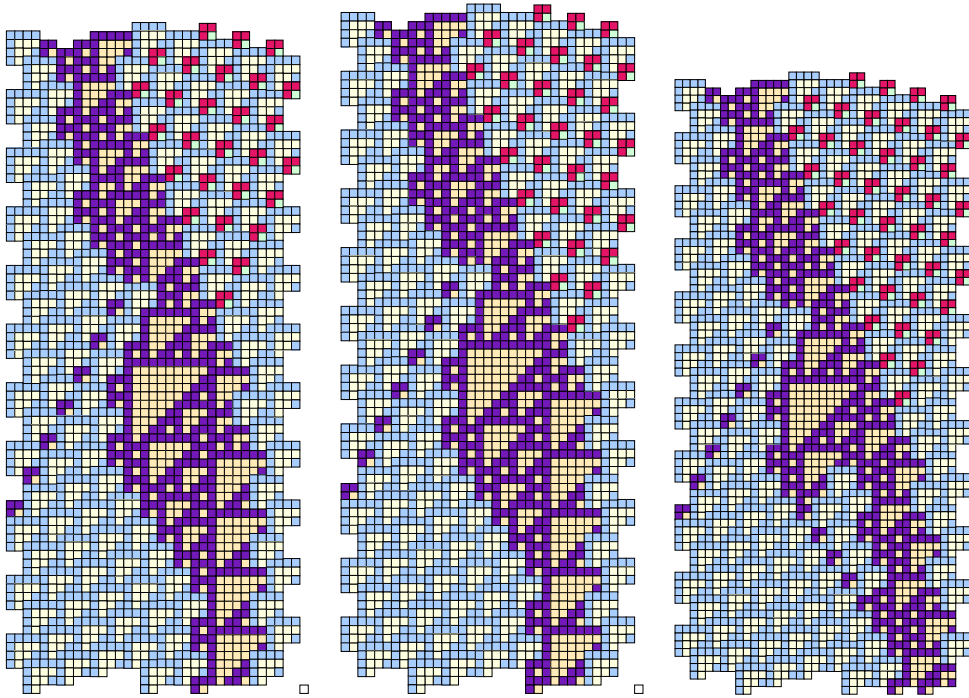


Figure 3.24: Three of the $n\text{BhiD1}$ collisions, for $n = 6, 7, 8$. The gradual growth of the period 8 margin of the region of B gliders can be seen. Every time the T1 cluster to the left of the T4 launches a new glider to the left, the B tally for the reaction must be incremented; otherwise the whole process is cyclic. Note that the A glider which transforms D1 into D2 is implicit in all three diagrams, which could be made more evident by changing the coloring of some of the T3's.

3.3.6 B - E collisions

Only one approach is possible, and invariably promotes E_n to E_{n+1} . Any number of B's can approach an E_n with arbitrary separations between them, without affecting the final result.

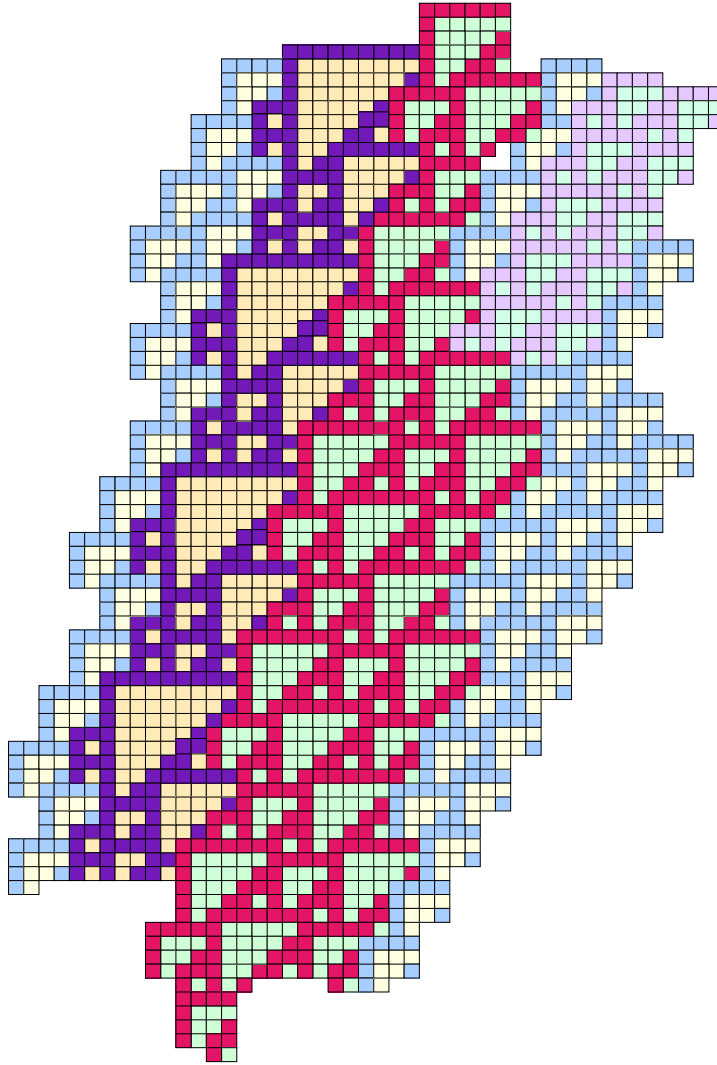


Figure 3.25: A swatch of E_5 glider, including the B 's which extended it from E_1 .

3.3.7 B - EBar collisions

There are two B - EBar collisions, both of them leaving the EBar advancing between three consecutive B precursors and working away from a pair of A's. Actually, the high aspect collision immediately switches over to a low aspect collision, with an attendant delay in becoming effective.

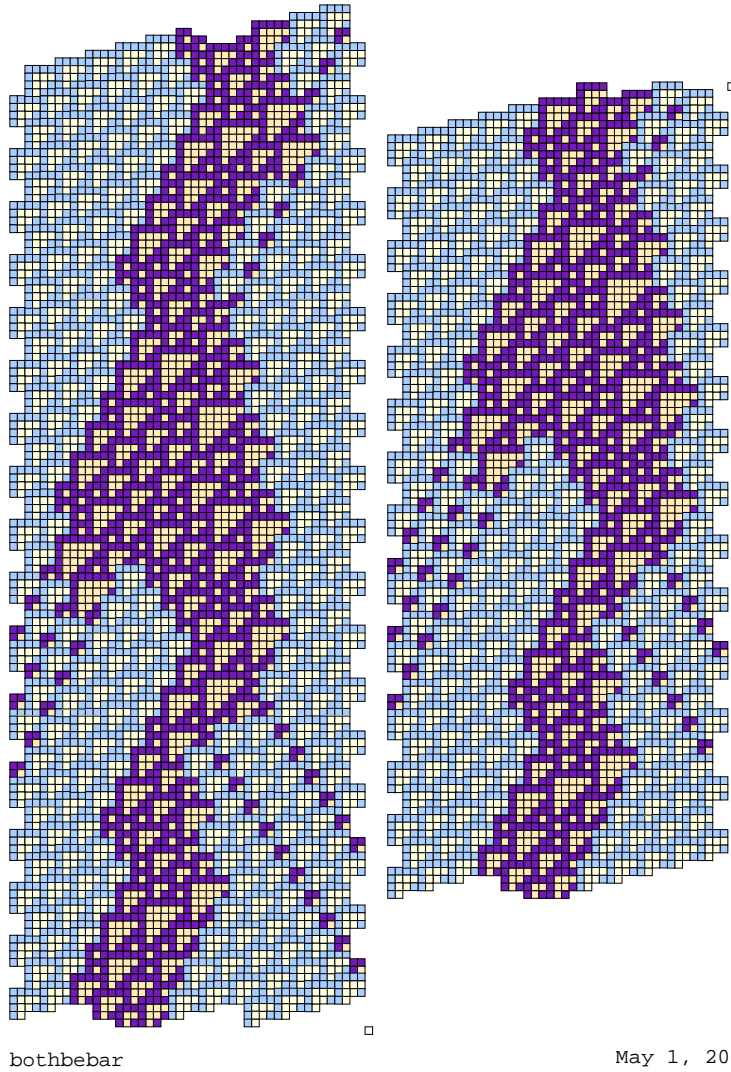


Figure 3.26: B and EBar collide in two aspects, leaving the EBar amidst a shower of sparks - two A's and a B triad.

3.3.8 B - F collisions

B gliders can approach an F glider from four alignments.

- 1st BBar + F
- 2nd D + A dimer
- 3rd B + F
- 4th BBar + F

There are four relative alignments between B and F gliders, two of which exchange the gliders for a BBar5 and an F, one of which is solitonic, and one of which leaves a residue travelling to the right.

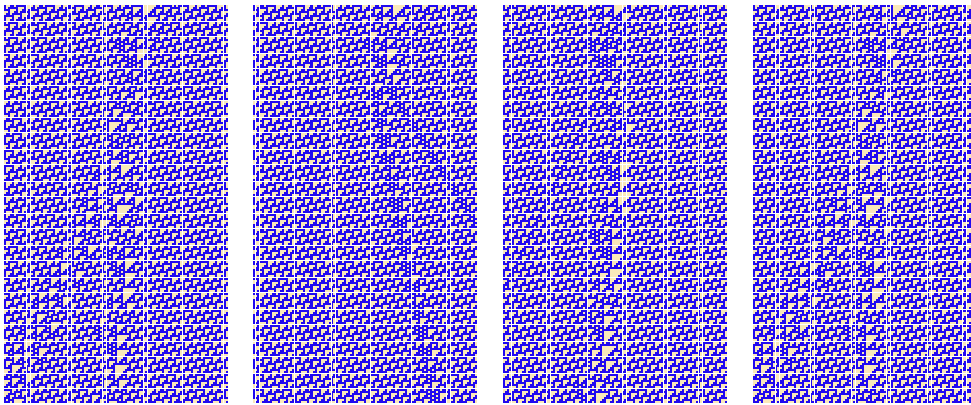


Figure 3.27: Left: The four B - F collisions.

3.3.9 B - G collisions

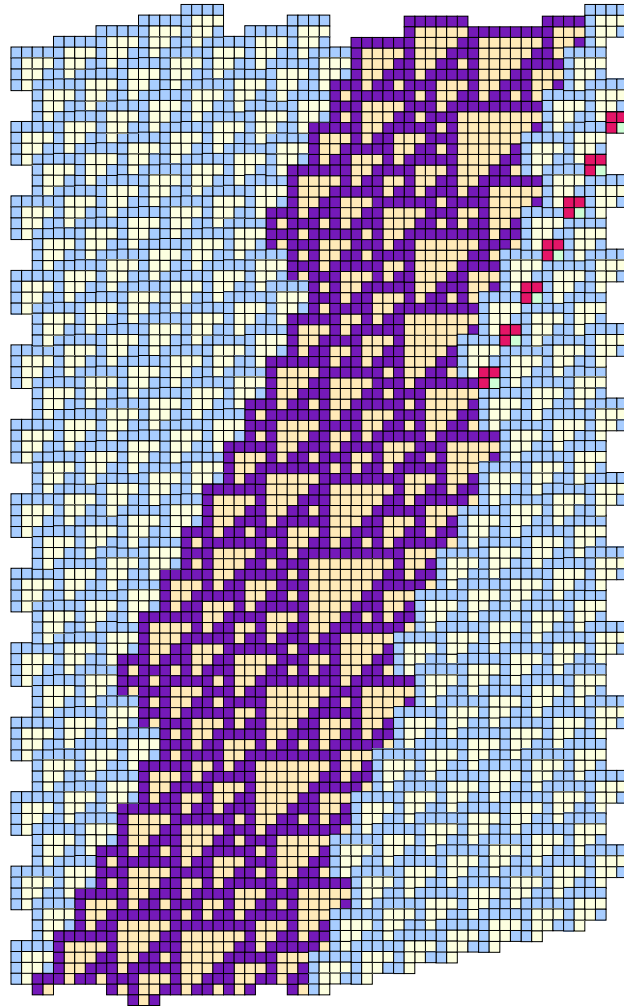


Figure 3.28: The collision of a B glider with a G glider is symmetrical between the T7 and the T8, from both of which a T5 protrudes as part of an incipient α lattice.

B gliders can extend a G glider from two alignments; both resemble B - E collisions, in which the incoming T1 grazes the protruding T5 creating a rearrangement which accomodates another T5. The process can be repeated arbitrtarily often, without any requirements on the spacing between B's.

3.4 Collisions with BBar5 gliders

3.4.1 BBar5 - C collisions

| | lo | mid | hi |
|----|------------|--------------------|----------------|
| C1 | D1 + A | EBar + 2 A dimer | F + 2 B |
| C2 | E + A | EBar + A dimer + A | BBar + F + 2 B |
| C3 | EBar + 2 A | EBar + 2 A | EBar + A dimer |

Table 3.15: BBar5-C collision

3.4.2 BBar5 - En collisions

When B's collide with E's or G's, an extension results. When BBars approach for a similar encounter, the results are variable. That is probably because the B's are a direct interface between the α 's and the ether, whilst the BBars are not.

| | |
|------|-------------------------|
| E1 | C1 + 4 B |
| E2 | E1 + B + 3 A + A trimer |
| E3 | E5 + A |
| E4 | E6 + A |
| E5 | E2 + 3 A |
| ... | ... |
| EBar | F + G + B + 3 A |

Table 3.16: BBar5-En collision

3.5 Collisions with BBar8 gliders

| | lo | mid | hi |
|----|----|-----|------------------|
| C1 | . | . | A, 3B, more |
| C2 | . | . | A dimer, 2B more |
| C3 | . | . | G, more |

Table 3.17: BBar8-C collision

3.6 Collisions with C gliders

The C gliders are static, readily interfacing to the ether on either the left or the right, and to an expanse of zeroes on the right. They can also be closely stacked, producing phalanxes of C's, and the attendant necessity to examine collisions with the phalanx in detail.

3.6.1 C - D collisions

| | D1 | D2 |
|----|--------------------|-----------------|
| C1 | A + A trimer + 3 B | A + A dimer + G |
| C2 | 2 A + 2 B | A + 2 B |
| C3 | A + 2 B | A + 3 B |

Table 3.18: Most C - D collisions cancel out into A's and B's, although sometimes after prolonged indecision during which various gliders almost materialize underneath a BBar leading edge.

3.6.2 C - E collisions

Any description of collisions with E gliders can become quite complicated simply because of the large variety of E gliders once their extensibility has been reckoned with. From a much larger perspective, there is far less variation because large E gliders are really margins of the alpha lattice, whose interface with other lattices is periodic on a sufficiently large scale.

| | E | | EBar | | | | F | |
|----|----------------|-----------------|--------------------|-------------|------------|------------|-----------------|-----------------|
| | Hi | Lo | eve: | | odd | | Hi | Lo |
| | | | Hi | Lo | Hi | Lo | | |
| C1 | A EBar F | A C2 D2 | C1 EBar | A pentam | A 3 B's | C1 EBar | C1 F | C2 EBar |
| C2 | A 2 B's | A C1 EBar | A 3 B's BBar | 3 B's | C1 F | C2 EBar | BBar C1 F | C2 F |
| C3 | A 3 B's | A G | C2 F | 4 B's | C1 C1 | 4 B's | C1 C2 | BBar C2 F |

Ccollis:

May 31, 19

Figure 3.29: Some selected collisions amongst C, E, EBar, and F gliders exhibit the properties of solitons.

C + En collisi

| | C1 | C2 | C3 |
|-------|---------------|----------------------------------|-------------|
| E1 h | EBar, F, A | A, 2 B's | A, 3 B's |
| E1 lo | C2, D2, A | C1, EBar, A | G, A |
| E2 hi | EBar, F | 2 B's | 3 B's |
| E2 lo | C2, D2 | C1, EBar | G |
| E3 hi | C2, EBar | 3 B's | 4 B's |
| E3 lo | A, 2 A dimers | A tetramer, 2 B's EBar, F, C2 | D1, EBar |
| E4 hi | D2, E | 4 B's | 5 B's |
| E4 lo | C1, E, 2 B's | C3, EBar | D1, EBar, A |
| E5 hi | E, EBar, A | 5 B's | 6 B's |
| E5 lo | | | |
| E6 hi | | 6 B's | 7 B's |
| E6 lo | | | |

CEncollis

June 24, 19

Figure 3.30: A pair of C's standing to the left can act as an En decremter similar to an A coming in from the left. Still others simply get eaten away as the En dissolves into a burst of B gliders which the next C in line refurbishes into another En.

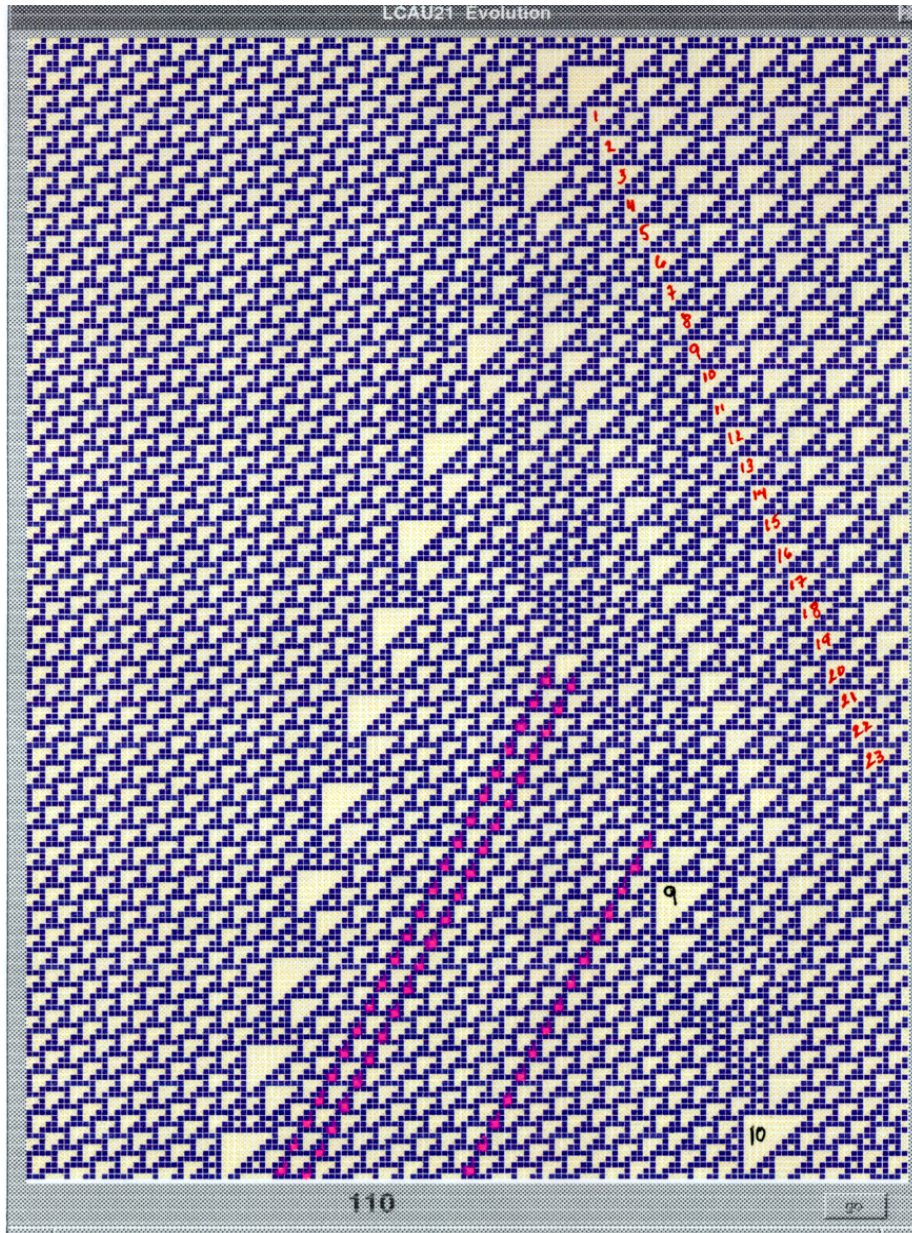


Figure 3.31: Many collisions with E complexes simply unravel the margin of an α domain, which means that they will always follow a predictable pattern.

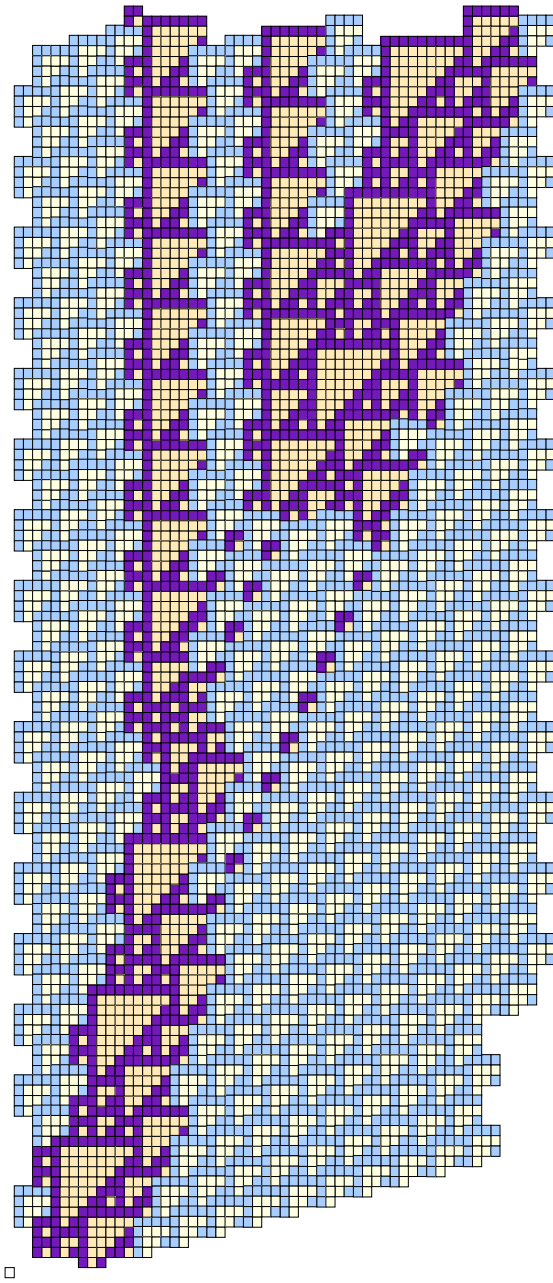


Figure 3.32: C2 collides with E, producing a shower of B's. These can collide with a waiting C2 to restore the E, but with decremented index.

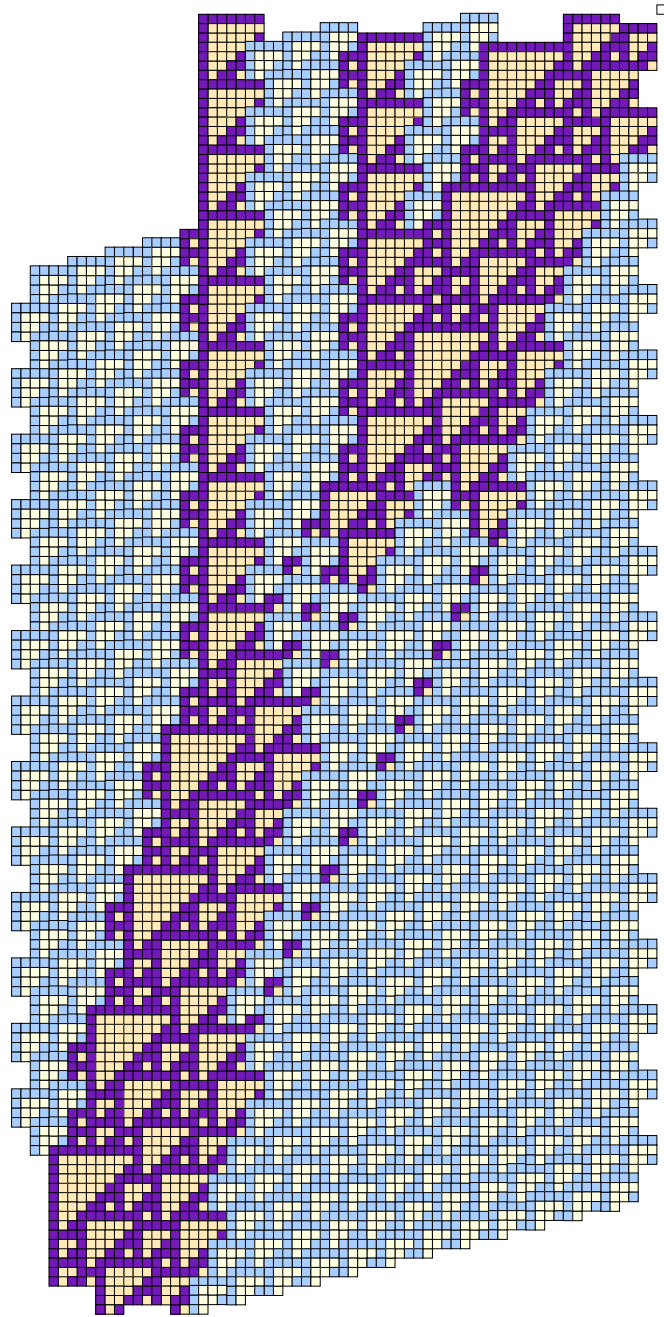


Figure 3.33: En eats up C3's, fattening itself in the process.

3.6.3 C - EBar collisions

| | high even | high odd | low even | low odd |
|----|-----------------|----------|----------|-----------|
| C1 | C1 + EBar | A penta | A + 3 B | C1 + EBar |
| C2 | A + 3 B + BBar5 | 3 B | C1 + F | C2 + EBar |
| C3 | C2 + F | 4 B | 2 C1 | 4 B |

The EBar glider can transport information from right to left across a line of C1's or C2's provided that it encounters them in the odd low aspect.

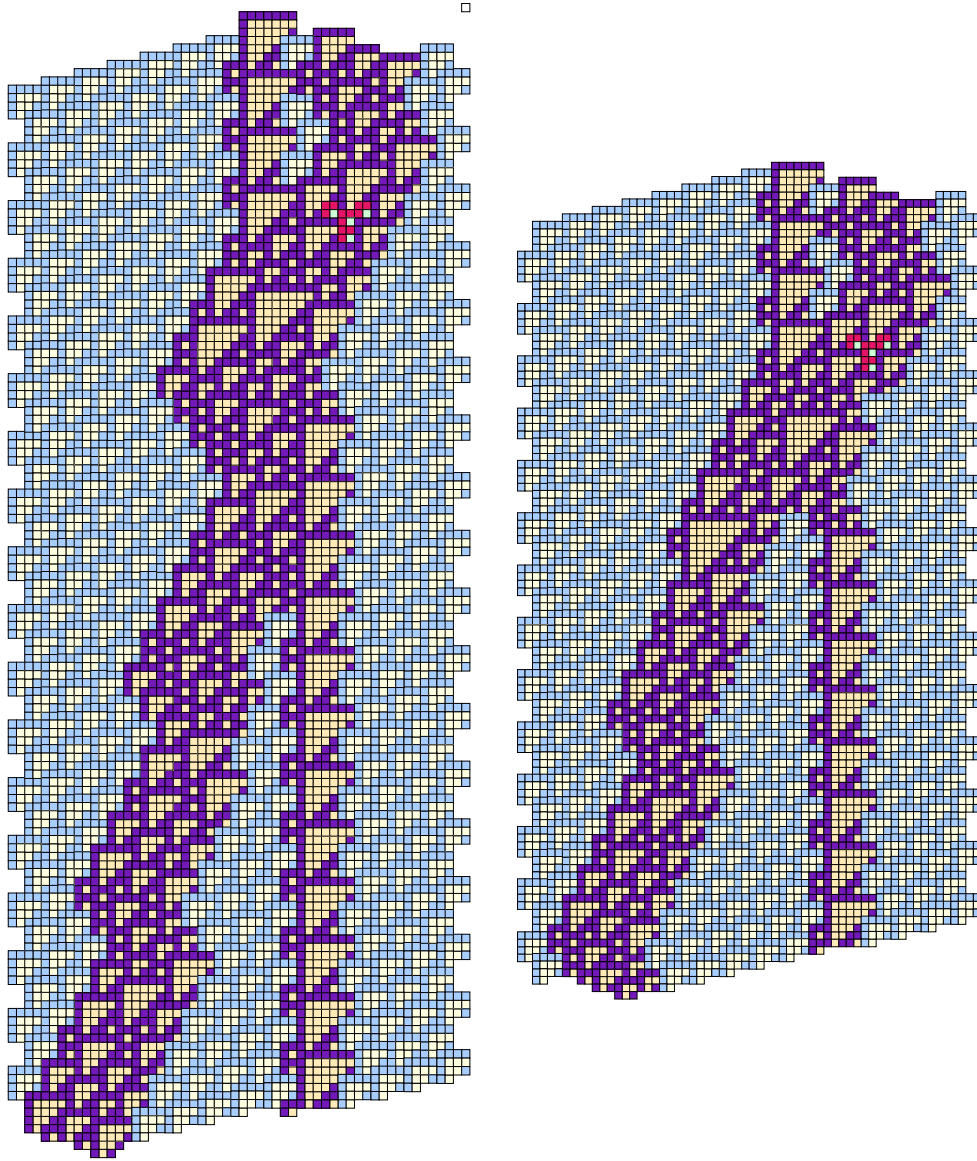


Figure 3.34: Although it has to be aligned correctly to do so, an EBar can pass by either a C1 or a C2, allowing it to carry information across a line of C's.

3.6.4 C - F collisions

| | F high | F low |
|----|---------------|---------------|
| C1 | EBar + C2 | F + C1 |
| C2 | F + C1 + BBar | F + C1 + BBar |
| C3 | C1 + C2 | F + C2 + BBar |

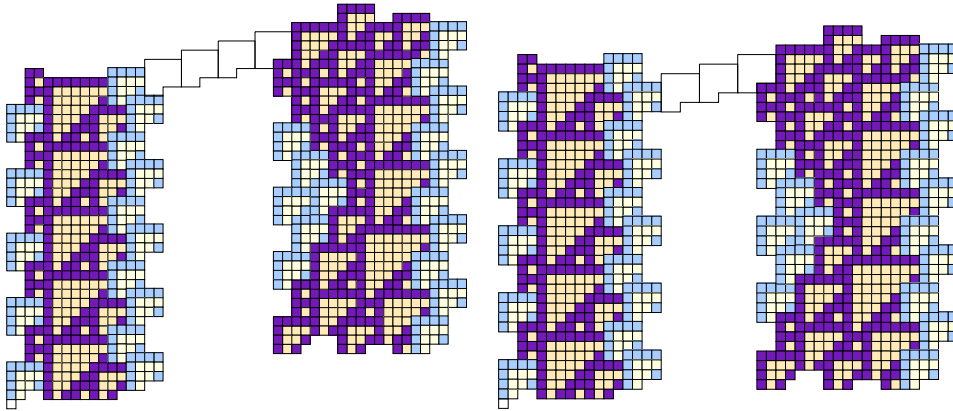


Figure 3.35: Illustrating the two different alignments for C - F collisions. They can be distinguished visually by whether an odd or an even number of ether tiles separate their two margins. Left: high aspect, Right: low aspect.

C gliders are static with period 7, while F gliders move left 4 every 36 generations, for a velocity of $-1/9$. Thus an F glider falls by one cell relative to the C chain, while coming 4 cells closer, every time it runs through its period.

Since the two gliders must be separated by an integral number of ether tiles, and there are two phases of ether tile which abut on the right side of a C, there are essentially two relative alignments for an F and any C.

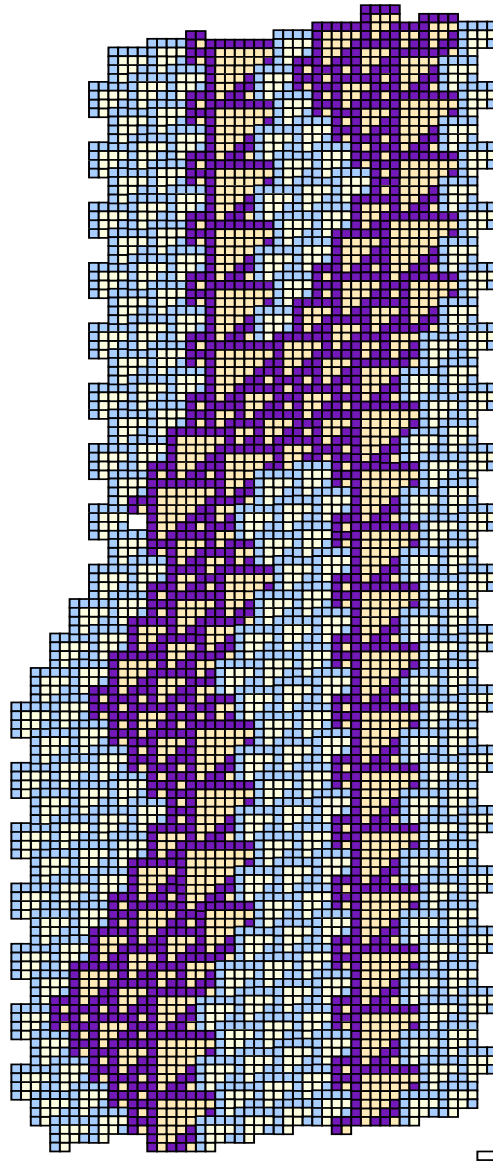


Figure 3.36: C1 collides with F in the low alignment, wherein they pass each other by.

3.6.5 C - G collisions

C gliders are static with period 7, while G gliders move left 14 every 42 generations, for a velocity of $-1/3$. Thus a G glider falls by one cell relative to the C chain, while coming 14 cells closer, every time it runs through its period. On the other hand, a G glider has a simple top margin consisting of three cycles of BBar margin, followed a drop of two ether tiles along an A dimer margin, there are essentially eleven positions for an oncoming G along a B line of sight, and only one B line of sight per C cell. These combinations are shown in Figure 3.37.

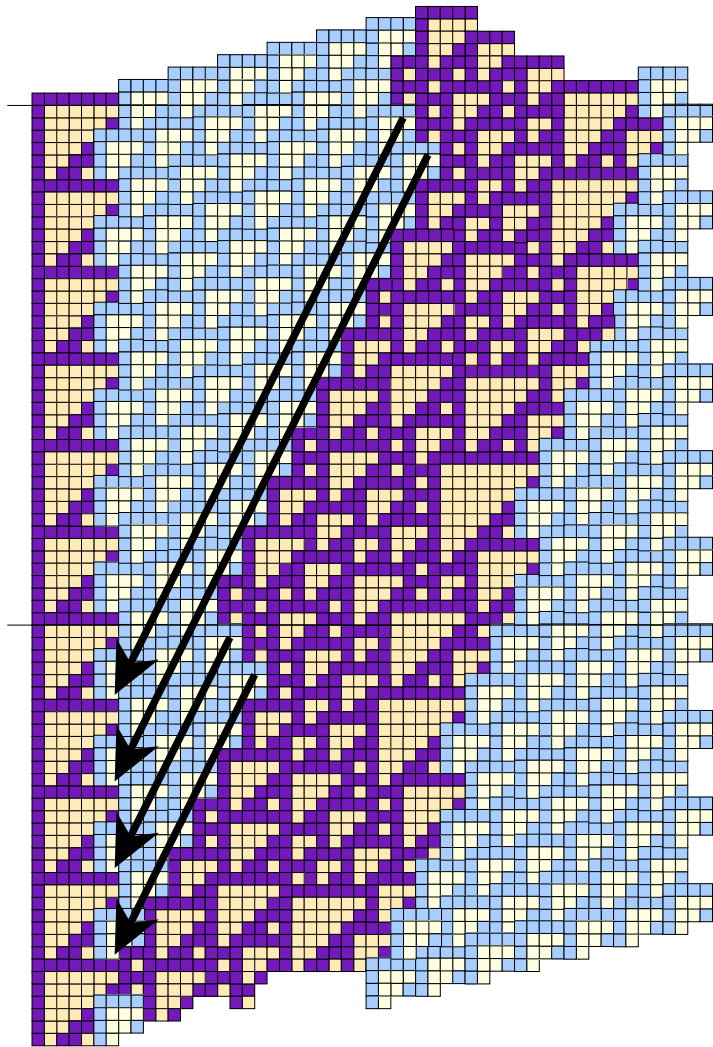


Figure 3.37: There are eleven aspects from which a G glider can approach a C glider.

It is then a matter of setting up each aspect for the three C gliders, and tabulating the results, as shown in Figure 3.38. The results vary in complexity, ranging from the

completely clean $C3 + G^{(6)} \rightarrow EBar$ to the two C2 collisions resulting in $A + C1 + D2 + EBar$. An EBar is by far the most common resultant, with most of the collisions producing varying numbers of A's; although B's arise almost as often. Sometimes a C glider will be left behind; usually a C2, but sometimes a C1, never a C3.

The BBaric periodicity of the G along the top margin, which is the part that reaches the C first, is very much in evidence; however it is not a rigorous periodicity because of the influence of the remainder of the environment.

| C1 - G colli | | C2 - G collision | | C3 - G collision | |
|--------------|-----------|------------------|---------------|------------------|-------------------|
| 1 | B dyad | 1 | 2A, | 1 | A, |
| 2 | 2A, | 2 | 2A, A*2, A*4, | 2 | B tetrad, C |
| 3 | A trimer, | 3 | A, C1, D | 3 | 3A, B triad, EBar |
| 4 | 2A, | 4 | A, | 4 | A trimer, C |
| 5 | B dyad | 5 | B triad | 5 | A, |
| 6 | A dimer, | 6 | 4A, B triad, | 6 | |
| 7 | 2A, | 7 | A*3, BBar5, | 7 | A, B dyad, C2, |
| 8 | B dyad | 8 | 2A, | 8 | A, |
| 9 | 2A, | 9 | 2A, A*2, A*4, | 9 | B tetrad, C |
| 10 | A trimer, | 10 | A, C1, D | 10 | 3A, B triad, EBar |
| 11 | 2A, | 11 | 2A, A*2, A*4, | 11 | B tetrad, C |

Figure 3.38: The thirty three different collisions between C gliders and G's.

3.7 Collisions with D gliders

3.7.1 D - E collisions

| | hi | mid | lo |
|----|---------------|---------------|---------|
| D1 | A dimer + 4 B | A dimer + 4 B | B dyad |
| D2 | 2 A dimer | G via T13 | B triad |

Table 3.19: D - E collisions mostly cancel out into A's and B's. a noteworthy exception being the D2E1mid collision which cleanly produces a G glider via a freestanding intermediary T13. In this respect the evolution resembles the commonplace production of an EBar from a single T10.

3.7.2 D - EBar collisions

3.7.3 D - F collisions

3.8 Collisions with E gliders

3.8.1 E - F collisions

En - F collisions tend to dissipate, sometimes after long intervals.

3.9 Collisions with EBar gliders

| | |
|-----------------|----------|
| 1 st | EBar + F |
| 2 nd | EBar + F |
| 3 rd | EBar + F |
| 4 th | B |

Table 3.20: Of the four relative alignments between an EBar and an F, the three highest let the EBar pass. The lowest removes them both leaving only a B to mark their presence.

3.10 Collisions with F gliders

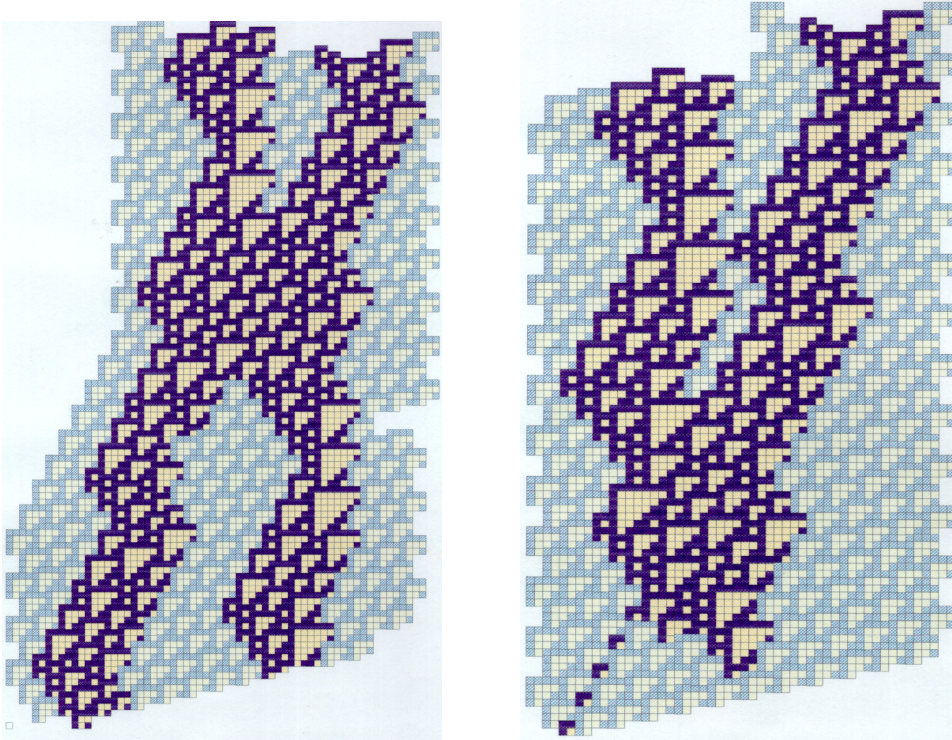


Figure 3.39: Left: EBar collides with F(1). Right: EBar collides with F(2).

Chapter 4

Running an Obstacle Course

Having enumerated binary collisions and examined some of their products, attention naturally turns to more complicated collisions. If the reactants are well separated, it is just a matter of combining the binary results. But given that collisions take time to resolve themselves, a third (or even more) gliders can intrude into the reaction area, changing the final result.

An intermediate type of collision consists of those where the interaction is perfectly predictable, but the combination of a whole series may turn out to be interesting. One example lies in the use of an E_n as a counter, which can be manipulated by two different mechanisms.

The outstanding characteristic of an E_n glider is that n will be incremented by B collisions, surely and independently of their relative spacing. Two of the possible collisions by an A glider decrement the index (taking E_0 as D1, and observing that B D1 can bring the E back, thereby allowing a mild deficit). Although symmetrical with respect to the indices, the arrival of the index modifying gliders from opposite directions recommends isolating the E_n , complicating any plans to use it as a tally.

The other index changing collision arrangement uses C gliders (which, of course, are static), relying upon the difference between C2 or C3 to get the sign of the index change. Whichever, the modifier sits on the same side, always the left, of the oncoming E. Creating a series of index changes depends on arranging the sign changing C's in the required linear order.

Running off the end of the series, with a non-existent E_0 , also has to be foreseen and provided for.

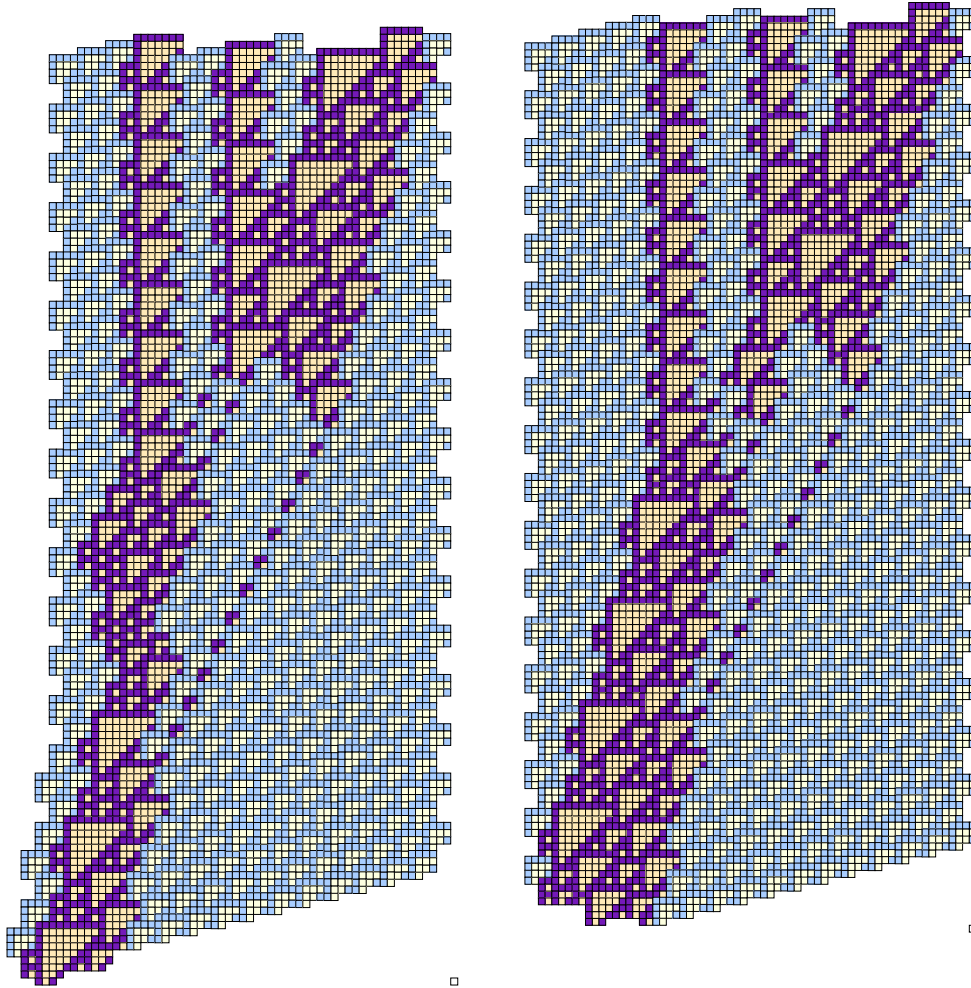


Figure 4.1: Left: A pair of C2's can decrement an En. Right: A pair of C3's can increment an En.

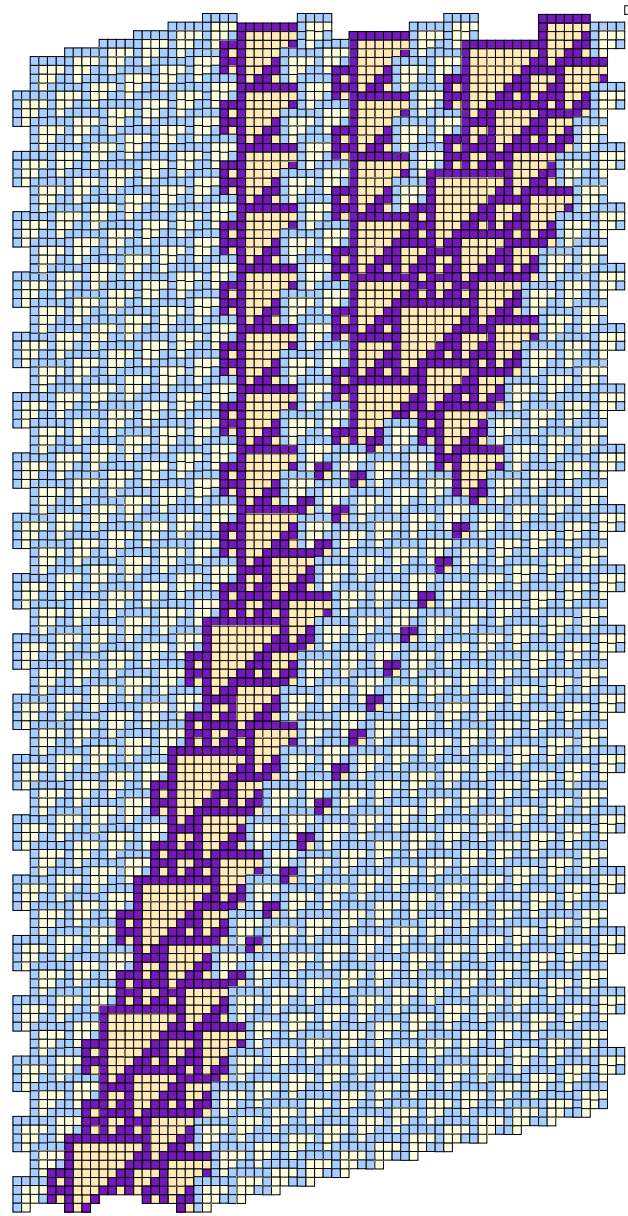


Figure 4.2: By alternating incrementation and decrementation, an En can maintain itself while erasing (right to left) C2, C3 pairs. Incrementing, followed by decremting, is secure; reversing the order could create an EBar as an intermediate.

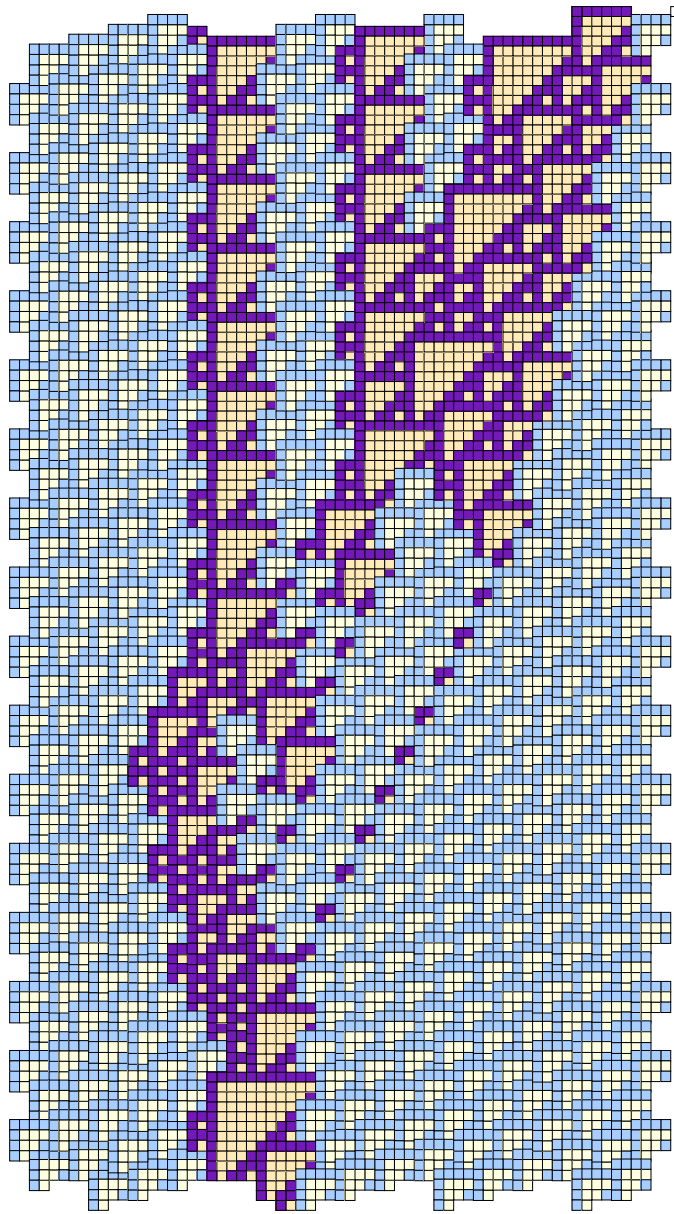


Figure 4.3: Unfortunately, reversing the order of C2 and C3 in an E_n sweep breaks the sequence, introducing EBars. The T10 visible at the bottom of the figure is a canonical EBar precursor.

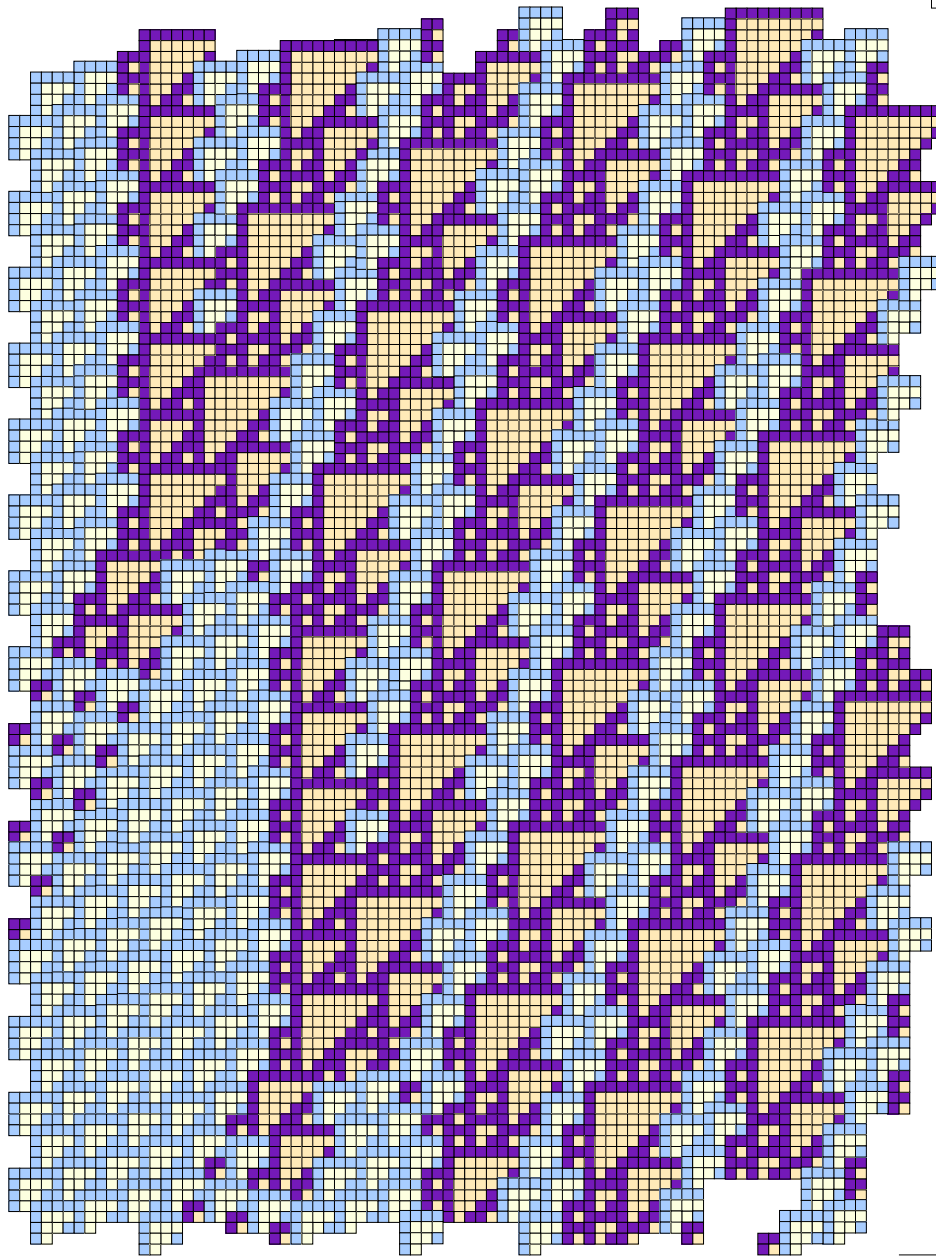


Figure 4.4: The C3 - E collision creates a B triad plus an A. But an A - E collision, high or low, produces a C3. Therefore a C3 can move to the right against an E stream at the expense of releasing three B gliders for every two E's which it absorbs. All those B's could be used to produce a huge E at some point, if that were desired.

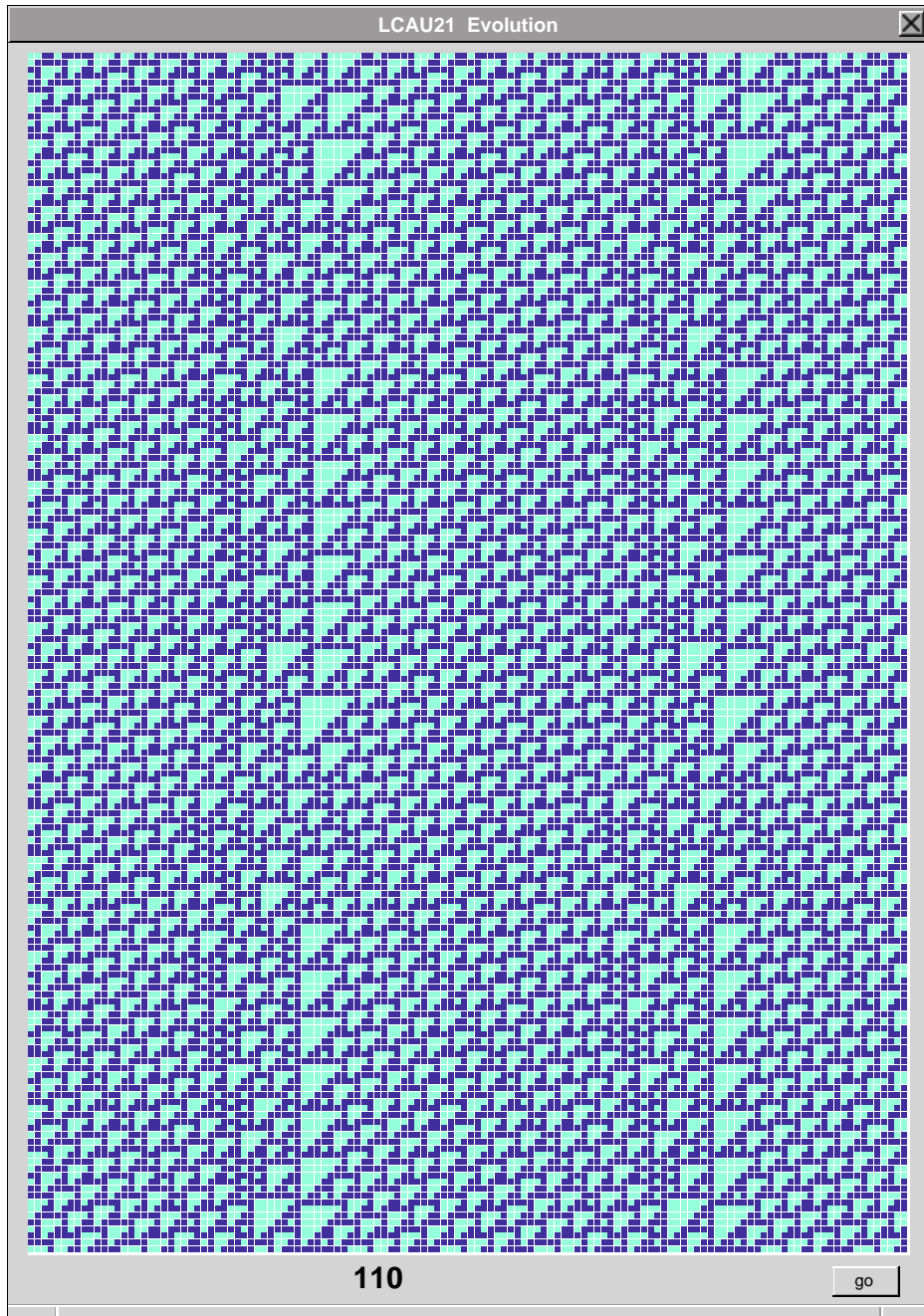


Figure 4.5: A slowly drifting complex can be formed from an infinite sequence of A, C2, and D2 gliders. Absorption of the A during the triple collision leads to regeneration of the C - D pair and the emission of a new A. The A's can be used to link successive pairs to get a figure with an overall shift period of 2 left every 86 generations.

Chapter 5

Conclusions

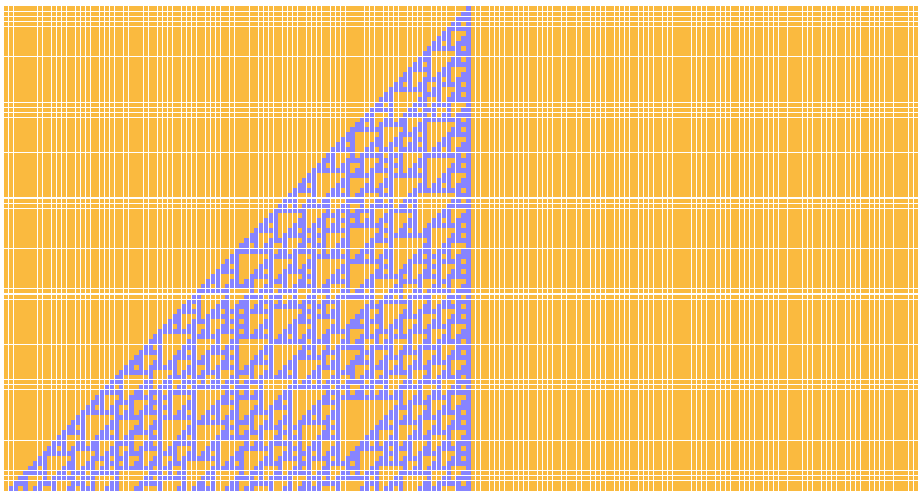


Figure 5.1: One of the reasons that large triangles do not occur often in evolutions is that they do not pack well. Extremely large triangles belong to the Garden of Eden.

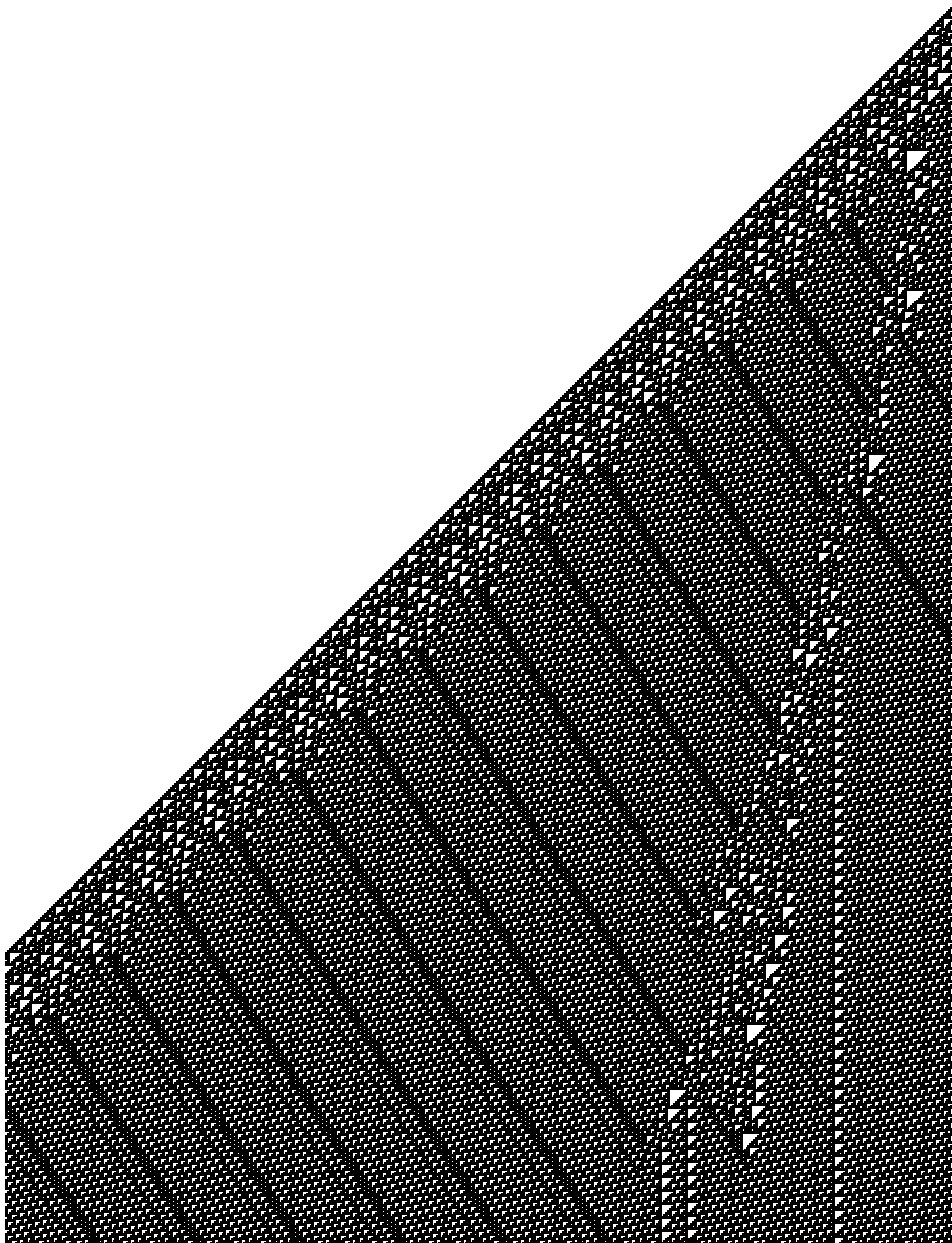


Figure 5.2: After the first few hundred generations, a boundary layer stabilizes along the advancing edge of the expansion of a single cell into the vacuum. It still has to come to terms with the right edge. (Figure courtesy Genaro Juarez Martinez)

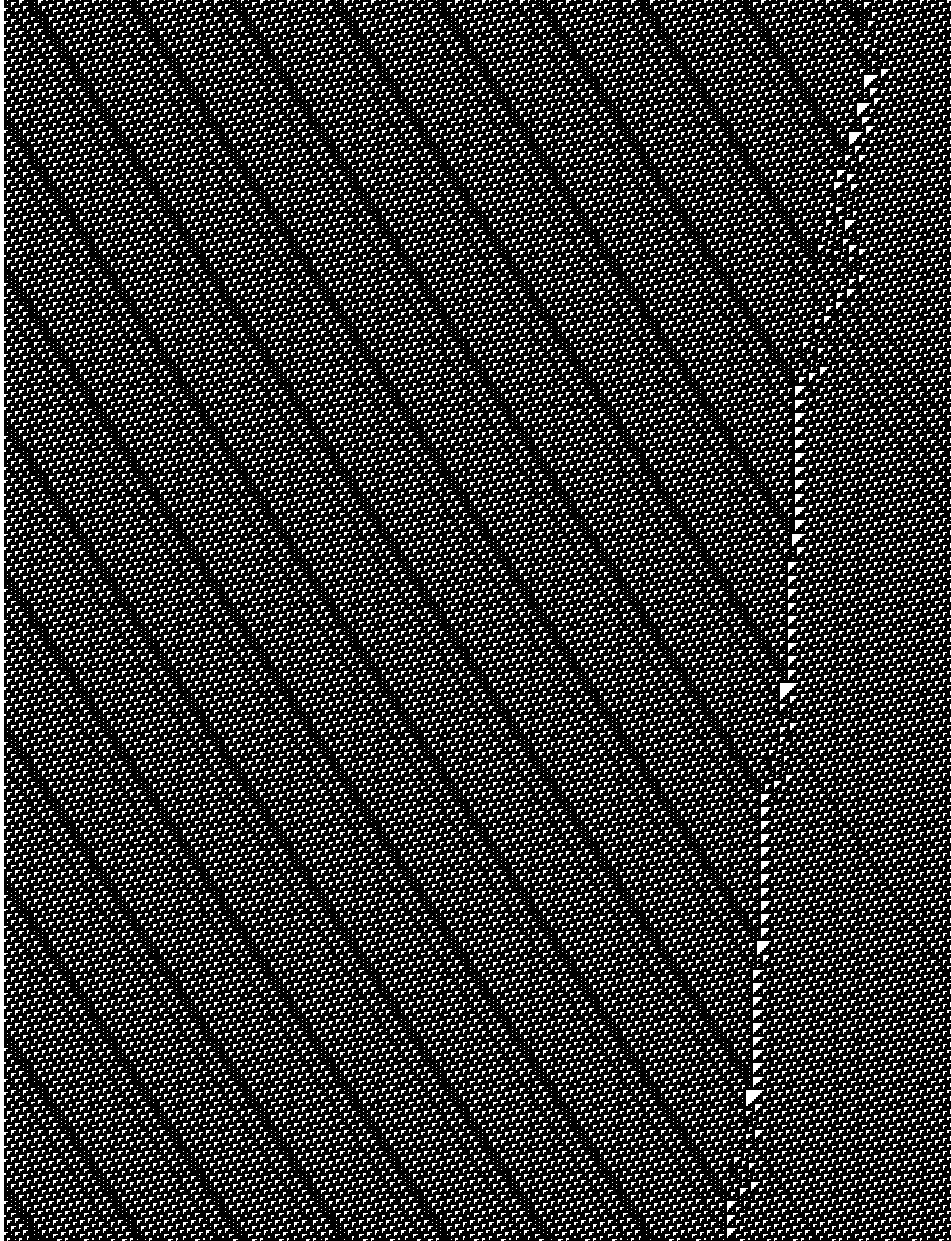


Figure 5.3: Eventually the expansion of a single cell into the vacuum comes into equilibrium, with A gliders from the left meeting C3's on the right in a reaction which displaces them slightly to the left. (Figure courtesy Genaro Juarez Martinez)

Using cyclic configurations to find gliders has limitations, especially when the gliders are sought against a textured background, as in the case of Rule 110. The idea of the straightjacket consists in fixing the boundary cells of an interval and looking at the evolution so constrained, which is certainly not a new idea by any means. In the case of gliders, the boundary can be staggered according to the velocity of the glider.

However, there is a complication, namely that the postulated boundary may not be compatible with the evolution of the full field, after all. The result is that running out the constrained basin diagram gives a necessary, but not sufficient, condition that the nuclear (transient-free) diagram defines gliders which can be inserted into the given background. Between necessity and sufficiency lies a compatibility problem, expressible via the Post Correspondence Principle, a/k/a the word problem, with a good likelihood of being undecidable: “It is undecidable whether there exists a glider of arbitrary velocity s/d (displacement/generation) in a textured automaton.”

“Textured” rules out arbitrary Class III automata unless agreement on an “ether” can be reached, whereas Class I and II automata do not have enough texture to raise the word problem out of triviality. In other words, it all depends on whether the sequence the straightjacket program generates is complex enough to create a word problem when checked against the boundary sequence.

Note a difference between the basin calculation and what is proposed here: Basin programs generate trees rooted on loops (and hence loop nuclei) because of the functional character of cyclic evolution. A stipulated boundary has to compensate the degradation of the automaton’s interval due to the discrepancy between neighborhood and cell; when there is shifting, it has to be thicker still. Therefore the map of a glider’s- width-interval always depends on some boundary cells, but still more at shift points. An interval will always have a successor, but possibly more than one, in contradistinction to the cyclic case; therefore nuclei need not be simple loops. Otherwise there would be no word problem.

As far as actually testing this, the gliders reported by Cook and Lind together with the margins they require imply a greater computational effort than that to which I have been accustomed.

5.1 Acknowledgements and Disclaimer

Visual inspection of the gliders in Cook’s [www](#) page [1] has been the source of all the tilings presented here. Beyond that, the further exchange of information via LifeMail has helped to clarify much of the structure and organization of his gliders. `NXLCAU21` is part of an extensive program development made possible by the NeXT workstation provided by the CONACYT.

Naturally one expects to fill a document such as this with correct information. Evolutions copied from the screen of a computer program are more likely to be correct than those drawn by hand; results obtained both ways verify one another but may still be erroneous. Therefore, a certain amount of scepticism should be exercised and the results viewed accordingly.

By far the most common error in the hand drawn diagrams arises from juxtaposing top margins; T tiles suffer more than the S tiles.

Bibliography

- [1] Matthew Cook, "Introduction to the activity of rule 110" (copyright 1994-1998 Matthew Cook) <http://w3.datanet.hu/~cook/Workshop/CellAut/Elementary/Rule110/110pics.html>
- [2] Branko Grünbaum and G. C. Shepard, *Tilings and Patterns*, W. H. Freeman and Company, New York, 1987 (ISBN 0-7167-1193-1).
- [3] Mariusz H. Jakubowski, Ken Steiglitz, and Richard K. Squier, "When can solitons compute?" *Complex Systems* **10** 1-21 (1996).
- [4] Wentian Li and Mats G. Nordahl, "Transient behavior of cellular automaton rule 110," *Physics Letters A* **166** 335-339 (1992).
- [5] Kristian Lindgren and Mats G. Nordahl, "Universal Computation in Simple One-Dimensional Cellular Automata," *Complex Systems* **4** 299-318 (1990).
- [6] Harold V. McIntosh, "Wolfram's Class IV automata and a good Life," *Physica D* **45** 105-121 (1990).
- [7] Christopher Moore and Arthur A. Drisko, "Algebraic properties of the block transformation on cellular automata" *Complex Systems* **10** 185-194 (1996).
- [8] Grzegorz Rozenberg and Arto Salomaa, *Cornerstones of Undecidability*, Prentice Hall, New York, 1994 (ISBN 0-13-297425-8 pbk).
- [9] Stephen Wolfram (Ed.), *Theory and Applications of Cellular Automata*, World Scientific Press, Singapore, 1986 (ISBN 9971-50-124-4 pbk).
- [10]
- [11] Andrew Wuensche and Mike Lesser, *The Global Dynamics of Cellular Automata*, Addison-Wesley, Reading, Massachusetts, 1992 (ISBN 0-201-55740-1).

August 5, 2001